THE NUCLEAR POLARIZATION OF GOLD 198 IN DILUTE SOLUTION IN GADOLINIUM METAL

Norman Mathieson Leitch

A Thesis Submitted for the Degree of PhD
at the
University of St Andrews

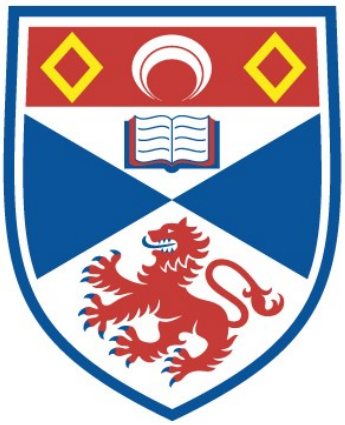

1964

THE NUCLEAR POLARIZATION OF THE NUCLEI OF GOLD 198 IN DILUTE SOLUTION IN GADOLINIUM METAL

being a thesis presented by

Norman Mathieson Leitch, B. Sc.,

to the University of St Andrews in

application for the degree of

Doctor of Philosophy.

ProQuest LLC.
789 East Eisenhower Parkway
P.O. Box 1346
Ann Arbor, MI 48106 – 1346

DECLARATION

I hereby declare that this thesis is entirely based on the results of work carried out by myself in the Laboratoire d'Electrostatique et de Physique du Métal, Institut Fourier, Grenoble, and in the School of Natural Philosophy, St Andrews University. The thesis is my own composition, and it has not been previously presented for a higher degree.

[redacted]

CERTIFICATE

I hereby certify that Norman Mathieson Leitch has spent nine terms in research work on the Nuclear Polarization of Au^{198} in Dilute Solution in Gadolinium Metal, that he has fulfilled the conditions of Ordinance 16 (St Andrews), and that he is qualified to submit this thesis in application for the degree of Doctor of Philosophy.

[redacted]

Research Supervisor.

16 October, 1963

Statement of Career

I matriculated in the University of St Andrews in the Martinmas term 1956, and was admitted to the degree of Bachelor of Science in June 1960.

I was awarded a N.A.T.O. Studentship to the Laboratoire d'Electrostatique et de Physique du Métal of the Centre National de la Recherche Scientifique in the Institut Fourier of the Université de Grenoble, France, where I began the research described in this thesis in October, 1960. I matriculated as a research student in the University of St Andrews in the Martinmas term, 1960. In the Martinmas term, 1962, I returned to residence in the University of St Andrews to complete the analysis of my results and the composition of this thesis.

CONTENTS

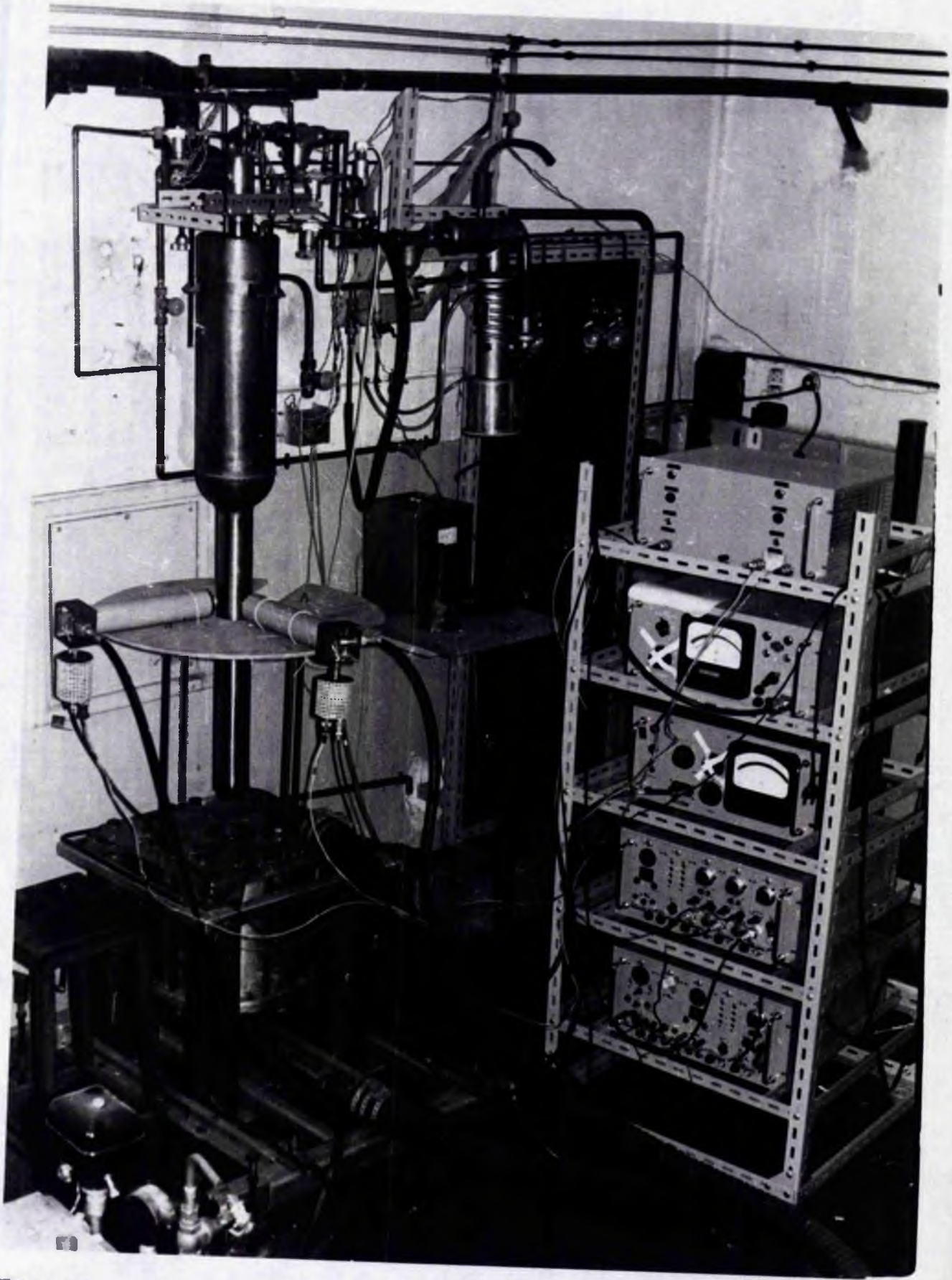

Plate 1. The Experiment Set Up.

Facing P.1.

CHAPTER I

General Introduction

I.1 Author's Preface

The author's interest in low temperature physics was first stimulated by Professor J.F. Allen, and it was with his encouragement that the author went to work under Professor Louis Weil at the Institut Fourier, Grenoble. During the first few months in Grenoble, the author gained experience in cryogenics by assisting colleagues with the measurements of the specific heats of metals both between $1^{\circ}K$ and $4^{\circ}K$ and below $1^{\circ}K$.

It was then decided to carry out a study of the nuclear orientation of the nuclei of diamagnetic elements in dilute solution in a ferromagnetic metal by a method first proposed by Samoilov[1]. This method makes use of the internal magnetic field in a magnetically saturated ferromagnetic metal to polarize the nuclei of the diamagnetic element in solution in it by interaction of the internal field with the magnetic moment of the nucleus. It was decided to establish whether or not this method could be applied to orientate

the nuclei of diamagnetic metals in solution in a ferromagnetic rare earth metal, and so obtain a value of the internal magnetic field in the rare earth which tends to orientate the nuclei of the diamagnetic metal. Gadolinium was chosen as the host metal of the alloy, and gold as the diamagnetic metal of the alloy.

This method of producing nuclear orientation requires that the specimens of the alloy be cooled to a temperature of below 5×10^{-2} °K. Such a temperature can only be obtained by the adiabatic demagnetization of a paramagnetic salt in thermal contact with the specimen. This entailed the construction of a high-power solenoid to produce intense magnetic fields, described in Chapter VII, and of a helium cryostat to produce the starting temperature for magnetic cooling. The construction of this apparatus is described in Chapter VI. Since the construction of the high-power solenoid was expensive, there was some delay before it could be authorized. The construction of the solenoid was completed in December 1961, and it was installed by March 1962.

The author was joined on the project by M. Jean Gizon of the Centre d'Etudes Nucléaires de Grenoble, whose responsibility it was to design and operate the gamma-ray counting apparatus, and to arrange the preparation and irradiation of the specimens.

The amount of time available for the completion of this research was limited by the duration of the author's Studentship which was limited to two years abroad, and also by the forthcoming transfer of the laboratory to new buildings, which took place in October 1962. This prevented investigation into nuclear orientation in other alloys, and limited the possibilities of modifying the apparatus as would have been done as a result of experience, had more time been available.

The author wishes to record his indebtedness to the North Atlantic Council for a NATO Studentship, and to the following members of the Laboratoire d'Electrostatique et de Physique du Métal for their help and cooperation:
Professeur Louis Weil, Dr B.B. Goodman, Messrs. J. Gizon, A. Lacaze, R. Geiser and to Professor J.F. Allen for his advice and encouragement.

I.2 The Scope of the Present Research and of Experiments which were Projected but not carried out.

In 1960, Samoilov, Sklyarevskii and Stepanov[1] reported a series of experiments on the nuclear polarization of the nuclei of diamagnetic elements in dilute solution in magnetically saturated iron.

These experiments were successful attempts to obtain nuclear polarization of the gamma-ray emitting nuclei of indium, antimony, and gold in dilute solution of iron. The specimens were cooled to about 0.03°K by adiabatic demagnetization of a pill of a paramagnetic salt in thermal contact with them, and were magnetized to saturation. Nuclear orientation in the specimens was detected by anisotropy in the gamma-ray emission which was measured by two scintillation counters arranged parallel and perpendicular to the direction of magnetization of the specimens. They concluded that nuclear orientation was due to interaction of the nuclei with a strong internal magnetic field within the alloy, and from the anisotropy of the gamma-ray emission they determined the order of magnitudes of the magnetic fields at these nuclei. Effective magnetic fields of the order of 7×10^5 gauss were estimated to act on the Au^{198} nuclei in iron where the magnetic 3d shell is close to the surface of the atom.

It was our intention to determine whether the deeply imbedded 4f electron shell of gadolinium could produce such a large hyperfine field as would polarize the gold nuclei in a dilute alloy of gold in gadolinium. A series of experiments on the nuclear polarization of gold in gadolinium by the method of Samoilov are reported

in this thesis. A review of the current state of the theory of internal magnetic fields in ferromagnetic materials is given in Chapter III. Much of the theoretical work reviewed here was published after the commencement of the work described in this thesis, and would certainly have suggested other experiments to be performed in this field, had it been published earlier.

We intended also, as part of this series of experiments, to investigate the nuclear polarization of the nuclei of suitable gadolinium isotopes in pure gadolinium metal in order to have complementary estimates of the internal magnetic field in gadolinium.

It was essential to use specimens in the form of thin discs for two reasons. It was desirable to decrease the demagnetization factor of the specimens, and it was necessary to have them circular in section so that the angular distribution of gamma radiation from a warm sample should be isotropic. The specimens were therefore punched from foils of the metal. Unfortunately, the bulk metal proved to be too brittle to roll into thin sheets at room temperature. We did not have facilities for heat treatment of the metal, and delivery dates for samples in laminar form were too long to allow the work to be completed in time.

We decided also to carry out an experiment on the nuclear orientation of Co^{60} in a 50% Co-Ni alloy to test the apparatus and the results are given in Chapter IX for interest and are compared with results obtained by other investigators.

CHAPTER II

Nuclear Alignment and Polarization

II.1 Definition of Alignment and Polarization

As an introduction, let us consider a nucleus of non-zero spin $\underline{I}$, and an axis of quantization which we will call the $\underline{z}$-axis. This axis may be defined by, for example, an externally applied magnetic field. If this magnetic field be of strength zero, the nucleus has $2I+1$ degenerate states, each characterised by a different value of I_z, the component of $\underline{I}$ along the z-axis. I_z can have any integral value from $+I$ to $-I$. In a disoriented assembly of nuclei, each of these degenerate sub-states is equally populated. If we let $m = I_z$, then each sub-state has an energy $E(m)$; the populations of the sub-states are then given by a Boltzmann function

$$a_m = Ae^{-E(m)/kT}.$$

At temperatures where $\beta = \frac{E(m+1) - E(m)}{kT}$ is small, the populations of each of the sub-states will be almost the same, and the orientation of the nuclei will be random. If $\beta \approx 1$, the populations of the sub-states will be unequal, and there will be nuclear orientation.

Nuclear orientation is a general term which is used to describe a situation where the populations of the sublevels of the nucleus are unequal, and refers to nuclear polarization or alignment without distinguishing between them.

Nuclear polarization occurs when the populations, a_m, of the sublevels m are such that $a_m \neq a_{-m} \neq a_{m=0}$. In other words, the nuclei are arranged such that more of their spins are orientated parallel to the z-axis than are orientated antiparallel or perpendicular to it. Nuclear alignment occurs when more nuclear spins are orientated equally parallel and antiparallel to the z-axis than perpendicular to it.

In order to be able to discuss the orientation of nuclei in more detail, we need to define numerical parameters to describe the orientation. The simplest such parameter is called the polarisation f_1, defined by the equation

$$f_1 = \frac{\sum m a_m}{I \sum a_m} \qquad (1)$$

Since m can take integral values from $-I$ to $+I$, f_1 can take values from -1 to $+1$, and f_1 is zero for a disorientated assembly of nuclei. It can be seen that a situation can arise where the force tending to orientate the nuclei is such that $a_m = a_{-m}$, though few nuclei are orientated perpendicular to the z-axis, $\dot{a}$.

the state of nuclear alignment. In this case $f_1 = 0$. Hence we see that though f_1 is adequate to describe a state of nuclear polarization, it is useless for the description of nuclear alignment.

The parameter used to describe nuclear orientation in this case is

$$f_2 = \frac{(\sum a_m m^2 - I(I+1)/3)}{I^2 \sum a_m} \qquad (2)$$

We can see that f_2 is zero for a disorientated assembly, since the a_m are all equal in this case. The definitions of alignment and polarisation can now be given in terms of the f parameters. When f_1 is not zero, the nuclei are said to be polarized; when f_1 is zero but f_2 is not zero, the nuclei are said to be aligned. The parameters f_1 and f_2 are not always sufficient to describe the nuclear orientation, since the force which orientates the nuclei does not always have axial symmetry. These and other parameters f_k are discussed more fully in Chapter IV. In general, f_1 is the statistical mean value of $\frac{I_z}{I}$, and f_2 is the statistical mean value of $\frac{I_z^2 - I(I+1)/3}{I^2}$.

II.2 Methods of Producing Polarized and Aligned Nuclei.

The methods of producing orientated nuclei

fall into two main classes: thermal equilibrium (static) and dynamic methods. The method used in this research was of the thermal equilibrium class, so we shall briefly consider the dynamic methods first, and the thermal equilibrium methods at greater length later.

II.2 (a) Dynamic Methods of Nuclear Orientation

All dynamic methods of nuclear orientation require the saturation of certain resonances of a system of coupled nuclear and electron spins in a steady external magnetic field.

The Overhauser method[2], which is applicable to the nuclei of atoms of a metallic solid, relies on the existence of the electron spin resonance of electrons in the conduction band. The interaction between the electron spin magnetic moment β_e and the nuclear spin magnetic moment β_n, which leads to nuclear polarization, is the hyperfine interaction of an s-electron

$$H = -(8\pi/3)\beta_e . \beta_n \delta(r) \qquad (1$$

where $\delta(r)$ is a delta function of the relative co-ordinate of the electron and nucleus under consideration. Nuclear polarization is produced

when the metallic sample, in a steady magnetic field $\mathcal{H}_o$, is irradiated with a perpendicular microwave field $2\mathcal{H}_1 \cos\omega t$, of frequency ω such as to satisfy the electron spin resonance criterion $\hbar\omega = 2\beta_e \mathcal{H}_o$. (4)

In a steady magnetic field, the spin magnetic moments of the conduction electrons of a metal align themselves parallel to the direction of the field, and if the metal is subjected also to a perpendicular alternating magnetic field of frequency such as to satisfy (4), the time variation of the difference between the number of conduction electrons aligned parallel and antiparallel to $\mathcal{H}_o$ is given by

$$\frac{dD}{dt} = (D_o - D)/T_1 - \alpha D \qquad (5)$$

where the equilibrium value of D is

$D_o = 3N\beta_e \mathcal{H}_o / 2\varepsilon_f$ with N the number of electrons per cubic cm, and ε_f the Fermi energy.

The first term in equation (5) is due to relaxation processes which establish the equilibrium degree of spin magnetization with a characteristic relaxation time T_1. The second term is due to the alternating field, which tends to decrease the magnetisation since more transitions are induced from the spin state of greater population. α is given by

$\alpha = 4\pi\beta_e^2 \mathcal{H}_1^2 / \hbar w$, where w is the integrated width of the electron spin resonance line.

A steady state will be reached such that $\frac{dD}{dt} = 0$, when the alternating field has been turned on. A net rate of spin flips in one direction due to $\mathcal{H}_1$ will be balanced by a similar rate in the opposite direction due to relaxation interactions of which those due to equation (3) will produce nuclear polarization. From equation (5) the steady state value of D is

$$D = D_o /(1 + \alpha T_1). \tag{6}$$

Since, in the limit of complete saturation of the resonance, i.e. large $\mathcal{H}_1$, $D \to 0$, we define a parameter s which is zero for $\mathcal{H}_1 = 0$ and unity for large $\mathcal{H}_1$:

$$s = 1 - \frac{D}{D_o}. \tag{7}$$

From equation (6), we find $s = \alpha T_1 /(1 + \alpha T_1)$

The nuclear polarization produced is proportional to s, which is a function only of αT_1.

In particles of lithium small compared to the skin depth the electron spin resonance line was found to be Lorentzian in shape, and for a line of Lorentzian shape, $w = \gamma \hbar / T_2$, where T_2 is the transverse relaxation time. The fractional saturation s can then be written

$$s = \gamma_e^2 \mathcal{H}_1^2 T_1 T_2 (1 + \gamma_e^2 \mathcal{H}_1^2 T_1 T_2) \tag{8}$$

where $2\beta_e/\hbar$ has been replaced by γ_e, the gyromagnetic ratio of the electron spin. From equation (8) we see that appreciable saturation exists only if $\gamma_e^2 \mathcal{H}_1^2 T_1 T_2$ is of the order of unity, i.e. $\mathcal{H}_1$ must be of the order of 5 oersteds.

The hyperfine interaction (equation (3)) leads

to a time rate of change in the populations of the electronic magnetic energy levels $(dD/dt)' = (D_o - D)/T_1' + G(\Delta_o - \Delta)/T_n'$ (9)

T_1' and T_n' are the electronic and nuclear relaxation times due to this interaction, and Δ is the difference in the populations of adjacent nuclear magnetic states whose equilibrium value is

$$\Delta_o = \frac{N\hbar\gamma_n\mathcal{H}_o}{(2I+1)k\Theta}$$ where Θ is the temperature,

and $G = \frac{2}{3} I(I+1)(2I+1)$.

Since equation (3) conserves the total spin angular momentum,

$(dD/dt)' = G(d\Delta/dt)' = 0$ in the equilibrium state after the alternating field has been turned on. If interactions of the form (3) are the only source of nuclear relaxation, then

$$T_n/T_n' = 1.$$

The steady state value of Δ, with the use of equation (7), is then

$$\Delta = \Delta_o + SD_oT_n'/T_1'G.$$

$$= \frac{N\hbar\mathcal{H}_o}{(2I+1)k\Theta} (\gamma_n + S/\gamma_e)$$

since $T_1'/T_n' = 8I(I+1)\epsilon_f/9k\Theta$

We define the nuclear polarization f_1 as

$$f_1 = \left| \sum_{m=-I}^{I} m_e^{mu} \right| \Big/ \left(I \sum_{mu=-I}^{I} {}_e^{mu} \right) \quad (10)$$

where the ratio of the populations of adjacent nuclear magnetic states is $M_m / M_{m-1} = e^{\mu}$, and

$$\mu = (\gamma_n + s|\gamma_e|)\, \hbar \mathcal{H}_o / k\theta$$

This method of nuclear polarization gives, substituting the following values for $I = \frac{3}{2}$, $\mathcal{H}_o = 10^4$ oe, $s = 0.8$ and $\mu = 0.54$, and equation (10) gives 42p.c. for the nuclear polarization.

The effect just described can occur only in metals, since the electrons in the unfilled band of a metal can change energy by small amounts, of the order of kθ, by small changes in momentum or wave number. This freedom is necessary in order that spin may be conserved during the simultaneous spin flip of an electron and a nucleus.

In order to produce nuclear polarization by this method, microwaves in the 1 cm. range are appropriate, but considerable power may be necessary, depending on the electronic relaxation time at liquid helium temperatures.

The Jeffries method[3] relies on saturating a weak 'forbidden' electron spin resonance line when the r.f. and d.c. magnetic fields on the specimen are parallel. This forbidden transition is one which in the Overhauser effect is induced only by relaxation effects which involve nuclear spin flips. The essential

difference with Jeffries' method lies in the fact that an external r.f. field provides the force tending to orientate the nuclei, instead of relying on relaxation effects, as in the Overhauser method. A temperature of about $1^{\circ}K$ is desirable. This method produces nuclear alignment. Jeffries has shown that his method works for Co^{60} by measuring the anisotropy of gamma-ray emission[4] from Co^{60}.

II.2 (b). Static Methods of Nuclear Orientation.

Hyperfine interaction in the solid state may arise through either electric or magnetic interaction, and is described by the spin Hamiltonian:

$$\mathcal{H} = g_{\parallel}\beta_e H_z S_z + g_{\perp}\beta_e (H_x S_x + H_y S_y) + D(S_z^2 - S(S+1)/3) + A S_z I_z + B(S_x I_x + S_y I_y) + Q(I_z^2 - I(I+1)/3) - g_n \beta_n \underline{H}.\underline{I} \quad (1$$

where $\underline{S}$ is the effective electron spin,

and $\underline{I}$ is the nuclear spin.

The first two terms represent the splitting of the electronic levels by the external magnetic field $\underline{H}$. $g_{\parallel}$ and $g_{\perp}$ are the atomic g-factors parallel and perpendicular to the z-axis. β_e and β_n are the Bohr and nuclear magnetons, respectively.

The term in D represents the splitting of the electronic levels by the crystalline electric

field, and the A and B terms represent the hyperfine structure splitting due to the interaction between the nuclear magnetic moment and the unfilled electron shells. The Q term is the nuclear electric quadrupole splitting in the crystalline electric field gradient. The last term gives the direct coupling between the nuclear magnetic dipole moment and the external magnetic field.

i) The earliest suggestion of a method for producing orientated nuclei was that of Simon in 1939. A large externally applied magnetic field will interact with the magnetic moments of the nuclei to remove the degeneracy in the nuclear energy levels. The separation of the levels is then $E = g_n \beta_n H$. This is characterized by the term $g_n \beta_n \underline{H}.\underline{I}$ in the spin Hamiltonian above. The populations of the individual states will then be proportional to $a = \frac{e^{m\beta}}{\Sigma e^{m\beta}}$, where $\beta = g_n \beta_n H/kTI$. As has been already observed on page 7, in order to achieve appreciable polarization, β must be of the order of unity, which requires the use of a very high magnetic field and a very low temperature. For example, for $g_n \beta_n = \frac{1}{2}$, values of $\frac{H}{T}$ of the order of 5×10^7 are required, i.e. a field of 50,000oe at $0.01^{\circ}K$. This temperature can only be obtained by magnetic cooling, so that the

condition of $\beta \approx 1$ is hard to achieve experimentally because of difficulty in obtaining thermal contact between the specimen and the cooling salt and the difficulty of producing such a large magnetic field. In principle, this method is applicable to all substances, but in practice it is restricted to metals because only in metals are nuclear spin-lattice relaxation times short enough. So far, this method has only been used with indium[5] and copper[6], the latter being an experiment on cooling by adiabatic nuclear demagnetization.

ii) Gorter[7] and Rose[8] independently suggested another method of producing nuclear orientation. They pointed out that the partially filled 3d and 4f electron shells produce a magnetic field at the nucleus of a paramagnetic ion of the order of 10^6 oersteds. This ought to be sufficiently large to produce nuclear polarization in the temperature range $0.1^{\circ}K$ to $0.01^{\circ}K$. The magnetic moments of the ions they thought should be polarized by the application of a magnetic field of the order of a few hundred oersted. The nuclei would become polarized if the temperature ~~is~~ were low enough. 500 oersteds at $0.05^{\circ}K$ is sufficient to polarize the ionic moments, but whether or not the nuclei are polarized depends on

the relative values of hyperfine splitting and temperature. In some cases alignment rather than polarization results. This is due to the influence of other internal magnetic fields. The substance to be investigated must be paramagnetic. This method of nuclear orientation depends on the A, B, and g terms in the spin Hamiltonian. The substance must be cooled by adiabatic demagnetization, and this is achieved either by the use of a separate paramagnetic salt with which the substance is mixed, or by using the substance as its own cooling agent. In this case, the field used for adiabatic demagnetization is not reduced to zero, but to about 500 oersted, which has the disadvantage that the final temperature obtained is somewhat higher. Many successful experiments using this method have been reported. The most popular cooling agent is cerium magnesium nitrate. It is the most suitable since it can be cooled to about $0.003^{\circ}K$, and shows marked magnetic anisotropy. This has the advantage that after cooling the salt by adiabatic demagnetization, the polarising field can be applied along the direction of small susceptibility, thereby confining reheating of the salt to a minimum. Nuclear orientation has been detected in ions of the transition metals and of the rare earths, usually by replacing some of the cerium ions or the magnesium ions with ions associated with

the nuclei to be investigated.

iii) Bleaney[9] suggested that nuclear alignment ($f_1 = 0, f_2 \neq 0$) could be obtained in single crystals by the interaction of inhomogeneous crystalline electric fields with the magnetic ions. This is based on the fact that the different orientations of the nuclear moment relative to a crystal axis may have different energy. The energy difference occurs through the influence that the crystalline fields have on the electronic orbits and as a result on their magnetic moments. The strong electric field set up by the neighbouring ions defines an axis of quantization. This interaction is often strong enough to ensure that even at temperatures between $10^{\circ}K$ and $100^{\circ}K$ only the lowest energy levels of the electron orbital magnetic moments are occupied. If these electric fields have axial symmetry, alignment of the electronic magnetic moments will take place. Hyperfine structure coupling will then produce nuclear alignment at sufficiently low temperatures. The required temperature of about $0.01^{\circ}K$ is most conveniently reached by adiabatic demagnetization of the paramagnetic single crystal. In this method of

producing nuclear alignment, $\underline{H} = 0$, and only the D, A, and B terms contribute to the spin Hamiltonian.

iv) The method suggested by Pound[10] uses the hyperfine structure associated with the nuclear quadrupole moment. This effect is produced by the interaction between the nuclear quadrupole moment and the electric field gradient at the nucleus produced by the surrounding electrons. In general, such gradients must be at least of the order of 10^5 e.s.u. to give a hyperfine structure splitting of the required magnitude, and they can be produced only by an asymmetrical distribution of the electron cloud immediately surrounding the nucleus. This distribution can be set up in homopolar bonds, and if these bonds have a parallel orientation for all similar nuclei, nuclear orientation will set in at sufficiently low temperatures. The axes of the electric field gradient tensor are related to the crystal axes, so a single crystal is needed. So far, only two successful experiments with this method have been reported (Dabbs[11], Johnson[12]).

v) In a ferro-magnetic substance, the electron moments, and hence the fields at the nuclei, are orientated parallel to certain directions in the crystal.

At sufficiently low temperatures, the nuclei become orientated in those directions. If a single crystal in zero magnetic field is used, an alignment ($f_1 = 0, f_2 \neq 0$) is produced, but a polarization ($f_1 \neq 0, f_2 = 0$) can be produced by applying an external magnetic field. Nuclear orientation in a ferromagnetic substance will be discussed extensively in the next chapter.

CHAPTER III

The Internal Magnetic Field in Ferromagnetic Metals

Orientation of the nuclei of ferromagnetic metals has been achieved through the interaction of the internal magnetic field in a ferromagnetic metal with the magnetic moment of its nuclei. Grace, Johnson, Scurlock and Taylor[13] have observed the nuclear orientation of radioactive Co^{60} nuclei in cobalt metal by the anisotropy of gamma-ray emission. Johnson and Scurlock[14] have repeated these measurements on alloys of cobalt in nickel, and cobalt in iron. On the other hand, Heer and Erickson[15] have measured the nuclear contribution to the specific heat of cobalt metal, and Kurti, Arp and Peterson[16] have measured the nuclear specific heat of pure cobalt and of a Co-Ni alloy, and so estimated the hyperfine contribution to the effective field on the nuclei.

III.1 Marshall's Estimate of the Internal Field in a Ferromagnetic.

The first attempt at a theoretical descript-

ion of nuclear orientation in ferromagnetics was made by Marshall[17] in 1958. He considered that the orientation of nuclei in ferromagnetics may be regarded as due to an effective magnetic field H given by

$$H = H_1 + H_c + H_a \,, \tag{12}$$

where H_1 is the local field at the nucleus, H_c is the internal field due to contact interaction between the conduction electrons and the nucleus, and H_a is the field due to the contact interaction between the nucleus and its orbital electrons.

This internal magnetic field gives in the case of radioactive Co^{60} an anisotropy in gamma-ray emission of

$$\varepsilon = \frac{W(\pi/2) - W(0)}{W(\pi/2)} \approx \frac{39(g_n \beta_n H)^2}{14(kT)^2} \,, \tag{13}$$

where W (θ) is the intensity of gamma-ray emission at an angle θ to the axis of orientation.

The local magnetic field at the nucleus is given by

$$H_1 = H_e - DM + \frac{4\pi M}{3} + H' \,. \tag{14}$$

H_e is the external field, -DM is the demagnetising field, and $\frac{4\pi M}{3}$ is the Lorentz field, and H' is the small remnant of the Lorentz field which exists only for non-cubic symmetry. H' is usually only about $1/10^3$ of the

normal Lorentz field, so it can be neglected.

The effective field H_c, which is due to contact interaction with the conduction electrons, can be considered as the sum of two parts. One part is that due to the conduction electron polarization p, and is proportional to $-(8\pi/3)\mu|\psi(0)|^2 n.p$, where μ is the Bohr magneton. $|\psi(0)|^2$ is the average probability density of a conduction electron evaluated at a lattice point, n is the number of conduction electrons per atom, and p is their polarization. The other part is that due to the mixing of the conduction electron band into the band below. This mixing can be expected to be fairly large (several percent.), but cannot readily be estimated. The sum of these two parts give an effective field

$$H_c = -(8\pi/3)\mu|\psi(0)|^2 \; n.\tilde{p} \qquad (15)$$

where $\tilde{p} = (p + 2\bar{S}a^2/n)$ is the effective polarization. $\bar{S}$ is the mean spin per atom, and a^2 is an average of the amount of s-electron wave function mixed into the band below. Both p and $\bar{S}$ are negative because the g-value for an electron is negative, so H_c is a positive field.

Marshall substitutes $|\psi(0)|^2 = \zeta|\psi(0)|^2_A$, where ζ is a correction factor, and $|\psi(0)|^2_A$ is the free atom value. He estimates p in the following

manner. The interaction between a conduction electron and an atom is written as $-2J\underline{S}.\underline{s}$, where $\underline{s}$ is the spin of a conduction electron spin and $\underline{S}$ is the atom spin. This interaction is equivalent to a magnetic field acting on the conduction electron of magnitude $J\bar{S}/\mu$. The Pauli paramagnetic susceptibility of a free electron gas is $3n\mu^2/2E_f$, where E_f is the Fermi energy. From these two quantities, $p = 3J\bar{S}/2E_f$, and hence H_c can be found.

For the next term, H_a, in the expression (12) for the effective magnetic field, Marshall uses the Van Vleck model of ferromagnetism, supposing that correlation effects are important. In order to treat this, he considers that on any particular atom of cobalt there will always be an integral number of 3d electrons coupled together according to Hund's Rule. He then assumes arbitrarily that 70 p.c. of the atoms are in the $3d^8\ ^3F$ state, and that 30 p.c. are in the $3d^9\ ^2D$ state. This then gives the required magnetic moment of 1.7μ per atom. He then uses this model to estimate the fields acting on the nucleus of an atom with a $(3d)^9$ and with a $(3d)^8$ configuration, and then averages the fields with the appropriate probabilities. The field for each electron configuration can be obtained from the spin Hamiltonian (11). The appropriate terms

are $\mathcal{H} = AS_zI_z + B(S_xI_x + S_yI_y)$. In a ferromagnetic (16
the electron spins are aligned by strong exchange interactions, which means that $S_x = S_y = 0$, and S_z can be replaced by S, the spin of the atom configuration. Marshall then derives the expression

$$H_a = - A\bar{S}/g\mu. \qquad (17$$

The coefficient A contains terms which take into account contact interaction with the inner 3s and 2s electrons, dipole-dipole interaction between the nuclear and electron spins, and the magnetic interaction between the nucleus and the unquenched part of the orbital magnetic moment. We call the contribution of these terms to the effective field H_{a_1}, H_{a_2}, H_{a_3}. The contact interaction with the inner s-electrons arises because these electrons see slightly different potentials depending on whether they are spin parallel or antiparallel to the spin of the 3d electrons. There is therefore a difference between their amplitudes at the nucleus which is appreciable because their probability densities at the nucleus are very large. This interaction has been experimentally observed to be constant for paramagnetic ions and neutral atoms, and for the effective field due to this interaction, ~~and~~ Marshall gives a value for $H_{a_1} = -12.8 \times 10^4$ oersted, which he assumes to hold also for the metal. The remain-

ing terms of the coefficient A depend on the symmetry of the crystal, and are discussed in the next paragraph.

Marshall has discussed cubic alloys of cobalt and pure hexagonal cobalt. He concluded that for cubic symmetry of the crystal for very high or very low concentration cobalt alloys, the dipole-dipole interaction between electron and nuclear spins was zero, but that this was not so for alloys of intermediate concentrations. The contribution of the dipole-dipole interaction to the effective field is denoted by H_{a_2}. One can hope that for alloys such as Co-Ni whose constituents are close together in the periodic table, the effect would be small even for a 50 p.c. concentration alloy, i.e. $H_{a_2} \approx 0$. Marshall then calculated the effect of spin-orbit coupling for a low concentration Co-Ni cubic alloy using the spin-orbit coupling parameters for Co and Ni and obtained a value for the contribution to the effective field by the spin-orbit coupling in cubic symmetry of $H_{a_3} = 5.4 \times 10^4$ oersted.

Marshall then calculated values for H_{a_2} and H_{a_3} for a hexagonal crystalline field potential and obtained the values

$$H_{a_2} = 8.1 \times 10^4 \text{ oersted.}$$

$$H_{a_3} = 8.3 \times 10^4 \text{ oersted.}$$

These gave a value for the effective magnetic field acting on Co nuclei in a cobalt single crystal of

$$H = \left[1.45\zeta\,(|p| + 2.43a^2) \times 10^6 + 3.6 \times 10^4\right] \text{ oersted} \quad (18)$$

For the effective field on Co^{60} nuclei in a low concentration alloy of cobalt in nickel, Marshall finds

$$H = \left[1.45\zeta\,(|p| + 2.43a^2) \times 10^6 - 7.4 \times 10^4\right] \text{ oersted.} \quad (19)$$

By comparing (18) with experimental values quoted in references (13), (15), and (16), and setting $\zeta = 1$, Marshall finds $a^2 = 0.032$. That is, he finds that the mainly 3d wave function contains about 3 p.c. of a 4s wave function. Incorporating this result into equation (19), Marshall shows that the effective magnetic field in a cubic cobalt alloy is 8.7×10^4 oersted, which should lead to an anisotropy in gamma-ray emission which is about 5 times smaller in a low concentration alloy of Co in Ni than is observed for hexagonal cobalt. This appears to be corroborated by comparison with work in references (13) and (14).

III.2 The Internal Field in a Ferromagnetic according to Watson and Freeman

Watson and Freeman[18] adopted a different

approach to determing the origin of effective fields in magnetic materials.

They first considered the effective fields on the nuclei of ions and free atoms, then extended their discussion to magnetic solids. Their investigations were based on accurate spin-polarized Hartree-Fock calculations for free transition-metal ions and neutral atoms, on calculations for ions in a crystalline field of the kind occurring in salts, and on calculations in which the wave functions and hence spin densities were modified so as to conform to energy band and neutron magnetic scattering measurements on the ferromagnetic metals. They showed that for transition metals the dominant contribution was the field arising from the exchange polarization of the core electrons by the spin density of the unpaired 3d electrons. They found that H_e was very sensitive to small variations in various parameters; e.g. crystal environments, expansion or contraction of the 3d spin density, and this led to an ambiguity in the values for H_e, but they reported a consistent set of calculations which agreed reasonably well with experimental data. They found also that in such ions as Fe^{++} and Co^{++}, large positive contributions from the unquenched orbital angular momentum competed with the core polar-

ization term, and used this concept to explain Mossbauer, NMR, and paramagnetic resonance measurements of the internal fields in ions. They pointed out that in rare earth ions orbital angular momentum contributions will predominate over the core polarization term except in ions with half-closed shells such as Eu^{++} and Gd^{3+}.

Watson and Freeman investigated the magnetic properties of solids by considering the contribution made by 'paired' electrons using the spin polarization mechanism in the Hartree-Fock formalism. They showed that the values of H_e obtained from consideration of the paired spin density of the core s-electrons agreed with experiment, and so confirmed that the spin polarization mechanism had an important effect in the effective magnetic field on the nucleus. The calculations also showed that the contribution of exchange polarization to an ion's magnetic interaction with neighbouring ions, and, in the solid state, with its own conduction electrons, was important in the explanation of the magnetic behaviour of rare earth ions. It was found that rare earth ions may seem to their neighbours to have spins antiparallel to the 4f spin direction, and that the negative field observed in some ferromagnetics[19] was due to the polarization of the core s-electrons.

In their Hartree-Fock calculations, Watson and Freeman relaxed the restriction that electrons in the same shell of the atom with different spin have the same radial wave functions. This restriction is inappropriate because electron systems with spin up have different exchange interactions from those with spin down. If this restriction is relaxed in the Hartree-Fock calculations, there is a non-zero spin density $|\psi_{\uparrow}(0)|^2 - |\psi_{\downarrow}(0)|^2$ for the closed s-electron shells. This leads to a non-vanishing Fermi contact interaction term for 'paired' s-electron shells, giving a 'polarizibility': $\chi = \frac{4\pi}{S} \sum_{s\ \text{shells}} \{\rho_{\uparrow}(0) - \rho_{\downarrow}(0)\}$ (20)

where S denotes the number of unpaired electrons. If χ is given in atomic units, H_o is found by using the conversion factor 1 a.u. = 4.21×10^4 oersted.

Abragam, Horowitz and Pryce have reported values of χ obtained from experimental data on divalent iron series ions which give a roughly constant value of $\chi = -3$ a.u., giving $\frac{H_o}{S} = -125$ koersted, where H_o is the contact term in the effective magnetic field. This field is antiparallel to the net spin of the ion, as is indicated by the negative sign. Watson and Freeman have calculated values of χ for each s-shell of divalent ions of the iron series, and conclude that

the effective fields are made up of competing terms each many times larger. They suggest that this is because the positive spin electrons of the 1s and 2s shells are attracted outwards, leaving a negative spin density in the region of the nucleus, but that the 3s shell overlaps the 3d shell, giving a small positive spin density in the vicinity of the nucleus. Watson and Freeman suggest that the competition between positive and negative terms in χ implies that the terms are sensitive to the ion's environment. By comparing their calculations for free ions and calculations for Ni^{++} in a cubic field they show that the individual terms of χ are increased, but the total χ has decreased in a cubic field. They also carried out investigations into the Mn^{++} ion which showed that H_c was sensitive to greater variational freedom for s wave functions near the nucleus and to small changes in the behaviour of all the orbitals.

Abragam, Horowitz and Pryce have also obtained, from experimental data, terms for the $3d^n4s^2$ states of the free neutral iron series atoms. They found that the values of χ are not constant at -3 a.u. as they had observed for the divalent ions, but fluctuate between 0 and -5 a.u. Watson and Freeman have done spin polarised Hartree-Fock calculations on these neutral atoms. Their computed values of χ do not

show the fluctuations exhibited by the experimental values, but tend to increase with increasing nuclear charge. They indicate that comparison of the neutral atom and divalent ion cases suggests that the experimentally observed fluctuations in χ are due to the 4s shells in which configuration interaction is known to be important. Configuration mixing, i.e. replacing the 4s orbital by other orbitals would reduce the 4s shell contribution, which, the greater the amount of configuration mixing, would give a value of χ closer to that obtained from consideration of the core electrons alone. This mixing of excited configurations with a ground configuration will produce a radial expansion in the spin densities of the atoms, which, in turn, will cause an increase in the values of χ due to the core electrons, because the spin densities are the source of spin polarization. Watson and Freeman also consider the individual 4s electron contributions to H_c, which indicate the behaviour of the 4s conduction bands in the metals. There is generally slightly less than one electron per atom in the conduction band in the metals, most of the contribution to the band being in the form of paired orbitals. They find that the individual 4s contributions parallel and antiparallel to the 3d spin direction both increase

with increase in nuclear charge, but the resultant H_c does not.

The internal effective fields on the nuclei of ferromagnetic solids have been determined by measurements of the hyperfine contribution to the specific heats of the metals, measurements of the Mossbauer effect, NMR, and nuclear alignment in a number of different hosts, including rare earth iron garnets, ferromagnetic oxides, and pure ferromagnetic metals and alloys. Mossbauer effect measurements by Hanna, et al.[19] have shown that the effective field at the nucleus in Fe^{57} is negative. The dominant contribution to H_e must therefore come from core polarization, since the other terms are presumed to be positive.

In order to estimate the positive contribution to H_e, Watson and Freeman considered the density of states curve for metallic iron. This curve shows that there is 0.4 electron in the 4s band for energies below the 3d band. Considering the non-magnetic state of the metal, if the energy levels are filled up until there are eight electrons per atom in the energy levels, one finds one electron in the 4s band, which means that there is 0.6 electron per atom in the region overlapping the 3d band. In order to

obtain the magnetic state of iron, one depopulates the electron states of one spin and populates the states of the other spin until there are 2.2 unpaired electrons per atom.

If we assume that the exchange interactions causing the net spin are of the same sign and magnitude for both the 4s and 3d shells, although there is reason to believe that the 4s exchange parameter is smaller, we can consider that there are about 0.05 to 0.1 unpaired electrons per atom in the 4s band. Considering that there are 0.8 paired and 0.05 unpaired electrons in the 4s band, Watson and Freeman calculated their contribution to the effective field to be 105 kOersted and 90 kOersted, respectively, from individual 4s electron contributions to H_e which they had calculated for the free iron atom.

The contributions of the core electrons to the effective field can be estimated by using the value of χ observed experimentally of -3 a.u. If we assume that the 2.2 unpaired electron spins are entirely in the 3d band, we obtain a contact term for the effective field of -275 kOersted, which is itself too small to account for the experimentally observed value of -333 kOe. [redacted]. If we take the value of χ computed by Watson and Freeman for the 3d orbital of the neutral Fe atom, the contact term of H_e becomes -320 kOersted,

which is still too small to overcome the positive terms to give the experimental value of H_e. The use of a value of χ calculated from the 3d orbital of the neutral atom or the divalent ion for the effective field in the bulk metal must therefore be inappropriate.

Watson and Freeman made full spin-polarized Hartree-Fock calculations for the Fe atom in both the $3d^6\ 4s^2$ and $3d^8$ configurations, but did not obtain a large enough increase in the negative value of the contact part of H_e to cancel the positive contribution from the 4s band. They then investigated the value of H_c as a function of the 3d-shell spin density by plotting H_c against the position of the maximum of the 3d orbital spin density for Fe in the $3d^8$ state. This showed that expansion or contraction of the 3d-shell spin density will give a value of H_c more than sufficiently large to overcome the positive 4s band contributions to give agreement with the experimental value of H_e. Such changes in the distribution of the 3d-shell spin density can be made as to give a value for H_c of -500 kOersted and remain compatible with neutron magnetic form factor measurements, but this is not necessarily a justification of these changes.

It has been suggested that apart from the positive contribution of H_e from the 4s-shell due to mixing of the 4s and 3d-shells there is a negative

antiferromagnetic contribution arising from covalent mixing of s and d wave functions. This could have four consequences. The positive and negative contributions could cancel each other. In order to preserve the net spin per atom, there would be an increase in the polarization of both the core and the paired 4s electrons. Unpaired 4s electrons would in any case contribute to the polarization of the core electrons, an effect not hitherto considered in our estimates of H_e for divalent ions and free atoms. If there is an anti-parallel net spin of the 4s electrons, the combined spin density per atom will appear contracted relative to the 3d spin density. Since the combined spin density of the atom is what is measured experimentally by neutron magnetic form factor measurements, the 3d spin density would appear to be more radially expanded than has been assumed in the estimate of H_e. This could have the effect of making H_e more negative than previously estimated, bringing it into closer agreement with the experimental value. Mossbauer effect measurements on the internal field at an Fe^{57} nucleus as an impurity in CoPd[20], and in Co and Ni[21], and in Cu-Ni alloy are in good agreement and indicate that the field at the iron nucleus depends mainly on its own electrons and only to a small degree on the

magnetization of its host. One can almost estimate H_e by calculating H_c and ignoring the conduction electrons, but although this works reasonably well for metallic iron and cobalt, it breaks down completely for metallic nickel.

The effective field has also been measured at the nuclei of non-magnetic atoms which are impurities in, or are alloyed with ferromagnetics. The Mossbauer effect has been used for studying Sn as an impurity in iron, cobalt, and nickel[22], and in alloy in manganese[22], Samoilov, et al.[24], have measured the internal field at the nuclei of gold, antimony, and indium as impurities in iron by a method of nuclear alignment. Possible explanations of the observed fields are: the admixture of the 3d spin density of the ferromagnetic atom into the closed shells of the non-magnetic atom produces an unpairing of its electron wave functions resulting in a contact effective field; the core of the non-magnetic atom is polarized by the exchange field of the magnetic shell of the ferromagnetic atom, producing unpaired s-electrons which create an effective field at the nucleus of the non-magnetic atom by the Fermi contact term; the conduction electrons are polarized and produce an effective field at the nucleus through the Fermi contact term. This/

This polarization can take place through the exchange polarization which is important for rare earth elements. For internal fields at rare earth nuclei, it appears that the dominant contribution for atoms with a half-closed shell such as gadolinium and europium arises in the exchange polarization of the core electrons by the unfilled 4f-shell electrons, whereas for the other rare earths, the main contribution arises in the orbital angular momentum of the 4f electrons which is almost completely unquenched.

The rare earth series of elements are unusual in having an unfilled magnetic 4f shell deep in the interior of the atom. Since the 4f electrons are well into the interior of the atom, they are comparatively unaffected by the environment of the atom. In the metal the three valence electrons of the atom form the conduction band. It is therefore convenient to treat the atoms in the solid state as free trivalent ions, since the 4f shell is little affected by its environment.

Freeman and Watson [25] have done approximate, non-relativistic Hartree-Fock calculations for the wave functions of the 4f electrons, and from these they investigated spin-orbit coupling, and hyperfine fields from exchange polarization. They pointed out that the main source of hyperfine field for Gd^{3+} and Eu^{2+} ions is the contact interaction from the exchange

polarization of the core electrons by the spin of the 4f electrons. In systems with a net spin, s-electrons in a given closed shell with differing spin experience different radial wave functions and a non-zero spin density at the nucleus. This effect is called exchange polarization.

Watson and Freeman[26] have done a spin-polarized Hartree-Fock calculation of 4f and core electron interaction for Gd^{3+}, but consider it inadequate because the calculations are non-relativistic and give a poor description of electron behaviour near the nucleus. Freeman and Watson[25], however, have estimated spin-polarization effects from experimental hyperfine data for S-state ions, such as Eu^{2+} and Gd^{3+}, and obtain a value of -335 kOersted for the hyperfine field in Eu^{2+}. From observations on iron group ^{6}S-state ions, they consider that the field at the Gd^{3+} nucleus will be rather smaller, and that the hyperfine field should be smaller the more covalent the environment of the rare earth ions. From these estimates they propose that the core polarization term for trivalent ions should be $(-90\ \text{kOe}) \times (g_J - 1)J$, where g_J is the Landé g-factor. From this we estimate the internal field at the Gd^{3+} nucleus to be -315 kOersted.

Watson and Freeman [26] have considered the exchange polarization and the magnetic interactions

of rare earth ions. They suggest that the rare earth ions have a negative 'paired' electron spin density in their outer layers. Since the unfilled 4f shell electrons are far into the interior of the ions, the negative outer spin distribution can have an important effect on the magnetic interactions of rare earth ions. It may even be that these ions will appear to their neighbours to have a negative spin. In a consideration of core electron spin density, calculated by Hartree-Fock methods, Watson and Freeman showed qualitatively that there were two regions of negative spin density. One, near the nucleus, produces the negative effective fields of the type already seen in iron; the other is important in interactions with neighbouring atoms. Nuclear magnetic studies in magnetic crystals of rare earth compounds have revealed large internal magnetic fields at the nuclei of normally diamagnetic ions. For example, NMR measurements have shown the presence of large internal magnetic fields at the nuclei of normally diamagnetic ions such as F^-. These are thought to be caused by unpairing in the fluoride ion orbitals. The unpairing is thought to originate either by a mixture of covalent bonding into a purely ionic configuration, or by an unpairing arising from a distortion due to a difference between the interaction of fluorine orbitals

of the same spin as the spin of the unfilled shell of the magnetic cation with that unfilled shell, and the interaction between orbitals of the fluorine atom of opposite spin and the unfilled magnetic shell of the cation.

Watson and Freeman, considering the rare earth salt GdF_3, investigated the possible effect of the negative spin density in the outer region of the Gd^{3+} ion. They suggested that the paired 5s and 5p orbitals of the Gd^{3+} ion will overlap the fluoride orbitals in a different way, causing a difference in their interactions which will result in a hyperfine interaction with the fluorine nucleus. They then calculated the overlap integrals between the outer orbitals of the Gd^{3+} ion and the 2s orbitals of the F^- ion at the nearest neighbour distance of 4.4 a.u. From their result they found that the effective field at the F^- nucleus due to the 5s and 5p orbitals of the Gd^{3+} ion was -7200 oersted, whereas the effective field due to the 4f overlap alone was +700 oersted. Considering work by Jaccarino, et al.,[27] on the NMR of Al^{27} in rare earth intermetallic compounds, they interpreted the negative Knight shift observed as being in part due to the outer region of negative spins, but mainly due to the negative spin density of the conduction 6s electrons of the gadolinium which would be the greater because of their

greater overlap with the aluminium electron wave functions.

CHAPTER IV

The Angular Distribution of Gamma Radiation from Oriented Nuclei

Tolhoek and Cox[28] gave a number of explicit expressions for the angular distribution of γ-radiation from oriented nuclei and from these one can readily calculate the angular distribution of the 411 keV γ-radiation of Au^{198} nuclei. An account of the derivation of these expressions will now be given.

We assume that the nuclei have an axis z of rotational symmetry, an angular momentum quantum number I, and a magnetic quantum number m, which is the component of I along z. Let a_m be the populations of the various energy levels defined by I and m. We call $J^{m_i}_{I_i}(\theta)$ the angular distribution of radiation from a nucleus in the state I_i, m_i; $W(\theta)$ is the angular distribution of the observed radiation, where θ is the angle between the direction of emission of the observed radiation and z.

Then $W(\theta)$ is given by $W(\theta) = \sum_m a_m J^{m_i}_{I_i}(\theta)$ (21)

When the angular distribution of radiation with angular momentum quantum number L and magnetic quantum number M is denoted by $F_L^M(\theta)$, we obtain

$$J_{I_i}^{M_i}(\theta) = \sum_M G_{m_i, m_i - M}^{I_i, LI_f} F_L^M(\theta) \qquad (22)$$

where the $G_{m_i, m_i - M}^{I_i LI_f}$ are the squares of the transformation coefficients for the addition of angular momenta.

Usually the transition under consideration will be preceded by a β or γ transition, $(I_o, m_o) \rightarrow (I_i, m_i)$. When this occurs the a_{m_o} give the original orientation of the nuclei, and we need to calculate the populations a_m of the states m_i so as to obtain $W(\theta)$ for the radiation emitted by the nuclei of spin $\underline{I}_i$. If $P(m_o, m_i)$ gives the relative transition probability for the transition $(I_o, m_o) \rightarrow (I_i, m_i)$, then

$$a_m = \sum_{m_o} a_{m_o} P(m_o, m_i) \qquad (23)$$

where $\sum_{m_i} P(m_o, m_i) = 1$.

IV.1 Description of the Orientation of Nuclei in Terms of the Parameters f_k.

In general, the state of orientation of an ensemble of nuclei, all with angular momentum $\underline{I}$, cannot be described by a single wave function. It is there-

fore necessary to use a density matrix ρ with $(2I+1)^2$ matrix elements. Now ρ is Hermitian and is normalized to

$$\Sigma_m \rho_{mm} = 1, \tag{24}$$

and with each state

$$\psi = \Sigma_m c_m \gamma_m \tag{25}$$

we associate a matrix

$$(\rho_\psi)_{mm'} = c_m c_m^* \tag{26}$$

The probability of finding a system described by the density matrix in the state ψ is then given by

$$W = \mathrm{Tr}(\rho\rho_\psi) \quad (\mathrm{Tr} \text{ is the trace of the matrix}) \tag{27}$$

If the axis $\underline{z}$ of rotational symmetry exists and is chosen as the axis of quantization, ρ is a diagonal matrix, and the probability of a state ψ_m is

$$a_m = \mathrm{Tr}(\rho\rho_{\psi_m}) = \rho_{mm} \tag{28}$$

ρ is determined by $2I+1$ numbers a_m, of which only $2I$ are independent since $\Sigma_m a_m = 1$. In fact, the a_m are always used in combinations of the form $\Sigma_m m^k a_m$, and we therefore define $2I$ independent combinations of this form, which are equivalent to the set of $2I$ numbers a_m.

$$\text{Let } f_k = \sum_{\nu=0}^{k} a_{k,\nu} \Sigma_m m^\nu a_m \tag{29a}$$

$$\text{and } f_k = 0, \text{ if } a_m = \sum_{p=0}^{k-1} A_p m^p \tag{29b}$$

$$\text{and } \alpha_{k,k} = 1^{-k} \tag{29c}$$

If we take $a_m = m^p$ $(p=0,\ldots..k-1)$, there are k linearly independent relations for the coefficients $\alpha_{k,0} \ldots \alpha_{k,k}$.

The condition (29c) is chosen so that the f_k remain finite as $I \to \infty$; thus the f_k are completely determined by the conditions (29). For an arbitrary orientation given by the a_m, a_m is given by the polynomial of degree 2I:

$$a_m = \sum_{p=0}^{2I} A_p m^p \tag{30}$$

Hence from the equations (29) and (30) we obtain $f_k = 0$, for $k \geq 2I+1$.

IV.2 The Values of the Parameters f_k for k = 0,1,2,3 and 4.

$\underline{k = 0}$, $\quad f_o = \alpha_{o,o} \sum_m m^o a_m = I^{-o} \sum_m a_m = 1$

$\underline{k = 1}$, $\quad f_1 = \sum_{\nu=0}^{1} \alpha_{1,\nu} \sum_{m=-I}^{I} m^\nu a_m = \alpha_{1,0} + \alpha_{1,1} \sum_m a_m$

Now, from (29b) $f_1 = 0$ if a_m is a constant,

hence $\alpha_{1,o} = 0$,

so $\quad f_1 = I^{-1} \sum_m m a_m \tag{31a}$

$\underline{k = 2}$, $\quad f_2 = \sum_{\nu=0}^{2} \alpha_{2,\nu} \sum_m m^\nu a_m$

$$= \alpha_{2,o} \sum_m a_m + \alpha_{2,1} \sum_m m a_m + \alpha_{2,2} \sum_m m^2 a_m$$

Now if $\quad a_m = \sum_{p=0}^{1} A_p m^p = A_o + A_1 m$, $f_2 = 0$ from (29b)

Then $\sum_{\nu=0}^{2} \alpha_{2\nu} \Sigma_m m^{\nu} (A_o + A_1 m) = 0$

i.e. $\sum_{\nu=0}^{2} \alpha_{2\nu} \Sigma_m m^{\nu} = 0$, and $\sum_{\nu=0}^{2} \alpha_{2\nu} \Sigma_m m^{\nu+1} = 0$

Hence $\begin{cases} \alpha_{2,o} \Sigma_m 1 + \alpha_{2,1} \Sigma_m m + \alpha_{2,2} \Sigma_m m^2 = 0 \\ \alpha_{2,o} \Sigma_m m + \alpha_{2,1} \Sigma_m m^2 + \alpha_{2,2} \Sigma_m m^3 = 0 \end{cases}$

i.e. $\begin{cases} \alpha_{2,o}(2I+1) + I^{-2} \Sigma_m m^2 = 0 \\ \alpha_{2,1} \Sigma_m m^2 = 0 \end{cases}$

Hence $\alpha_{2,1} = 0$, and $\alpha_{2,o} = - \dfrac{\Sigma_m m^2}{I^2(2I+1)} = - \dfrac{I+1}{3I}$

Then $f_2 = I^{-2} \left(\Sigma_m m^2 a_m - \dfrac{I(I+1)}{3} \right)$ (31b)

and $\Sigma_m m^2 a_m$ is the average value of I_z^2.

For random orientation, a_m is independent of m, hence

$f_2 = I^{-2} \left(\sum_{m=-I}^{I} m^2 - \dfrac{I(I+1)}{3} \right) a_m = I^{-2} \left(\dfrac{1}{2I+1} \cdot \dfrac{I(I+1)(2I+1)}{3} - \dfrac{I(I+1)}{3} \right) = 0$

$f_2 > 0$ corresponds to nuclear alignment parallel to $\underline{z}$;

$f_2 < 0$ corresponds to nuclear alignment perpendicular to $\underline{z}$.

$\underline{k = 3}$,

$f_3 = \sum_{\nu=0}^{3} \alpha_{3,\nu} \Sigma_m m^{\nu} a_m = \alpha_{3,o} + \alpha_{3,1} \Sigma_m m a_m + \alpha_{3,2} \Sigma_m m^2 a_m + \alpha_{3,3} \Sigma_m m^3$

The condition $f_3 = 0$, for $a_m = \sum_{p=0}^{2} A_p m^p$, gives the following

conditions,

$$\sum_{\gamma=0}^{3} \alpha_{3,\gamma} \sum_m m^{\gamma} = 0, \quad \sum_{\gamma=0}^{3} \alpha_{3,\gamma} \sum_m m^{\gamma+1} = 0, \text{ and } \sum_{\gamma=0}^{3} \alpha_{3,\gamma} \sum_m m^{\gamma+2} = 0,$$

which gives the following simultaneous equations:

$$\begin{cases} \alpha_{3,0}(2I+1) + \alpha_{3,2} \sum_m m^2 = 0 \\ \alpha_{3,1} \sum_m m^2 + I^{-3} \sum_m m^4 = 0 \\ \alpha_{3,0} \sum_m m^2 + \alpha_{3,2} \sum_m m^4 = 0 \end{cases}$$

The first and third equations of the system give the results

$\alpha_{3,0} = \alpha_{3,2} = 0$, and we obtain from the second:

$$\alpha_{3,1} = -I^{-3} \frac{\sum_m m^4}{\sum_m m^2} = -\frac{3I^2+3I-1}{5I^3}$$

whence $$f_3 = I^{-3} \left(\sum_{-I}^{I} m^3 a_m - \frac{3I^2+3I-1}{5} \sum_{-I}^{I} m a_m \right) \qquad (31c)$$

k = 4,

$$f_4 = \sum_{\gamma=0}^{4} \alpha_{4,\gamma} \sum_m m^{\gamma} a_m = \alpha_{4,0} + \alpha_{4,1} \sum_m m a_m + \alpha_{4,2} \sum_m m^2 a_m + \alpha_{4,3} \sum_m m^3 a_m + \alpha_{4,4} \sum_m m^4 a_m$$

The condition that $f_4 = 0$ for $a_m = \sum_{p=0}^{3} A_p n^p$ gives the following equations $\sum_{\gamma=0}^{4} \alpha_{4,\gamma} \sum_m m^{\gamma} = 0$ $\sum_{\gamma=0}^{4} \alpha_{4,\gamma} \sum_m m^{\gamma+1} = 0$

$$\sum_{\gamma=0}^{4} \alpha_{4,\gamma} \sum_m m^{\gamma+2} = 0 \quad \sum_{\gamma=0}^{4} \alpha_{4,\gamma} \sum_m m^{\gamma+3} = 0$$

which gives the following simultaneous equations:

$$\begin{cases} \alpha_{4,0}(2I+1) + \alpha_{4,2}\sum_m m^2 + I^{-4}\sum_m m^4 = 0 \\ \alpha_{4,1}\sum_m m^2 + \alpha_{4,3}\sum_m m^4 = 0 \\ \alpha_{4,0}\sum_m m^2 + \alpha_{4,2}\sum_m m^4 + I^{-4}\sum_m m^6 = 0 \\ \alpha_{4,1}\sum_m m^4 + \alpha_{4,3}\sum_m m^6 = 0 \end{cases}$$

Equations 2 and 4 of this system give $\alpha_{4,1} = \alpha_{4,3} = 0$. Solution of the equations 1 and 3 gives:

$$\alpha_{4,0} = \frac{3}{35} I^{-3}(I-1)(I+1)(I+2)$$

$$\alpha_{4,2} = -\frac{I^{-4}(6I^2 + 6I - 5)}{7}$$

Hence, for f_4 we have

$$f_4 = I^{-4}\left(\sum_{-I}^{I} m^4 a - \frac{6I^2+6I-5}{7}\sum_{-I}^{I} m^2 a + \frac{3}{35} I(I-1)(I+1)(I+2)\right) \quad (31$$

For nuclear orientation of Au^{198} nuclei, the nuclear spin I = 2 for the 411 keV level, so we need consider only the parameters f_1, f_2, f_3, and f_4, because $f_k = 0$ for $k \geq 2I+1$.

For totally oriented nuclei, $a_m = \delta_{mI}$, and we obtain:

$$f_1 = 1, \qquad f_2 = (2I-1)/(3I),$$

$$f_3 = (I-1)(2I-1)/5I^2, \quad f_4 = \frac{2(I-1)(2I-1)(2I-3)}{35I^3}.$$

IV.3 The Values of f_k for Values of a_m given by a Boltzmann Distribution.

In order to determine the angular distribution

of radiation from an ensemble of oriented nuclei, we must know the populations of the various energy levels of the nuclei. We suppose the populations to have a Boltzmann distribution

$$a_m = Ce^{\beta m}, \text{ where } \beta = \mu H/kTI.$$

If $\beta I << 1$, we can write a_m approximately as

$$a_m = C(1+\beta m + \tfrac{1}{2}\beta^2 m^2 + \tfrac{1}{6}\beta^3 m^3 + \tfrac{1}{24}\beta^4 m^4)$$

$$= C(1 + A_1 m + A_2 m^2 + A_3 m^3 + A_4 m^4) \quad \text{(say)}$$

Then from equations (31), $f_1 = I^{-1}\Sigma_m m a_m = I^{-1} C \Sigma_m (A_1 m^2 + A_3 m^4)$

$$= C\frac{(I+1)(2I+1)}{3}\left(A_1 + \frac{(3I^2+3I-1)}{5} A_3\right) \quad (3$$

We determine C in the following manner.

Identically $\Sigma_m a_m = 1$, so

$$C\Sigma_m(1 + A_1 m + A_2 m^2 + A_3 m^3 + A_4 m^4) = 1.$$

Therefore $\frac{1}{C} = (2I+1)\left\{1 + \frac{I(I+1)}{3} A_2 + \frac{I(I+1)(3I^2+3I-1)}{15} A_4 \cdot \right\}$

Similarly $f_2 = I^{-2}\left\{C.\Sigma_m(m^2 + A_2 m^4 + A_4 m^6) - I(I+1)/3\right\}$

$$= \frac{(2I-1)(I+1)(2I+1)(2I+3)}{45I} \cdot C \left\{A_2 + \frac{6I^2+6I-5}{7} \cdot A_4\right\} \quad (32b$$

and $$f_3 = C. \frac{(I-1)(2I-1)(I+1)(2I+1)(2I+3)}{175I^2} \cdot A_3 \quad (32c$$

$$f_4 = C. \frac{4(2I-3)(2I-1)(I-1)(I+1)(2I+1)(2I+3)(I+2)(2I+5)}{(105)^2 I^3} \cdot A_4 \quad (32d$$

For the 2+ level of Au^{198} of spin I = 2, the four orient-

ation parameters are

$$f_1 = 5C \left\{ A_1 + \frac{17}{5} A_3 \right\}$$

$$f_2 = \frac{7}{2}C \left\{ A_2 + \frac{31}{7} A_4 \right\}$$

$$f_3 = \frac{9}{5}C.\ A_3$$

$$f_4 = \frac{6}{7}C.\ A_4 \text{ where } \frac{1}{C} = 5\left(1 + 2A_2 + \frac{34}{5}A_4\right)$$

We can now calculate the energy level populations a_m as functions of the orientation parameters f_k for a nuclear spin I = 2. From the equations (31) we obtain:

$$f_1 = a_2 - a_{-2} + \frac{a_1 - a_{-1}}{2}$$

$$f_2 = a_2 + a_{-2} + \frac{a_1 + a_{-1}}{4} - \frac{1}{2}$$

$$f_3 = \frac{3}{20}(a_2 - a_{-2}) - \frac{3}{10}(a_1 - a_{-1})$$

$$f_4 = -\frac{3}{14}\left\{ \frac{a_2 + a_{-2}}{2} + a_1 + a_{-1} - \frac{3}{5} \right\}$$

These give four simultaneous equations for the a_m in terms of f_k:

$$2a_2 + a_1 - a_{-1} - 2a_{-2} = 2f_1$$

$$4a_2 + a_1 + a_{-1} + 4a_{-2} = 4f_2 + 2$$

$$a_2 - 2a_1 + 2a_{-1} - a_{-2} = \frac{20}{3} f_3$$

$$a_2 + 2a_{+1} + 2a_{-1} + a_{-2} = -\frac{28}{3}f_4 + \frac{6}{5}$$

The solution of these equations give the populations of

the five magnetic sublevels of nuclei of spin I = 2 as functions of the f_k.

$$a_2 = 2/5\, f_1 + 4/7\, f_2 + 2/3\, f_3 + 2/3\, f_4 + 1/5$$

$$a_1 = 1/5\, f_1 - 2/7\, f_2 - 4/3\, f_3 - 8/3\, f_4 + 1/5$$

$$a_{-1} = -1/5\, f_1 - 2/7\, f_2 + 4/3\, f_3 - 8/3\, f_4 + 1/5$$

$$a_{-2} = -2/5\, f_1 + 4/7\, f_2 - 2/3\, f_3 + 2/3\, f_4 + 1/5 \qquad (33)$$

and, since $\sum_m a_m = 1$, $a_o = -4/7\, f_2 + 4 f_4 + 1/5$

IV.4 The Angular Distribution of γ-Radiation from Orientated Nuclei.

The angular distribution of the observed radiation from orientated nuclei can be obtained from equations (21) and (22), and is given by

$$W(\theta) = \sum_{mi,M} a_{mi} G^{Ii,Lf}_{mi,mi-M^2} F^M_L(\theta) \qquad (34)$$

Tolhoek and Cox [28] give the values of $F^M_L(\theta)$ for L = 1, and L = 2 obtained by considering Maxwell's electromagnetic theory. We consider an electromagnetic field with a vector potential $\underline{A} = \underline{A} e^{-ickt}$. The Poynting vector is defined by $\underline{P}^M_L = \frac{c}{4\pi} (\underline{E} \wedge \underline{H})$,

$$\text{where } \underline{E} = -\frac{1}{c} \frac{\partial}{\partial t} \underline{A} = ik\underline{A}$$

$$\text{and } \underline{H} = \text{rot } \underline{A}.$$

If $\underline{n}$ is a unit vector in the direction of $\underline{P}^M_L$, then

$$\underline{n}.\underline{P}^M_L = \frac{ck^2}{8\pi} . \underline{A}.\underline{A}^* \qquad (35)$$

We define $F_L^M(\theta) = 32\pi^3 r^2 c^{-1} \cdot \underline{n} \cdot \underline{P}_L^M$ (36

where $F_L^M(\theta)$ is normalised so that $\int F_L^M(\theta) d\Omega = 8\pi$.

Then from equations (34) and (35)

$$F_L^M(\theta) = 4\pi^2 r^2 k^2 \underline{A} \cdot \underline{A}^* \quad (37$$

and $$F_L^M(\theta) = 4\pi^2 r^2 k^2 \underline{E} \cdot \underline{E}^* \quad (38$$

From the general expression for $\underline{A}$ we obtain the following expression for $F_L^M(\theta)$, where the Y_L^M are spherical harmonics:

$$F_L^M(\theta) = \frac{4\pi}{L(L+1)} \left\{ 2M^2 \left| Y_L^M \right|^2 + (L-M)(L+M+1) \left| Y_L^M \right|^2 + (L+M)(L-M+1) \left| Y_L^M \right|^2 \right\}$$

For dipole radiation, L = 1, and for quadrupole radiation, L = 2, so we obtain

$$F_1^0(\theta) = 3(1-\cos^2\theta)$$

$$F_1^{\pm 1}(\theta) = \tfrac{3}{2}(1 + \cos^2\theta)$$

$$F_2^0(\theta) = \tfrac{5}{2}(6\cos^2\theta - 6\cos^2\theta)$$

$$F_2^{\pm 1}(\theta) = \tfrac{5}{2}(1 - 3\cos^2\theta + 4\cos^4\theta)$$

$$F_2^{\pm 2}(\theta) = \tfrac{5}{2}(1 - \cos^4\theta)$$

In equation (34), the transformation coefficients $G^{Ii, LI_f}_{mi,\ mi-M}$ are the Clebsch-Gordan coefficients for the addition of angular moments, and we rewrite them as $C(I_f L I_o, m_f M m_o) = (-I)^{Io+m_o} \sqrt{(2I_o+1)}\, V(I_f L I_o, m_f M - m_o)$, where the subscripts o and f refer to the initial and final states of the system. We may thus write the angular distribution of the γ-radiation as

$$W(\theta) = \sum_{m_o,M}(-1)^{I_o+m_o}\sqrt{(2I_o+1)}\,a_{m_o}\,V(I_fLI_o, m_fM - m_o)F_L^M(\theta),$$

where V is an operator introduced by Racah.

Now in the case of the quadrupole radiation from the transition $2+ \longrightarrow 0$, $I_o = 2$, $L = 2$, and $I_f = 0$, whence $m_o = M$.

Therefore $W(\theta) = \sum_{m_o=-2}^{2}(-1)^{m_o}\sqrt{5}\,a_{m_o}\,V(022, 0m_o - m_o)F_2^{m_o}(\theta)$.

Now $V(022, 0m_o - m_o) = (-1)^{m_o}/\sqrt{5}$, hence $W(\theta) = \sum_{m_o=-2}^{2} a_m F_2^m(\theta)$,

i.e. $W(\theta) = (a_2 + a_{-2})F_2^2(\theta) + (a_1 + a_{-1})F_2^1(\theta) + a_oF_2^o(\theta)$.

Expressing the a_m as functions of the parameters f_k, and replacing the functions $F_L^M(\theta)$ by their expressions, we have

$$W(\theta) = 5(\tfrac{4}{7}f_2 + \tfrac{2}{3}f_4 + \tfrac{1}{5})(1 - \cos^4\theta) - 5(\tfrac{2}{7}f_2 + \tfrac{8}{3}f_4 - \tfrac{1}{5})(1 - 3\cos^2\theta + 4\cos^4\theta) - 15(\tfrac{4}{7}f_2 - 4f_4 - \tfrac{1}{5})\cos^2\theta(1 - \cos^2\theta)$$

$$= 1 - \tfrac{10}{7}f_2P_2(\cos\theta) - \tfrac{40}{3}f_4P_4(\cos\theta) \qquad (39)$$

where $P_2(\cos\theta)$ and $P_4(\cos\theta)$ are Legendre polynomials of order 2 and 4 respectively.

The definitions of the f_k parameters may be justified by the use of tensor methods:

From the analysis one obtains a parameter

$$\overline{f}_k = \sum_m (-1)^{I-m}C(IIk, m - m0)a_m \qquad (40)$$

which differs from the f_k already defined only by a constant factor ω_k and which satisfies the conditions (29a,b). The value of ω_k can be obtained

with the use of equation (29c), giving

$$\omega_k(I_i) = \frac{f_k}{\bar{f}_k} = \left(\frac{k!}{2k!}\right)^2 I_i^{-k} \left[\frac{(2I_i + k + 1)!}{(2k+1)(2I_i-k)!}\right]^{\frac{1}{2}} \qquad (41)$$

and from equations (40) and (41) we obtain

$$f_k(I_i) = \omega_k(I_i) \sum_{mi} (-1)^{I_i+k-m_i} \sqrt{(2k+1)}\, V(I_i I_i k, m_i\ -m_i\ 0)\, a_{m_i}^{(42)}.$$

IV.5 The Influence of preceding Transitions on the Angular Distribution of Radiation.

Hitherto we have considered only the simplest case of nuclear orientation; that of orientated nuclei which decay by a single γ-emission. However, in the majority of cases, the orientated nuclei will be β-active with a sufficiently long half-life, and the β-decay will be followed by one or more gamma transitions in cascade, so that it is necessary to consider the relations between the initial state of orientation and that existing after the β-decay and before the γ-emission.

In β-decay the change of spin of an orientated nucleus is equal to the total angular momentum L of the emitted electron and neutrino. In forbidden or allowed first order transitions, L can take the values 0, 1, and 2. The relative probabilities of these values we call α_0, α_1, and α_2, where $\alpha_0 + \alpha_1 + \alpha_2 = 1$.

If $\vec{l}$, $\vec{s}_e$ and $\vec{s}_\nu$ designate the orbital moment, the spin of the electron, and the spin of the neutrino, then

$L = 0$ for $\vec{s}_e + \vec{s}_\nu = \begin{cases} 0 \\ 1\uparrow \end{cases}$ and $\vec{l} = \begin{cases} 0 \text{ (s-electron)} \\ 1\downarrow \text{(p-electron)} \end{cases}$ corresponds to α_0

$L = 1$ for $\vec{s}_e + \vec{s}_\nu = \begin{cases} 0 \\ 1\uparrow \end{cases}$ and $\vec{l} = \begin{cases} 1 \\ 0 \end{cases}$ corresponds to α_1

$L = 2$ for $\vec{s}_e + \vec{s}_\nu = \begin{cases} 0 \\ 1\uparrow \end{cases}$ and $\vec{l} = \begin{cases} 2\uparrow \text{(d-electron)} \\ 1\uparrow \\ 3\downarrow \text{(f-electron)} \end{cases}$ corresponds to α_2

When $\alpha_1 \neq 0$, and $\alpha_2 \neq 0$, there is a reduction in the orientation. That is, the transition $I_o \rightarrow I_i$ causes a tendency for the populations of the sub-levels to equalise, since each sub-level m_o can decay to several sub-levels m_i according to the selection rules.

The probability of a β-decay is proportional to the square of the matrix element $\langle \tau_i I_i m_i | H_{\beta(L,M)} | \tau_o I_o m_o \rangle$ which gives, from the Wigner-Eckart theorem

$$\langle \tau_i I_i m_i | H_{\beta(L,M)} | \tau_o I_o m_o \rangle = \langle \tau_i I_i \| H_{\beta(L)} \| \tau_o I_o \rangle \sqrt{2I_o+1} \times V(I_i L I_o, m_i M-m_o)$$

where τ_i and τ_o symbolise the other quantum numbers characteristic of the system, and $H_{\beta(L,M)}$ is the interaction Hamiltonian.

The populations a_{m_i} of the sub-levels after

β-decay are related to the original populations a_{m_o} by the equation

$$a_{m_i} = \sum_{m_o} \sum_{L=0}^{2} \sum_{M=-L}^{L} \alpha_L a_{m_o} (2I_o+1) V^2 (I_i L I_o, m_i M - m_o)$$

where α_L = const. $\langle \zeta_i I_i \| H_{\beta(L)} \| \zeta_o I_o \rangle^2$

where the constant is determined by $\sum_L \alpha_L = 1$.

In the particular case of Au^{198} the decay scheme shows a principal (99 p.c.) β-transition of 959 keV between the ground state of Au^{198} and the 411 keV excited state of Hg^{198}. In the experiments on the nuclear orientation of Au^{198} the 411 keV γ-emission was measured, that is the orientation of the 2+ level of Hg^{198} was studied, whereas the experiment concerned the orientation of the 2- level of Au^{198}. The earlier calculations of the angular distribution of the γ-radiation were made without taking into account the transition 2- $\xrightarrow{\beta}$ 2+. The influence of this transition will now be considered.

Substituting for a_{m_i} in equation (42) its value in terms of a_{m_o} we obtain

$$f_k(I_i) = \omega_k(I_i) \sum_{L, m_i, m_o} (-1)^{(I_i+k-m_i)} \sqrt{(2k+1)}(2I_o+1) \times$$

$$\alpha_L V(I_i I_i k, m_i - m_i 0) \times V(I_i L I_o, m_i M - m_o) a_{m_o}$$

From the rule for summation of Clebsch-Gordan coefficients

$$f_k(I_i) = \omega_k(I_i) \sum_{L,m_o} (-1)^{(3I_i+L-k+m)_o} \sqrt{(2k+1)}\alpha_L V(I_o k I_o, m_o 0 - m_o \times W(I_o I_i I_o I_i, Lk) a_{m_o}$$

where W is Racah's Operator.

Putting $V(I_o k I_o, m_o 0 - m_o) = (-1)^{I_o} V(I_o I_o k, m_o - m_o 0)$,

then $f_k(I_i) = \omega_k(I_i) \sum_L (-1)^{(3I_i+L-I_o-k)} \alpha_L (2I_o+1) \times$

$$W(I_i I_o I_i I_o, Lk) \sum_{m_o} (-1)^{(I_o+k-m_o)} \sqrt{(2k+1)} V(I_o I_o k, m_o - m_o 0)$$

Introducing the parameter $f_k(I_o)$ to represent the initial state of orientation

$$f_k(I_i) = \frac{\omega_k(I_i)}{\omega_k(I_o)} f_k(I_o)(2I_o+1) \sum_L \alpha_L W(I_i L k I_o, I_o I_i) \qquad (43)$$

IV.6 The Angular Distribution of 411 keV γ-Radiation from Au^{198}.

In the case of Au^{198}, $I_o = I_i = 2$, and L = 0, 1, and 2. Substituting these values in equation (43), we have

$$f_k(I_i) = 5 f_k(I_o) \sum_{L=0} \alpha_L W(2Lk2, 22).$$

For k = 2,

$$f_2(I_i) = 5 f_2(I_o) \{\alpha_o W(2022, 22) + \alpha_1 W(2122, 22) + \alpha_2 W(2222, 22)$$

Now, W(2022,22) = 1/5, W(2122,22) = 1/10, W(2222,22) = -3/70.

Hence $f_2(I_i) = (\alpha_o + \frac{\alpha_1}{2} - \frac{3}{14}\alpha_2) f_2(I_o)$

$= (1 - \frac{\alpha_1}{2} - \frac{17}{14}\alpha_2) f_2(I_o)$ since $\sum_L \alpha_L = 1$

$$= B_2 f_2(I_o) \qquad (44)$$

The probabilities $\alpha_2 = 1$, and $\alpha_o = 1$ give the limits of B_2

$-\frac{3}{14} \leq B_2 \leq 1$. But if there is anisotropy it is positive hence $0 \leq B_2 \leq 1$.

For $k = 4$,

$$f_4(I_1) = 5f_4(I_o) \left\{ \alpha_o W(2042,22) + \alpha_1 W(2142,22) + \alpha_2 W(2242,22 \right.$$

Now $W(2042,22) = 1/5$, $W(2142,22) = -2/15$, $W(2242,22) = 2/3$

Hence $f_4(I_1) = (1 - \frac{5}{3}\alpha_1 - \frac{5}{7}\alpha_2) f_4(I_o) = B_4 f_4(I_o)$ (45)

Hence, substituting in equation (39)

$$W(\theta) = 1 - \frac{10}{7} f_2(I_o) B_2 P_2(\cos\theta) - \frac{40}{3} f_4(I_o) B_4 P_4(\cos\theta) \qquad (46)$$

Stone and Turrell[29] from an experiment on the nuclear polarization of Au^{198} in solution in iron have proposed for $\alpha_2 = 0$, $B_2 = 0.7$, and $B_4 = 0$, hence $f_2(I_1) = 0.7 f_2(I_o)$ and $f_4(I_1) = 0$. This can only be considered as an approximation since the contribution $L = 2$, although small, is not negligible. An approximate calculation for Au^{198} shows that for $B_2 = 0.7$, and $\beta = \frac{\mu H}{kTI} \approx 0.3$, the most populated sub-level loses 10 p.c. of its population as a result of the β-decay.

IV.7 The Anisotropy of γ-Radiation from Orientated Au^{198} Nuclei.

It is convenient to define a parameter, ϵ, to

describe the anisotropy of radiation emitted by orientated nuclei.

We define $\varepsilon = \frac{W(\pi/2) - W(0)}{W(\pi/2)}$, where $W(\pi/2)$ and $W(0)$ (1
are the intensities of radiation in the directions perpendicular and parallel to the axis of orientation of the nuclei. If the γ transition is pure,

$\varepsilon < 0$ for a dipolar transition,

and $\varepsilon > 0$ for a quadrupolar transition.

Thus it is possible to determine the multipolar character of the radiation by measuring ε. Also, one can determine the spin of the emitter level if the spin of the final energy level of the nucleus is known, and vice versa.

From equation (39) we obtain

$$\varepsilon = \frac{15/7\ f_2 + 25/3\ f_4}{1 + 5/7\ f_2 - 5f_4}$$

Substituting for f_2 and f_4 from equations (32b,d), we obtain $\varepsilon = \frac{3}{2}\cdot\frac{A_2 + 113/21\ A_4}{1 + \frac{5}{2}A_2 + \frac{571}{70}A_4}$ where $A_2 = \frac{\beta^2}{2!}$, and $A_4 = \frac{\beta^4}{4!}$

$\beta = \frac{\mu H}{kTI}$, where μ is the nuclear moment, H is the effective magnetic field on the nucleus, k is Boltzmann's constant and T is the absolute temperature. If β is small $\varepsilon \approx \frac{3}{2} A_2 = \frac{3}{16}\left(\frac{H}{kTI}\right)^2$. If we measure experimentally the anisotropy, ε, of the emitted radiation, and the temperature, T, of the specimen, we can determine the internal magnetic field in the specimen which orientates the

emitting nuclei. Rewriting equation (41), we have

$$H = \sqrt{\frac{4}{3}} \cdot \frac{kTI}{\mu} \cdot \sqrt{\varepsilon}.$$

For the 2+ level of Au^{198}, I = 2, and $\mu = 0.5\mu_n$, where $\mu_n = 5.05 \times 10^{-24}$ erg/oersted. Thus $H = 1.24 \times 10^8 . T\sqrt{\varepsilon}$ oersted.

If we take into account the influence of the β-transition which precedes the γ-emission, equation (48) is modified to give, from equation (46)

$$\varepsilon = \frac{\frac{15}{7}f_2 B_2 + \frac{25}{3}f_4 B_4}{1 + \frac{5}{7}f_2 B_2 - 5f_4 B_4} \qquad (48$$

If we take $B_2 = 0.7$ and $B_4 = 0$,

$$\varepsilon = \frac{1.5 f_2}{1 + 0.5 f_2}$$

$$\text{and } \varepsilon = 1.05 \frac{A_2 + 4.75 A_4}{1 + 2.35 A_2 + 8.35 A_4}$$

$$\text{if } \beta = \frac{\mu H}{kTI} \ll 1, \varepsilon \approx 1.05 A_2 = \frac{1.05^2}{8}\left(\frac{\mu H}{kTI}\right)^2$$

That is, $H \approx 1.5 \times 10^8 T\sqrt{\varepsilon}$ oersteds.

Therefore, the field obtained by taking into account the β-decay is greater by 20 p.c. than that calculated when the effect of the β-decay is disregarded.

CHAPTER V

The Specimens and the Measuring Equipment

V.1 The Specimens.

Two series of experiments were performed. The first series was carried out with the object of determining the internal magnetic field in a gadolinium-gold alloy by measuring the orientation of the gold nuclei. The object of the second series was to determine the internal magnetic field in a cobalt-nickel alloy by measuring the nuclear orientation of the cobalt nuclei.

The specimens used for the first series of experiments had to be alloys of a small percentage of a diamagnetic metal with gadolinium. Very little had previously been done with gadolinium alloys, and the section on gadolinium in Hansen's book 'The Structure of Binary Alloys' was confined to discussions of gadolinium hydrides and nitrides, and alloys and intermetallic compounds of gadolinium with ferromagnetic and paramagnetic metals, and with other rare

earth metals.

We had at first hoped to make alloys of gadolinium with the three diamagnetic metals that Samoilov had used - antimony, indium, and gold. Calculations based on Hume-Rothery's rule for binary alloys showed that of these three metals only gold could be expected to alloy readily with gadolinium. From discussions with M. Forrat of the CENG it appeared that gold and gadolinium would alloy in any proportion. Attempts were then made to produce an alloy of gold and gadolinium in an electric furnace in an atmosphere of argon, and also under high vacuum, but these resulted only in the oxidation of the gadolinium, presumably due to impurities in the argon or a leak in the furnace. We did not attempt to make the alloy in the furnace in an atmosphere of hydrogen because of the risk of producing hydrides. As we were unsuccessful in producing a gadolinium - gold alloy we did not attempt to produce a gadolinium - antimony or a gadolinium - indium alloy, so we placed an order with Messrs Johnson - Matthey for foils of a 1 p.c. gold in gadolinium alloy.

It was important for the experiment that the gold should be properly dissolved in the gadolinium.

If the gold were present as aggregations of several gold atoms in the lattice, the results obtained would be unreliable since the magnetic field in an aggregate of gold atoms would not be that in the lattice. For experimental accuracy it is essential that single gold atoms be distributed homogeneously in the gadolinium lattice.

These specimens were submitted to gamma ray spectroscopy which revealed the presence of a very small quantity of terbium. X-ray analyses of the specimens did not show any lines characteristic of gold, which indicates that the gold atoms were incorporated into the gadolinium lattice, but since the proportion of gold present was very small, this does not confirm that the distribution of the gold in the gadolinium was homogeneous. However, any effect due to this could be compensated for by the fact that many runs were carried through using specimens from different foils and from different parts of each foil.

The sheets of the alloy were 0.1 mm. thick and from these, discs of 5 mm. diameter were punched. The specimens were made in the form of a thin disc so as to reduce its demagnetization factor to a minimum so that the magnetization of the specimen should be a maximum. It is necessary also that the specimen

should be circular in section so that γ-ray emission should be isotropic from a 'warm' specimen. These specimens were irradiated with thermal neutrons of flux 5×10^{12} neutrons/cm^2/sec. in the Grenoble reactor 'Melusine' to produce nuclei of Au^{198} of activity of 10 to 20μC. This nucleus emits gamma radiation of energy 411 keV.

In the second series of experiments a 50 p.c. alloy of cobalt and nickel was obtained from the CENG and cut into discs of 5 mm. diameter and 0.2 mm. thickness. After annealing for one hour at 900°C in an atmosphere of hydrogen, the specimens were irradiated in 'Melusine' with thermal neutrons of flux 5×10^{12} neutrons/cm^2/sec. The specimens were left for a few days after removal from the reactor to allow the activity from the Ni^{65} also formed to diminish to a level very low in comparison to that of the Co^{60}. The half-life of Ni^{65} is 2.6 hrs, and the half-life of Co^{60} is 5.2 years. The activity of the Co^{60} was then 50μC. The gamma radiation has an energy of 1.17 MeV.

V.2 The Counting Equipment.

In order to measure the anisotropy of the gamma radiation emitted from the specimens, it was necessary to use two separate systems of counting

equipment. Each system consisted of a scintillation counter, a light guide, a photomultiplier, a scaler, and associated power packs which supplied the photomultipliers.

The scintillation counters were crystals of sodium iodide activated with thallium, each of one inch diameter and depth. Each was covered with aluminium. The base of each crystal was in optical contact with the head of the light guide, and cemented to it with silicone grease.

The light guides were inserted between the scintillation counters and the photomultipliers in order to remove the latter from the magnetic field of the Helmholtz coils surrounding the specimen. This was necessary in order to avoid interference with the working of the photomultipliers due to deflection of the electrons from the dynodes of the photomultipliers by the magnetic field, which would result in significant losses in the numbers of photons reaching the photocathode.

A light guide should have good resolution and good transmission. Perspex of refractive index 1.45 was used for the light guides which had a profile in the shape of logarithmic spiral. If a photon entering the end surface of the light guide is reflected at an angle λ, total reflection of all photons, i.e. 100 p.c.

Fig. 1.

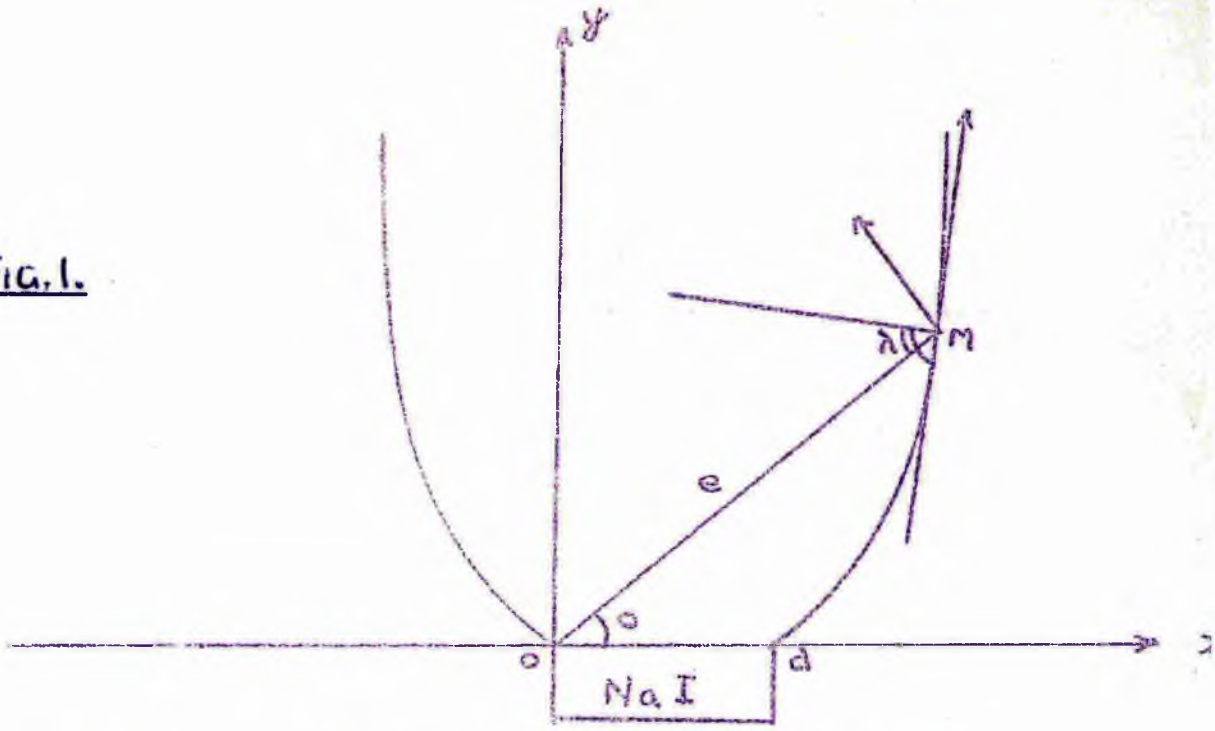

SKETCH OF THE HEAD OF THE LIGHT-GUIDE

Fig. 2

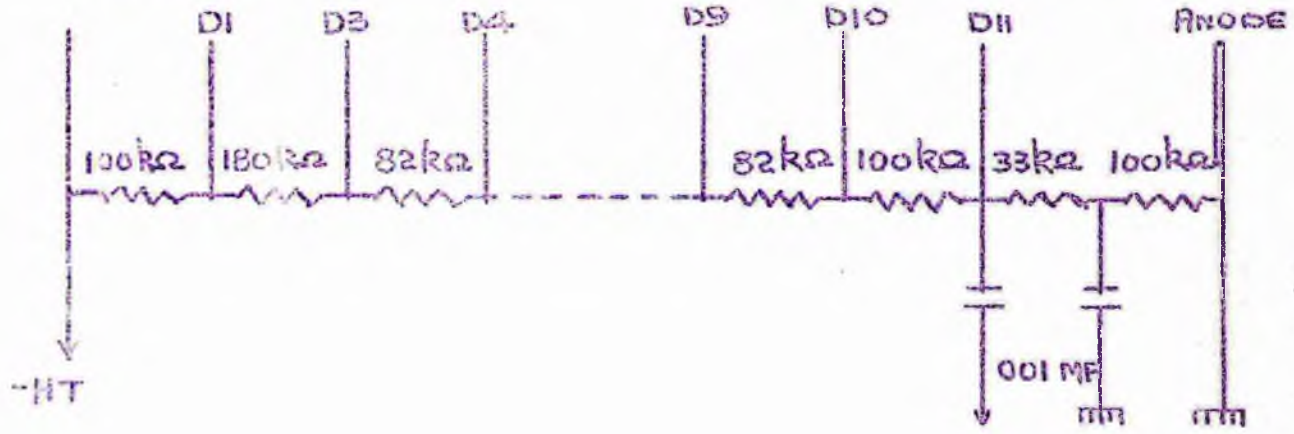

CATHODE FOLLOWER

gathering power is achieved for $\lambda \geqslant \sin^{-1} \frac{1}{n} = 43^{\circ}$. Using the notation shown in the figure (1) the equation of the spiral is $\rho = d.\exp(-\theta \tan\lambda)$. Then the entry diameter d and the maximum diameter D of the light are related by:

$$D/d = (2\cos\lambda_o \exp -\lambda_o \tan\lambda_o) - 1,$$

where $\lambda_o = \sin^{-1} \frac{1}{n}$.

Thus for $\lambda \geqslant \lambda_o = 43^{\circ}$, $d/D = 0.54$. Hence if we take d = 29 mm., the diameter of the sodium iodide crystal, then D = 54 mm. The dimensions, therefore, of the guides were as follows: Entry diameter = 29 mm., maximum diameter = 55 mm., exit diameter = 32 mm. The overall length was 162 mm. Measurements of the energy of pulses from Cs^{137} registered by the scintillators were made with an oscilloscope when the light guide was present between scintillator and photomultipliers, and compared with measurements made without the light guide. From the measurements we found that for 100 p.c. collection of photons there was 23 p.c. absorption and 21 p.c. of losses in the light guides.

The photomultipliers were Radiotechnique 11 dynode 51 AVP, and the associated circuit is shown in the figure (2). The positive signal from the last dynode D goes to the cathode follower. The photomultipliers were magnetically screened by a cylinder of

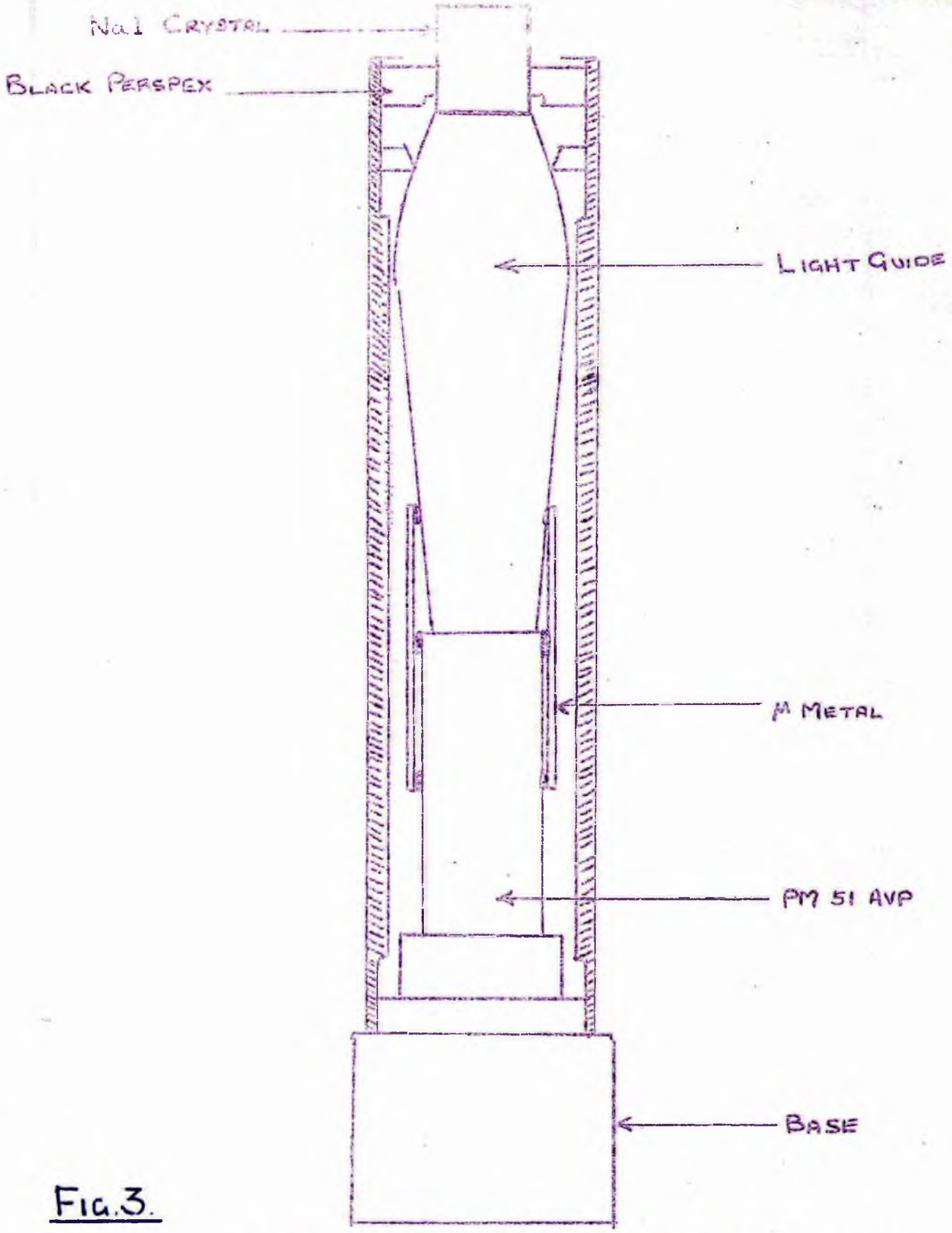

Fig.3.

SKETCH OF γ-RAY DETECTOR ASSEMBLY

μ-metal which extended beyond the surface of the photocathode by a distance at least equal to its radius in order to eliminate all end effects, since the effect of a magnetic field on the photomultiplier is most important between the photocathode and the first dynode. In the figure opposite, (fig. 3), the whole assembly of scintillation crystal, light guide, and photomultiplier is shown. The assembly was contained within a cylinder of mild steel which acted as a magnetic screen, and ensured the centring of the crystal, the photomultiplier, and the light guide, and rendered the whole assembly light-tight.

The influence of a magnetic field on a photomultiplier was investigated using a copper-wound solenoid having the same magnetic moment (5700 emu) as the Helmholtz coils surrounding the specimen in the cryostat. The solenoid was submerged in liquid air in order to reduce the resistance of the copper wire used, thus permitting the use of a smaller coil to give the same magnetic moment. The resistivity of copper diminishes by a factor of 10 on cooling to liquid air temperature ($97^{\circ}K$), so that a current 10 times as large may be passed through it at $97^{\circ}K$ as at room temperature. This experiment showed that a field of less than one oersted has no effect ~~on the~~

on the photomultiplier, and that the precautions taken to shield the photomultiplier and separate it from the crystal by a light-guide were adequate.

Pulses from the last dynode of each of the photomultipliers were fed into a pre-amplifier (incorporating a cathode-follower) and an amplifier. The rest of the counting equipment consisted in one case, of a single channel selector with adjustable energy band width and adjustable pulse height discriminator, and a binary scaler calibrated decimally. The signals from the other photomultiplier were supplied to equipment consisting of an amplifier and a pulse amplitude discriminator and a system of pulse amplitude selectors. This was followed by a binary scaler calibrated decimally. Incorporated in one system was a timing device which allowed both counting systems to be started simultaneously and stopped simultaneously after a predetermined period. There was also two power packs to provide the H.T. supply to the photomultipliers.

V.3 The Alternating Current Hartshorn Bridge.

For measuring the magnetic susceptibility of the salt pill, measurements of the mutual inductance

THE A. C. HARTSHORN BRIDGE

FIG. 4.

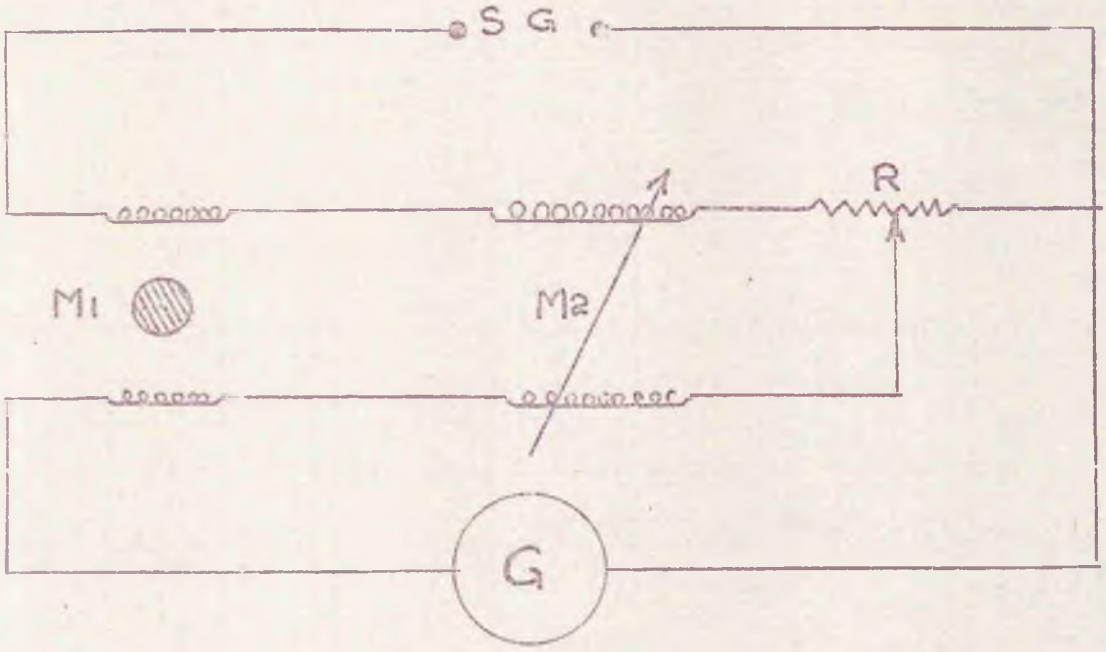

M1 IS THE SUSCEPTIBILITY MEASURING COIL

M2 IS STANDARD MUTUAL INDUCTANCE

S.G IS SIGNAL GENERATOR

G IS DETECTOR

of a pair of coils surrounding the salt pill were made with a Hartshorn A.C. Bridge, the circuit of which is shown opposite, (figure 4).

The signal generator used was a Phillips audio-frequency generator. The output of this was supplied to the primary of the measuring coils, the primary of a Tinsley standard mutual inductance, and a bank of AOIP variable resistances providing a range of 0 to 10 kohms. The secondary of the measuring coils was connected in series with the secondary of the standard mutual inductance. The signal in this circuit went to the input of an amplifier which supplied a valve voltmeter which had several ranges of sensitivity. This valve voltmeter was sensitive to signals of the order of 0.1 mV from the amplifier. The Tinsley standard mutual inductance had three decades and a continuous variometer which provided a range of 0 to 10000μH, with a precision of 0.1 μH.

If the susceptibility of the salt be represented by $\chi = \chi^{1} - i\chi^{11}$, then M_1 fulfills the relation $M_1 = M_o + \beta(\chi^{1} - i\chi^{11})$, where M_o is the mutual inductance of the empty coils. Only $M_o + \beta\chi^{1}$ can be balanced by adjusting M_2 since they both give rise to voltages in quadrature with the primary current. The voltage due to $\beta\chi^{11}$ is in phase with the primary current and hence it can be balanced by

setting the potentiometer R. It is found that the equilibrium conditions of the bridge are

$$M_2 = M_o + \beta\chi^{I}$$

$$R = \beta\chi^{II}$$

In fact we were not interested in the value of χ^{II} since it was very small, so we measured only the variation M_2.

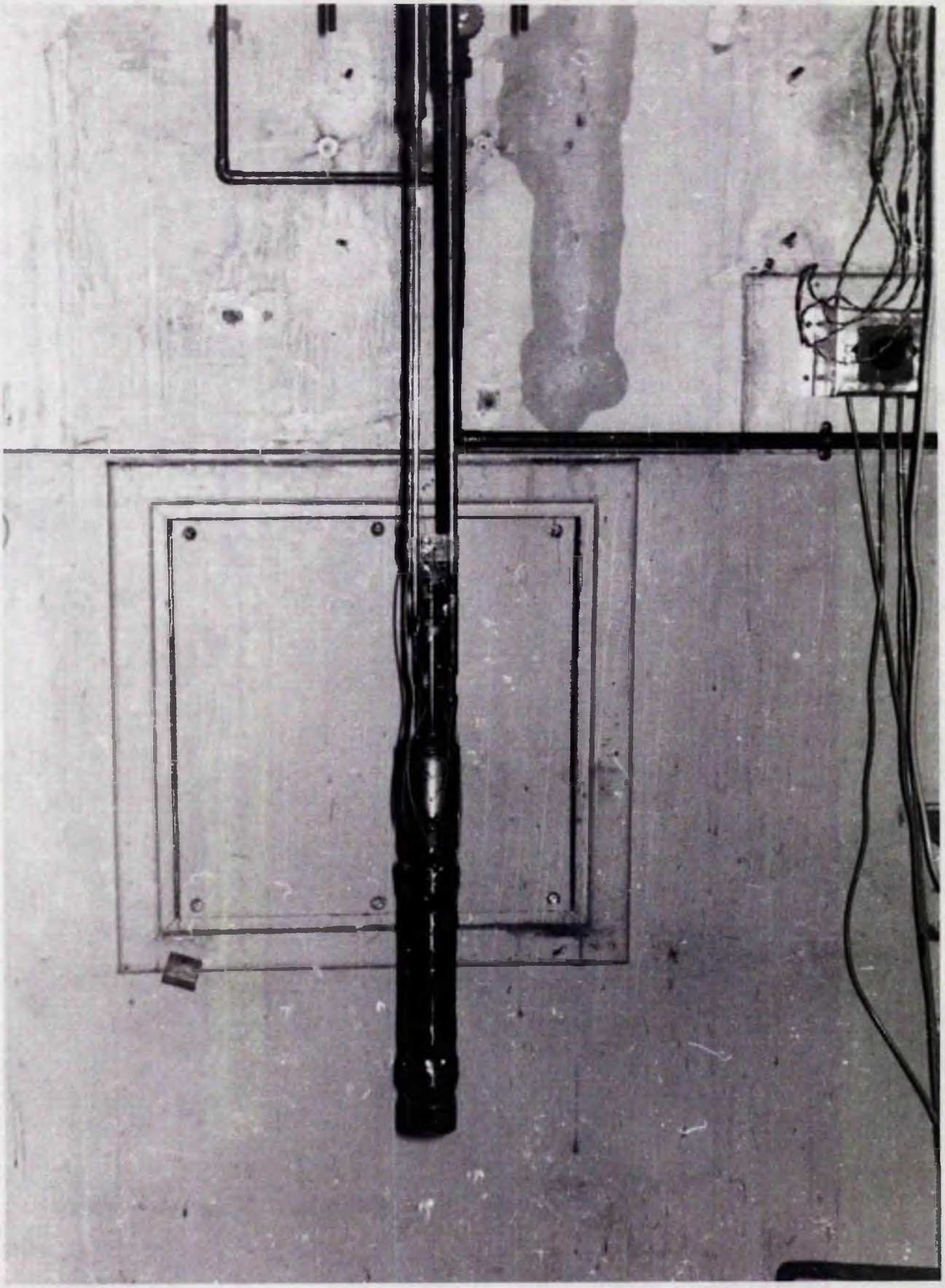

Plate 2. The Cryostat, showing the Mutual Inductance and Magnetization Coils.

Facing p. 73.

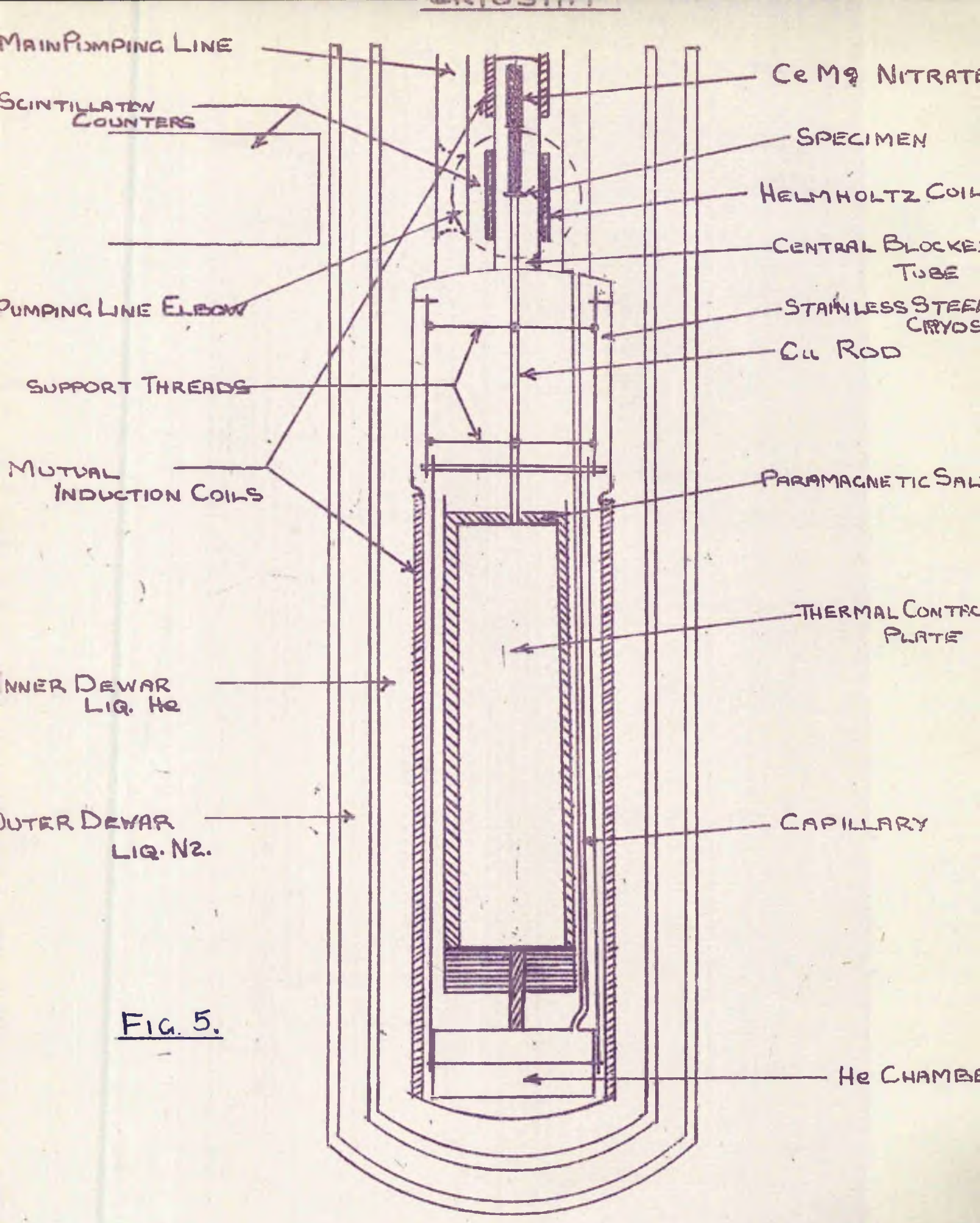
Main Pumping Line
Scintillation Counters
Pumping Line Elbow
Support Threads
Mutual Induction Coils
Inner Dewar Liq. He
Outer Dewar Liq. N2.
Ce Mg Nitrate
Specimen
Helmholtz Coil
Central Blocked Tube
Stainless Steel Cryos
Cu Rod
Paramagnetic Sal
Thermal Contro Plate
Capillary
He Chambe

Fig. 5.

CHAPTER VI

The Apparatus

An apparatus for producing very low temperatures by the method of adiabatic demagnetization of a paramagnetic salt was built. The construction of a liquid helium-four cryostat and its two surrounding Dewars, the design of mutual inductance and magnetization coils, the preparation of the salt pill, and the mounting of the specimen are described in this chapter.

VI.1 The Construction of the Cryostat.

The cryostat was a can of stainless steel connected to a high vacuum pumping system by stainless steel tubing. The details are shown in figure (5). The can was 40 cm. long, with a diameter of 50 mm. over the upper 10 cm., and a diameter of 40m.m. mm. over the rest. The walls were 1 mm. thick. The stainless steel can was completed at the top by a copper cap into which were soldered three wide bore tubes. The can was soldered to the cap with Wood's metal. The tubes in the cap were, respectively, from

right to left, the high vacuum line for evacuation of the can, a central blocked tube to enclose the specimen, and a line for the evacuation and filling of the helium chamber. The can itself was made of stainless steel so that mutual inductance measurements of salt susceptibility would not be affected by eddy currents in the can. Stainless steel has a high resistivity, and is non-magnetic at very low temperatures. The central tube in the can was of stainless steel for the same reason. The pumping lines were partly of stainless steel and partly of copper. That part of each which extended down from the helium line manifold was of stainless steel, so as to reduce the heat conducted down into the helium bath. For a short distance above the cap of the cryostat, the tubes were of copper, and incorporated elbows which prevented radiation from above heating the salt pill, and which were so placed at the height of the specimen as to provide a clear line of sight for the γ-rays along the axis of the specimen. The diameters of the three tubes were respectively 12, 10, and 6 mm.

A cylindrical copper chamber of about 2 cubic cm. capacity was provided inside the can near the bottom, and fitted with a thermal link to the salt pill, which will be described below. A small heating coil

High Vacuum System for Cryostat

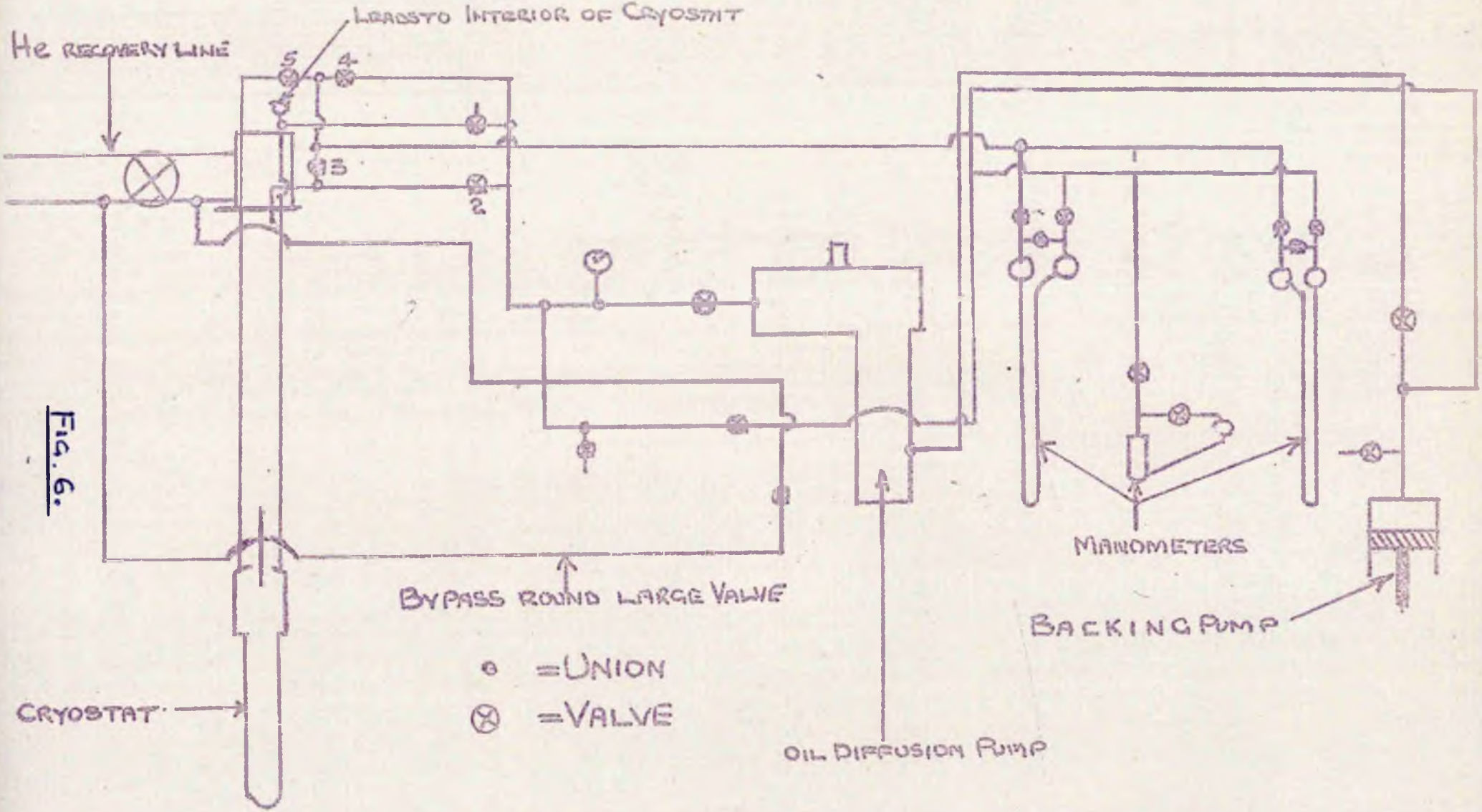

Fig. 6.

was wound round the chamber so that the liquid helium in it could be boiled off if required. The chamber was connected to the vacuum system by a stainless steel capillary of 2 mm. diameter and wall thickness 0.1 mm. To the cryostat cap was screwed a cage of brass rods and nylon annuli which provided a rigid support for the salt pill and the helium chamber.

VI.2 The Vacuum System.

The vacuum system was of an orthodox type except that provision was made for filling the small chamber with helium and for pumping it to a hard vacuum. A sketch of the system is shown opposite (fig. 6).

A rotary and an oil diffusion pump were used to obtain the vacuum. Appropriate valves were provided on either side of the diffusion pump so that it could be isolated from the system, allowing the rotary pump to pump directly on the system via a line by-passing the diffusion pump. A liquid air trap was mounted directly on the diffusion pump. The valve for shutting off the high vacuum side of the diffusion pump was mounted directly on the liquid air trap, and from this a wide bore tube led to the cryostat. An ionisation vacuum gauge was fitted to this tube. The

by-pass from the rotary pump joined the main pumping line at this point. Two branches led from this line; one narrow bore tube went to the manifold of the helium line to enable the interior of the helium Dewar to be evacuated via the valve (2), the other of wide bore went to another union. From this union, one branch led to the cryostat via the valve (1). The other branch was used to evacuate the helium chamber via the valves (4) and (5). From a union between the valves (4) and (5) there was a link to the interior of the helium Dewar via the valve (3). From this link there was a connection to the 'high-pressure' side of each of the three manometers. The other side of each of the two outer manometers was joined to the diffusion pump by-pass. The third was a differential manometer, so that no connection to the rotary pump was necessary.

The manifold was connected to the recovery line through a large valve which was passed by a narrow-bore tube which could be closed by a valve so that finer control of the rate of pumping on the liquid helium could be achieved. So it can be seen that the pumping line to the helium chamber communicated also with the interior of the helium Dewar and the cryostat, and also with the manometers.

Helium gas could be admitted at a precisely known pressure to the chamber as follows. With valves

THE DEWARS

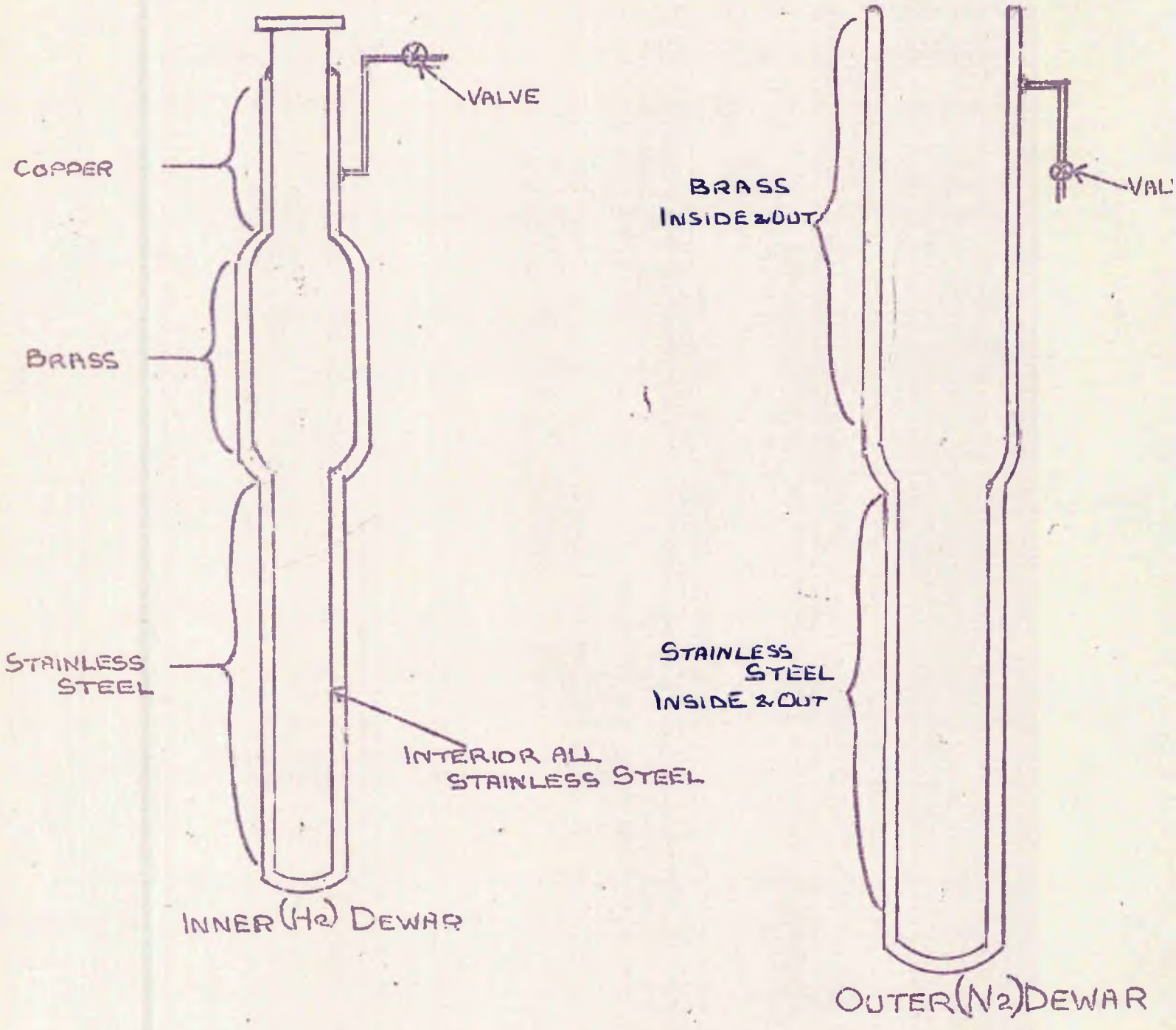

FIG. 7

(2), (4), and (5) closed, the manometers gave the pressure in the helium Dewar. If (3) were closed and (5) opened, helium gas would be admitted to the chamber from the manometers. This process could be repeated until the desired pressure in the chamber was obtained. The chamber could be evacuated with valves (4) and (5) open and valves (1), (2), and (3) closed.

The helium recovery line manifold was provided with an aperture for siphoning liquid helium into the Dewar, and with vacuum-tight seals through which electrical wiring could be introduced.

VI.3 The Dewars.

The outer and inner Dewars could be removed separately, and were of all-metal construction. They were of the form indicated in the sketch opposite, (fig. 7).

The inner helium Dewar had a stainless steel inner wall on which was mounted a flange over which could be screwed a nut which pulled the flange against an O-ring seal in the manifold. The outer wall of the Dewar was of brass over the wide section with a stainless steel tail. The internal diameter of the wide section was about 120 mm., and of the tail, about 60 mm. The external length of the tail was about 80 cm. The

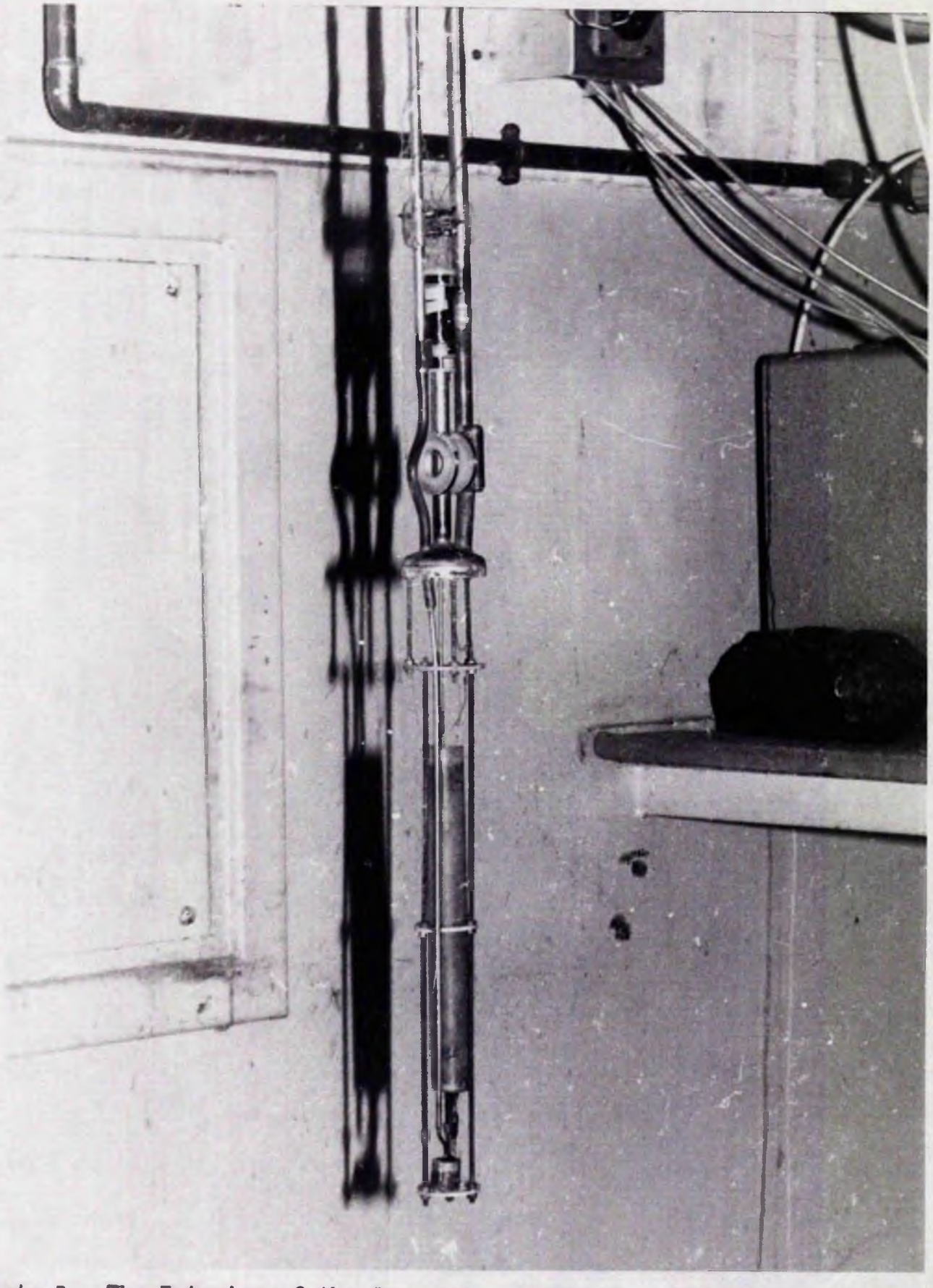

Plate 3. The Interior of the Cryostat, showing the Salt Pill, the Small Mutual Inductance, and the Helmholtz Coils.

Facing p. 78.

walls were about 0.5 mm. thick, which was about the practical limit for combining a reduction of thermal conduction down into the liquid helium with mechanical strength. When mounted over the cryostat, this Dewar hold about five litres of liquid helium.

The upper part of the outer Dewar was of brass, and the tail was of stainless steel. The length of the tail was about 90 cm. outside, and the external diameter was 9 cm. so that it would enter the solenoid. The Dewars had stainless steel tails so that mutual inductance measurements were not disturbed by eddy currents in the tails of the Dewars.

VI. 4 The Preparation of the Salt Pills and the Mounting of the Specimen.

The salt used for the magnetic cooling was chromium potassium alum. The salt pill was prepared in the following manner.

The salt was finely ground and mixed into a slurry with a mixture of 75 p.c. glycerine and 25 p.c. water. Thermal contact between the salt and the helium chamber and the specimen was arranged as follows. A thin sheet of copper was wound into a spiral to the ends of which were brazed cruciform plates. To each of the plates was brazed a copper rod of 2 mm. diameter

and length 3 cm., in one case and 22 cm. in the other. The other end of each of these rods was screw cut. This device was slid into a nylon tube of internal diameter 22 mm. which was blocked at one end with a nylon bung, pierced with a hole to allow the 3 cm. long rod to pass. This rod was then screwed into a socket on the top of the helium chamber. The salt slurry was then poured into the tube and packed against the copper sheet. The thermal link was designed in this way in order to avoid eddy currents which could disturb measurements of mutual inductance.

The temperature of the specimen could be measured independently by measuring the magnetic susceptibility of a single crystal of cerium magnesium nitrate in thermal contact with it. A thin sheet of copper of dimensions 40x60x0.1 mm. was silver-soldered into a slot at the end of a copper rod which could be screwed into a copper cylinder of length and diameter 4 mm., which was tapped by a blind hole of 2 mm. diameter. A single crystal of cerium magnesium nitrate was cut in half along its principal axis, and one surface of each half was ground flat. The two halves were stuck on either side of the copper sheet with silicone grease and bound on with cotton thread soaked with varnish. This was done in such a way that the

principal axis of the crystal was vertical.

The specimen of gadolinium alloy, which was in the form of a disc, was glued between two copper cylinders of the above dimensions with araldite which afforded reasonable thermal contact. The assembly of specimen and cylinders was then screwed on the end of the 22 cm. rod which emerged from the salt pill, and the rod holding the single crystal of cerium magnesium nitrate was then screwed into the other copper block.

The whole assembly of salt pill, specimen, and single crystal was then mounted in the cryostat by introducing the rods supporting the specimen and the single crystal into the central tube in the cap of the cryostat, and screwing the rod emerging from the other end of the salt pill into a socket on the top of the helium chamber. The specimen and single crystal were prevented from touching the sides of the tube by nylon spacers fitted on the rods. The cage was then mounted round this, by screwing it to the cryostat cap. The assembly was then secured to the cage with nylon thread or cotton thread soaked in varnish. The cryostat was then sealed by soldering the can to its cap. The mounting of the salt pill is shown in plate (3).

VI.5 The Mutual Inductance and Magnetization Coils.

Two coils were made for measuring the temper-

ature of the salt pill and the specimen.

The first was made to fit tightly over the cryostat and the length of the narrower part of the cryostat can was fixed by the length of the measuring coils. The length of the coils was fixed by their diameter, which itself was determined by the diameter of the cryostat can.

The form and direction of the windings as determined was directed towards producing a very uniform field over the length of the salt pill, with compensating reverse windings at the ends of both primary and secondary in order to produce a sharp cut-off of the field so as to avoid measuring stray susceptibilities.

The coil for measuring the susceptibility of the potassium chrome alum was wound on a former made of a roll of thin paper which was subsequently varnished. This method was chosen so that one turn of the paper at a time could be removed from the inside until a tight fit over the cryostat was obtained. The overall length of the windings was about 30 cm., and the internal diameter 44 mm. Copper wire of diameter 0.3 mm. was chosen for the primary, and of diameter 0.2 mm. for the secondary. Basic units of winding of 60 and 90 turns/cm. were chosen for the primary and secondary, respectively. The actual turns density at

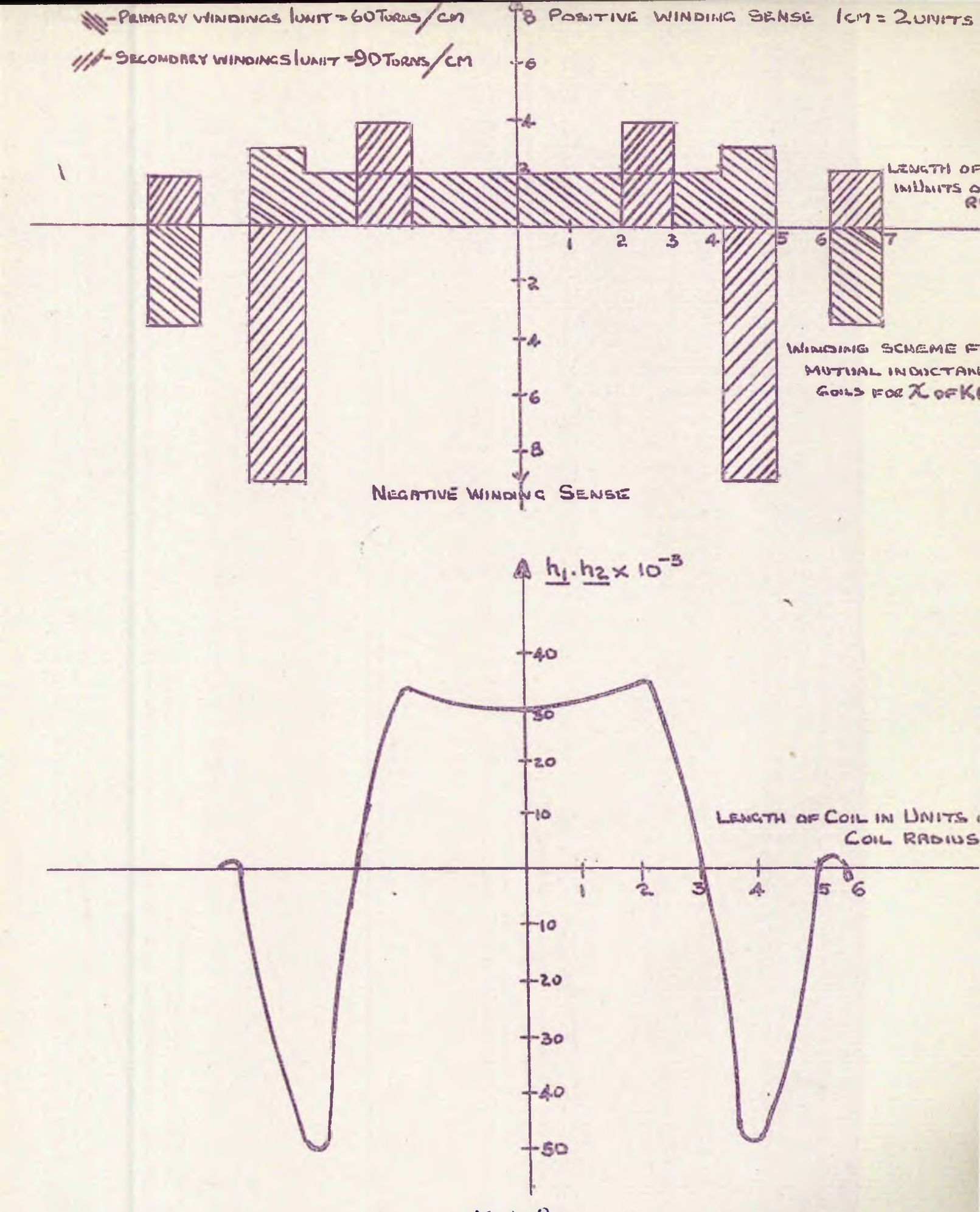
-PRIMARY WINDINGS 1UNIT = 60 TURNS/CM
-SECONDRY WINDINGS 1UNIT = 90 TURNS/CM
POSITIVE WINDING SENSE 1CM = 2UNITS
LENGTH OF
IN UNITS O
R
WINDING SCHEME F
MUTUAL INDUCTAN
GOILS FOR X OF K
NEGATIVE WINDING SENSE
$h_1 \cdot h_2 \times 10^{-3}$
LENGTH OF COIL IN UNITS
COIL RADIUS

FIG. 8.

PRIMARY - 1 UNIT = 100 TURNS/CM

SECONARY - 1 UNIT = 1000 TURNS/CM

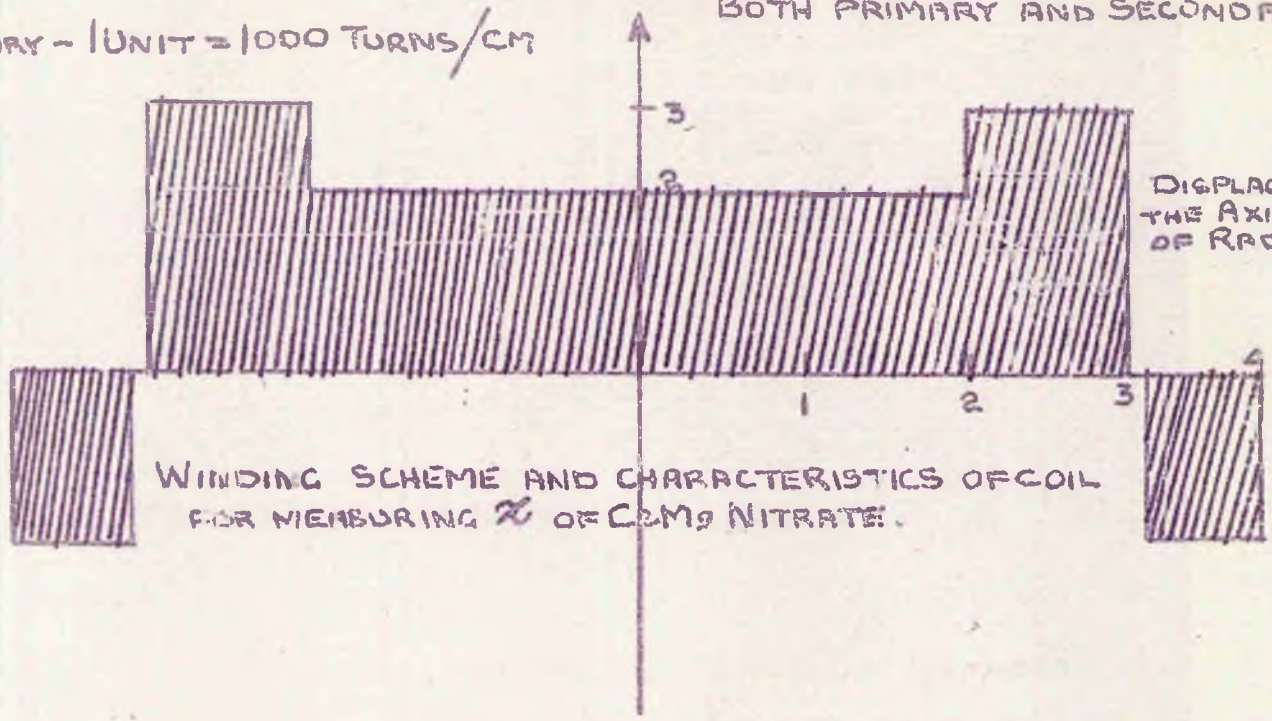

WINDING SCHEME AND CHARACTERISTICS OF COIL FOR MEASURING α OF $CoMg$ NITRATE.

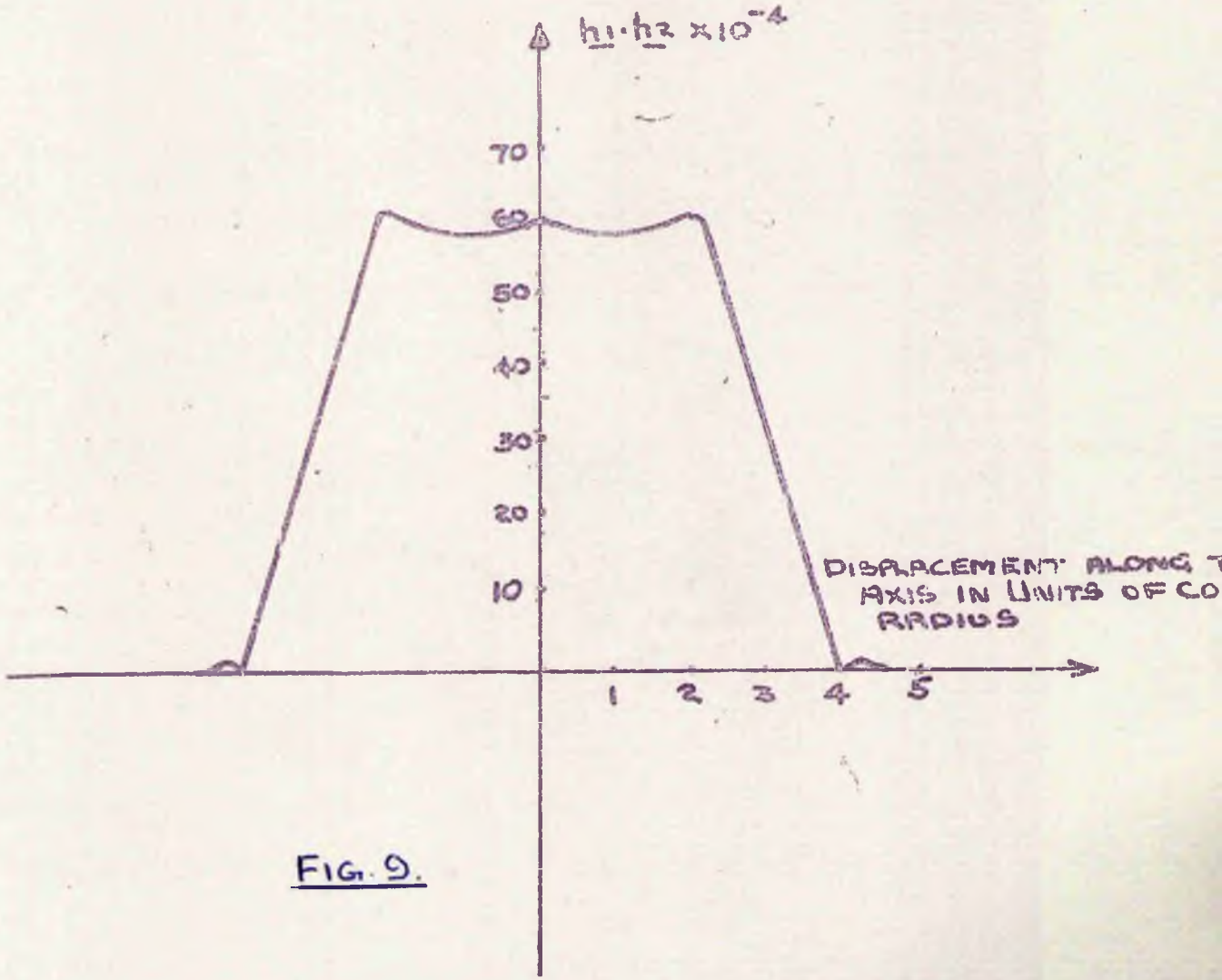

FIG. 9.

various points along the coil is as shown in the diagram where the vertical axis represents arbitrary positive and negative directions of winding. The change in mutual inductance due to the presence of the salt in the coils is given by

$$\Delta M = \int \underline{h}_1 . \underline{h}_2 \, \chi_{eff.} \, d\tau$$

where $\underline{h}_1$ and $\underline{h}_2$ are the fields per unit current due to the primary and secondary windings and χ_{eff} is the effective susceptibility of the salt. A plot of $\underline{h}_1 . \underline{h}_2$ as a function of distance along the coil axis is given opposite, (fig. 8).

The coils for measuring the susceptibility of the single crystal of cerium magnesium nitrate were wound on a nylon former machined to provide separators for the various parts of the coils. The overall length of the windings was 50 mm., and their internal diameter was 12mm. The windings were of copper, 0.15 mm. for the primary, and 0.07 mm. for the secondary. The winding schemes and a graph of $\underline{h}_1 . \underline{h}_2$ as a function of the distance along the axis of the coils are shown opposite, (fig. 9).

The alternating current passed through the primary of each of the mutual inductance coils was chosen to be 4 mA, at a frequency of 250 c/s, and for this value, the leads to the coils could be of small

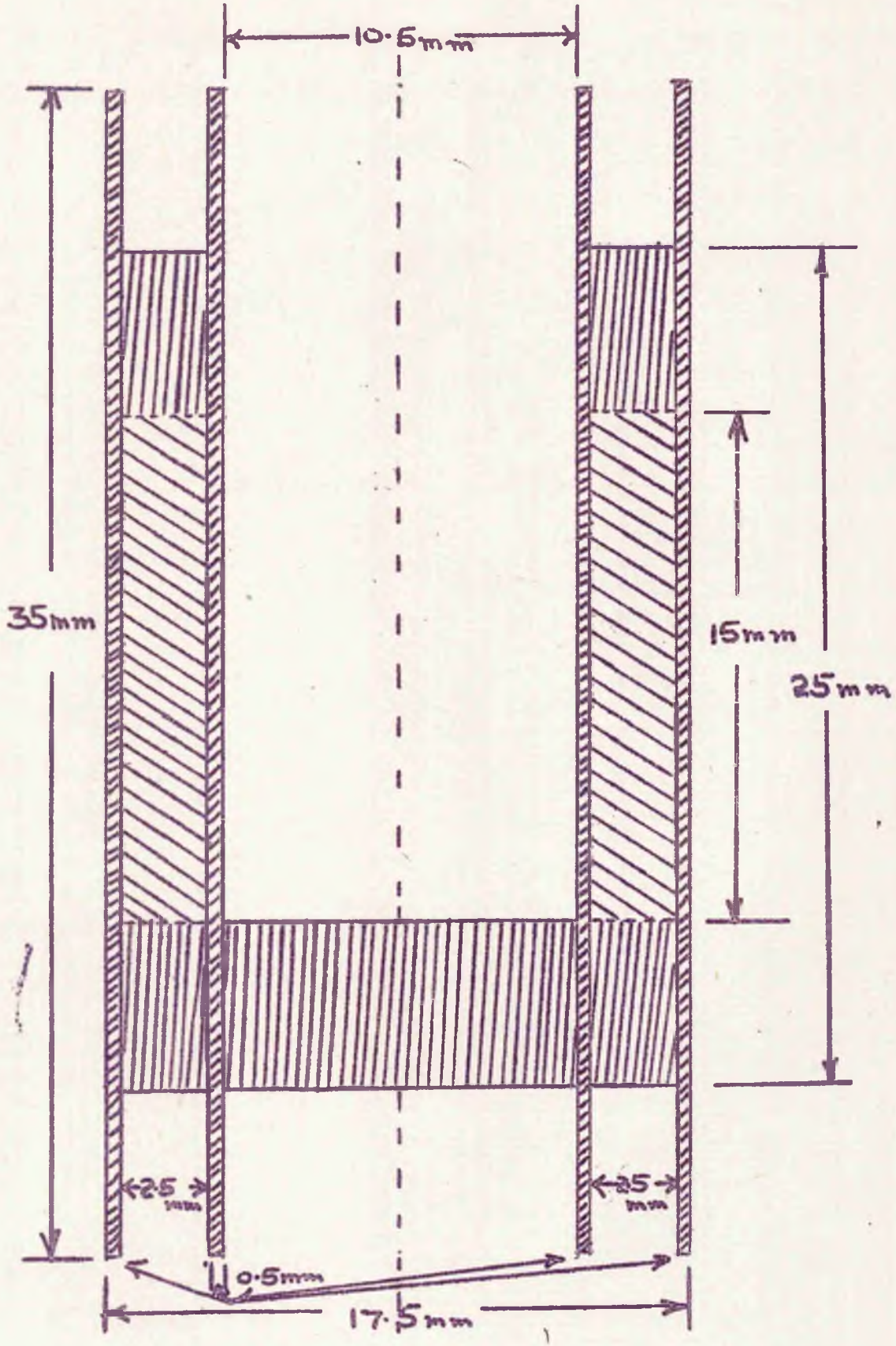

NYLON FORMER FOR HELMHOLTZ COILS

FIG. 2.0

cross-section. Leads of diameter 0.15 mm. were used so that the amount of heat conducted down into the liquid helium would be small. The leads were wound helically to increase their resistance to thermal conduction.

A Helmholtz pair of coils was used for magnetizing the specimen. The former for the coils was machined from nylon, to the dimensions indicated on the sketch overleaf. Each coil of the pair was wound with 950 turns of niobium wire of 0.003" diameter. A superconductor was used for the windings so that no power would be dissipated in the coil, thus avoiding excessive boiling of the liquid helium bath. The only heat dissipated in the liquid helium due to the coils was that produced in the copper leads to the coils. The diameter of the leads was fixed by minimising mathematically the total heat flow into the liquid helium due to power dissipation and thermal conduction down the leads from the rest of the apparatus. The optimum diameter was found to be 0.7 mm., but 0.95 mm. diameter wire was used since it was available, and little affected the result.

In practice it was found that the 5 litres of liquid helium in the Dewar lasted between 24 and 30 hours depending on the number of adiabatic demagnetizations carried out. This was much longer than was necessary for the experiment.

CHAPTER VII

The Design and Construction of the High-Power Solenoid

In order to cool the specimens to very low temperatures by the adiabatic demagnetization of paramagnetic potassium chromium alum, a high-power solenoid, cooled by demineralized water, was built according to a design by Geiser[29]. The solenoid produced a magnetic field of 39 oersted/amp. which was constant to better than 1 p.c. over a length of 8 cm. along the axis of the solenoid. The solenoid was energised by an electric current of 500 amp. and consumed a power of 138 kW. The internal diameter was 9 cm. which was sufficient to accommodate any cryostat used in the laboratory. It was mounted on hydraulic jacks on a mobile chassis. The jacks could raise it by 45 cm.

VII.1 The Theory of the Solenoid.

The magnetic field at the centre of a solenoid is given by Fabry's formula $H(0) = G\sqrt{\frac{W.\lambda}{\rho.a,}}$ (49)

where G is a dimensionless factor which depends on the shape of the solenoid.

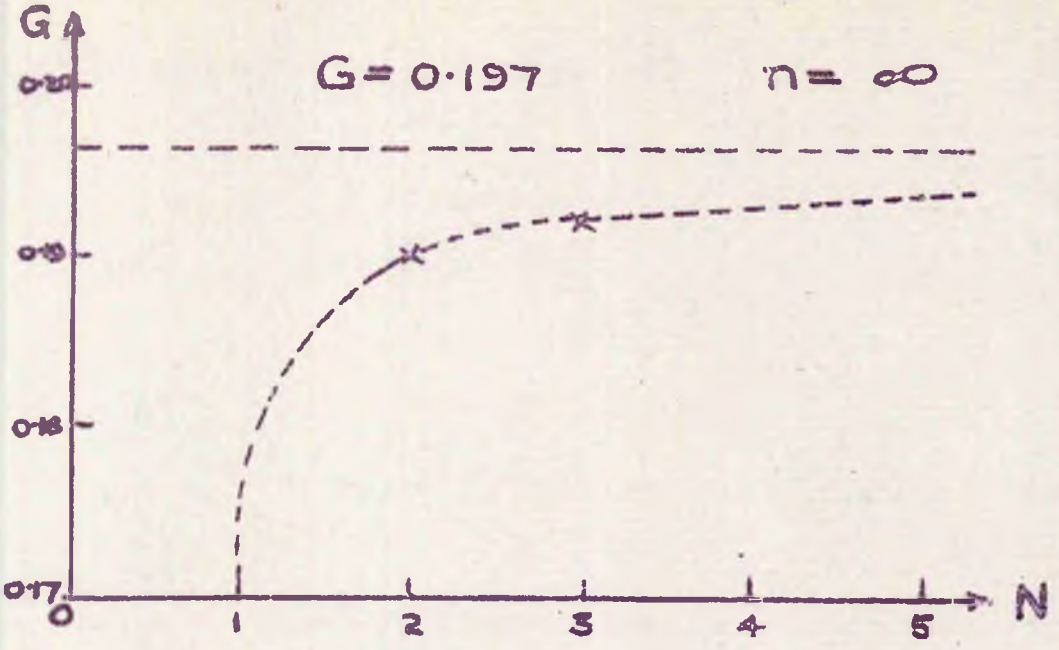

G AS A FUNCTION OF n

FIG. 10

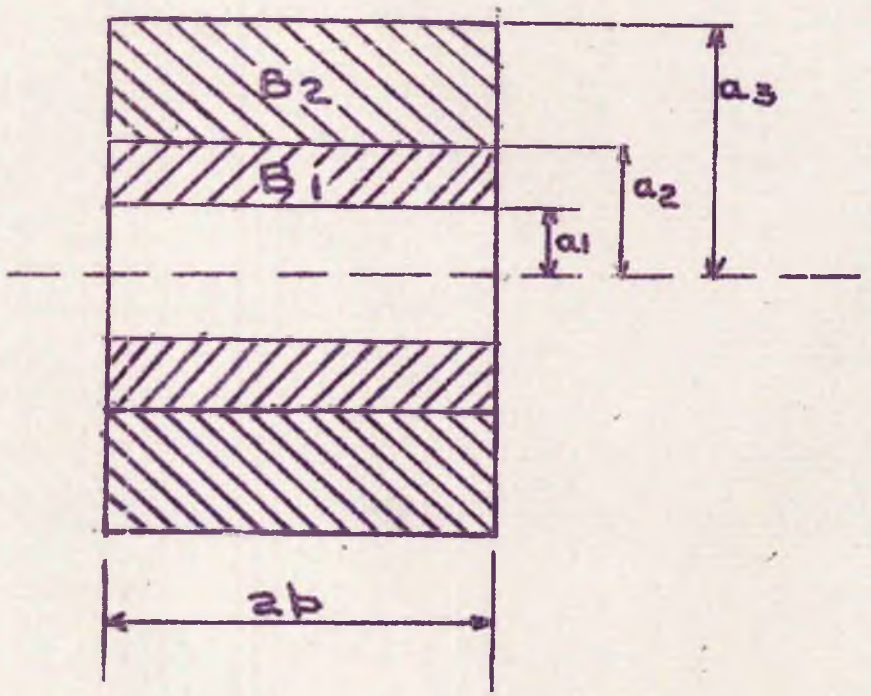

FIG. 11

NOTATION USED FOR DIMENSIONS OF SOLENOID

W is the power dissipated in the solenoid, in megawatts,
H(0) is the field at the centre in kilogauss,
ρ is the resistivity of the windings in ohm-cm.,
a_1 is the internal radius of the solenoid in cm.,
and λ is the filling factor of the solenoid, that is, the fraction of the volume of the solenoid which is occupied by conductor. We use the following notation to describe the dimensions of the solenoid: (fig.11.)

If a_2 is the external radius of the solenoid, $\frac{a_2}{a_1} = \alpha$.

If 2b is the overall length of the windings, $\frac{b}{a_1} = \beta$.

From equation (49) we see that the maximum field is obtained with a configuration such that G and λ are as large as possible. The problem here is to vary the current density as a function of the distance of the windings from the axis of the solenoid. This can best be done by considering the solenoid as composed of a number of separate superimposed coaxial coils.

Let n be the number of superimposed coils. In figure 10, a graph is shown of the value of G as a function of n for a solenoid with $\alpha = 4$, $\beta = 3$. It can be seen from this that the maximum value of G occurs for $n = \infty$, which is a condition satisfied approximately by having a different current density in each layer of the windings. This method of maxi-

mising G can be discarded as impracticable. The idea of having constant current density throughout the windings was rejected also because this gives a value of G 15 p.c. smaller than is given by n = 3. The value n = 2 was chosen since this gives a value of G only 3.5 p.c. smaller than the theoretical maximum. The value of G is not significantly increased by the use of three or more different current densities, and is undesirable for practical reasons.

VII.2 The Specification of the Solenoid.

The choice thus fell on a solenoid of two coaxial coils B_1 and B_2 with the three radii a_1, a_2, and a_3. It was decided to make provision for using the solenoid with the two sets of windings in series or parallel so that the solenoid could be used with the same voltage, but with double the current density in each set of windings. This imposes the condition that the two sets of windings have equal resistance, thus ensuring that equal power is dissipated in each coil. It was intended also to design the solenoid so that the field at the centre was uniform. The condition for this is that the second derivative of the field be zero at the centre.

In order to choose the values of α and β for

the solenoid, Table I, quoted by Tournier[30], should be considered. The table gives the values of G and G^* as functions of α and β, where G^* is the value of G obtained when the solenoid has been modified to give a uniform field at the centre. The Values of E give the percentage by which the field has been reduced by making it uniform at the centre.

Table I.

α	β	G	E	G^*
6	4	0.196	1.7 p.c.	0.1930
8	4	0.203	1.7 p.c.	0.1990
6	3	0.209	3.22 p.c.	0.202
6	2	0.218	8.23 p.c.	0.200
4	3	0.197	2.82 p.c.	0.192
4	2	0.208	8.45 p.c.	0.190

In spite of the fact that high values of G are obtained only for the higher values of α, a value of $\alpha = 4$ was chosen for economic reasons. From the table, for $\alpha = 4$, we see that G is greater for $\beta = 2$, whereas G^* is greater for $\beta = 3$. Accordingly, $\beta = 2.5$ was chosen. For $\alpha = 4$, $\beta = 2.5$, and the condition of equal resistances for the two coils, calculation shows that $\frac{a_1}{a_2} = 0.5$.

The method of removing some of the windings

SECTION OF THE SOLENOID

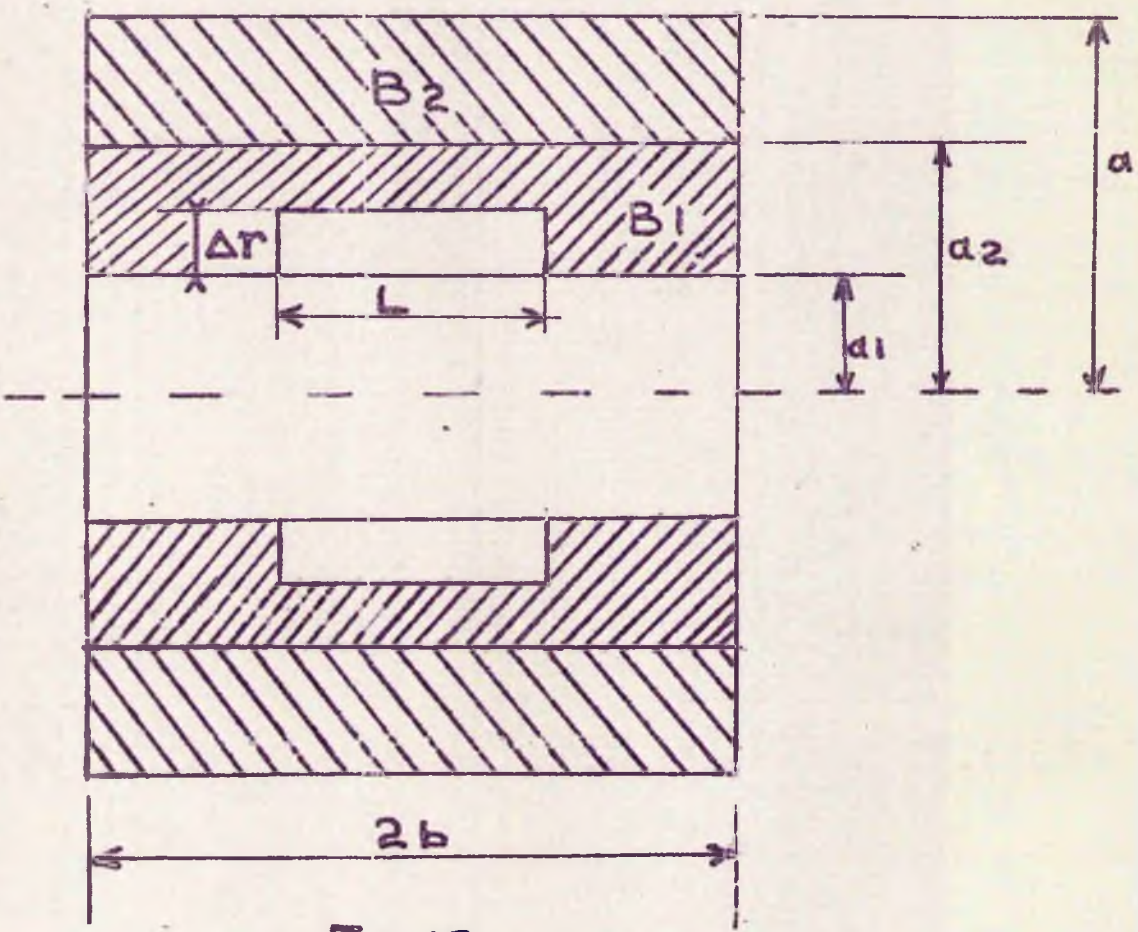

FIG. 12

Δ^r = 1·5cm

L = 3·7cm

in the middle of the solenoid was used to make the field uniform at the centre of the solenoid. This was done over a length of about 3.7 cm. and a thickness of 1.5 cm. by substituting one turn of copper sheet of the same thickness as one layer of winding for the appropriate number of turns of the wire. This gave a field constant to 1 p.c. along about 8 cm. of the axis of the solenoid around the centre, but by doing this, the field at the centre was reduced by about 9 p.c.

VII.3 The Characteristics of the Solenoid.

Since a generator producing 500 amp. at a maximum voltage of 300 V was available, it was decided to build a solenoid producing 20000 oersted in a volume of radius 4.5 cm. A section of the solenoid is shown in figure 12. The former of the solenoid was copper tube of internal diameter 8.9 cm. and length 39 cm., which was covered by fibreglass to ensure insulation. The internal winding B_1 was wound round this tube, and the winding B_2 was wound on B_1. The windings B_1 and B_2 were contained between two fibreglass discs which were designed to distribute the cooling water over the whole end surface of the windings. All of this was encased in a brass cylinder with two brass end plates

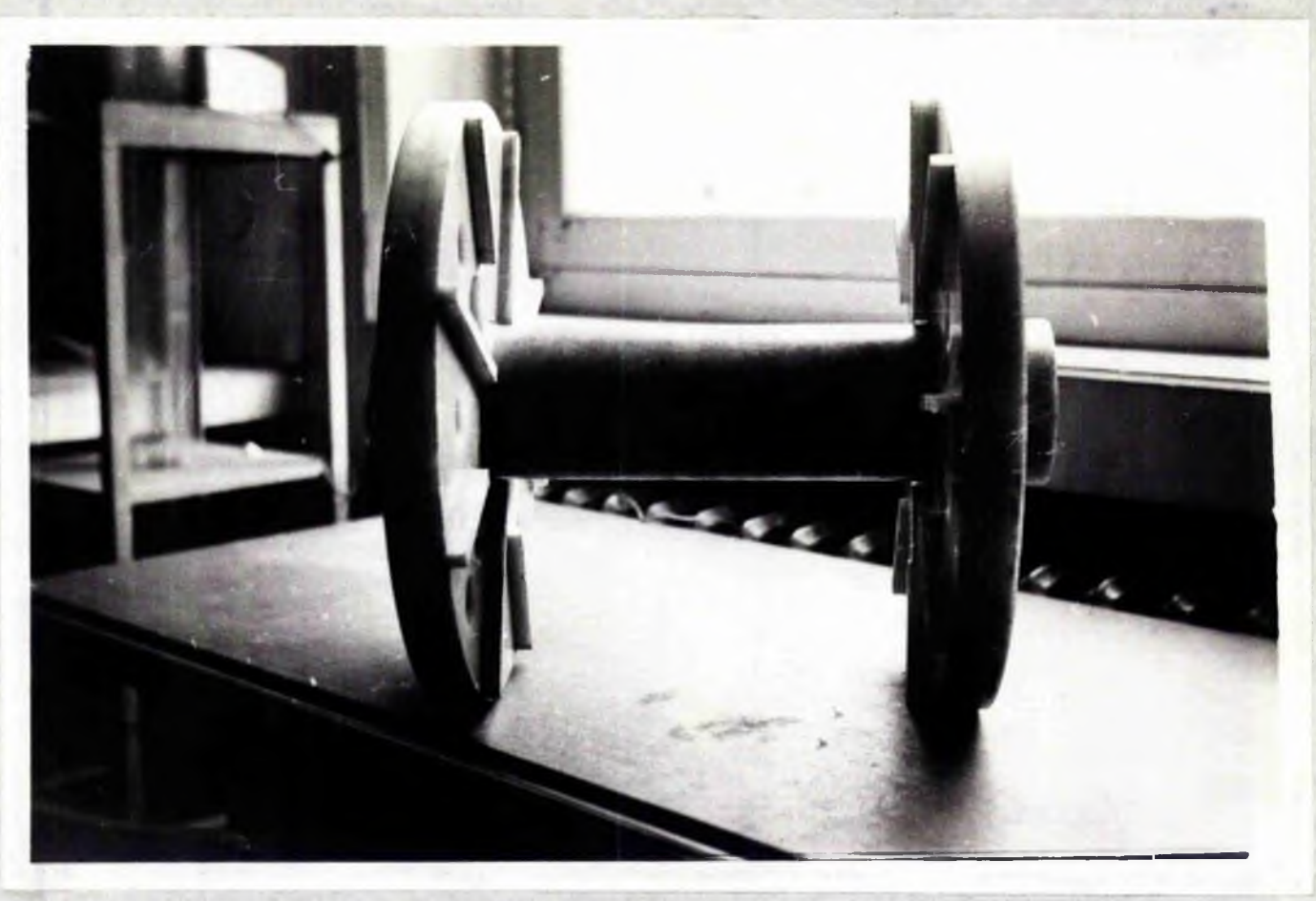

Plate 4. The Fibre-glass Former for the Solenoid.

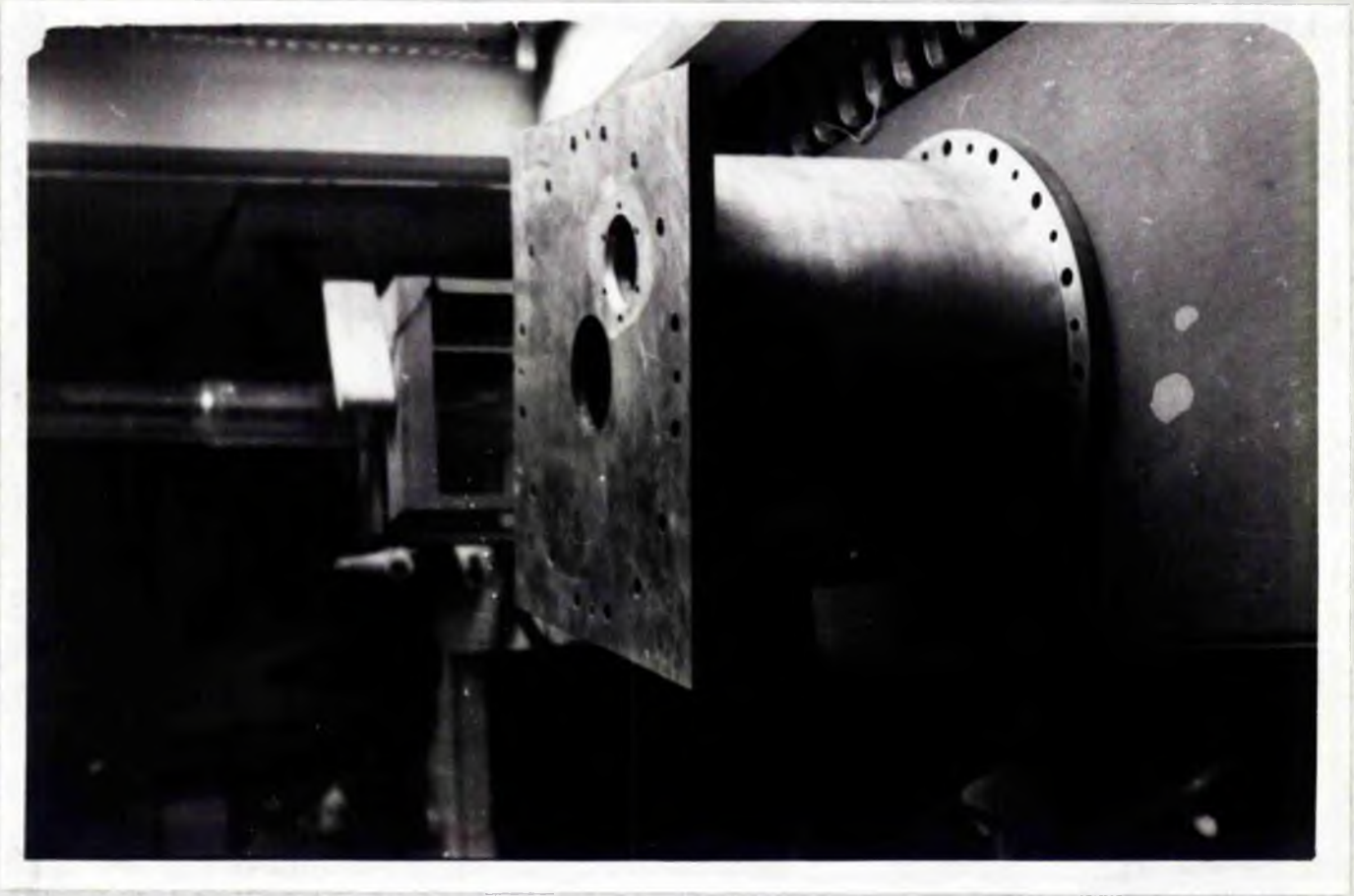

Plate 5. The Casing of the Solenoid.

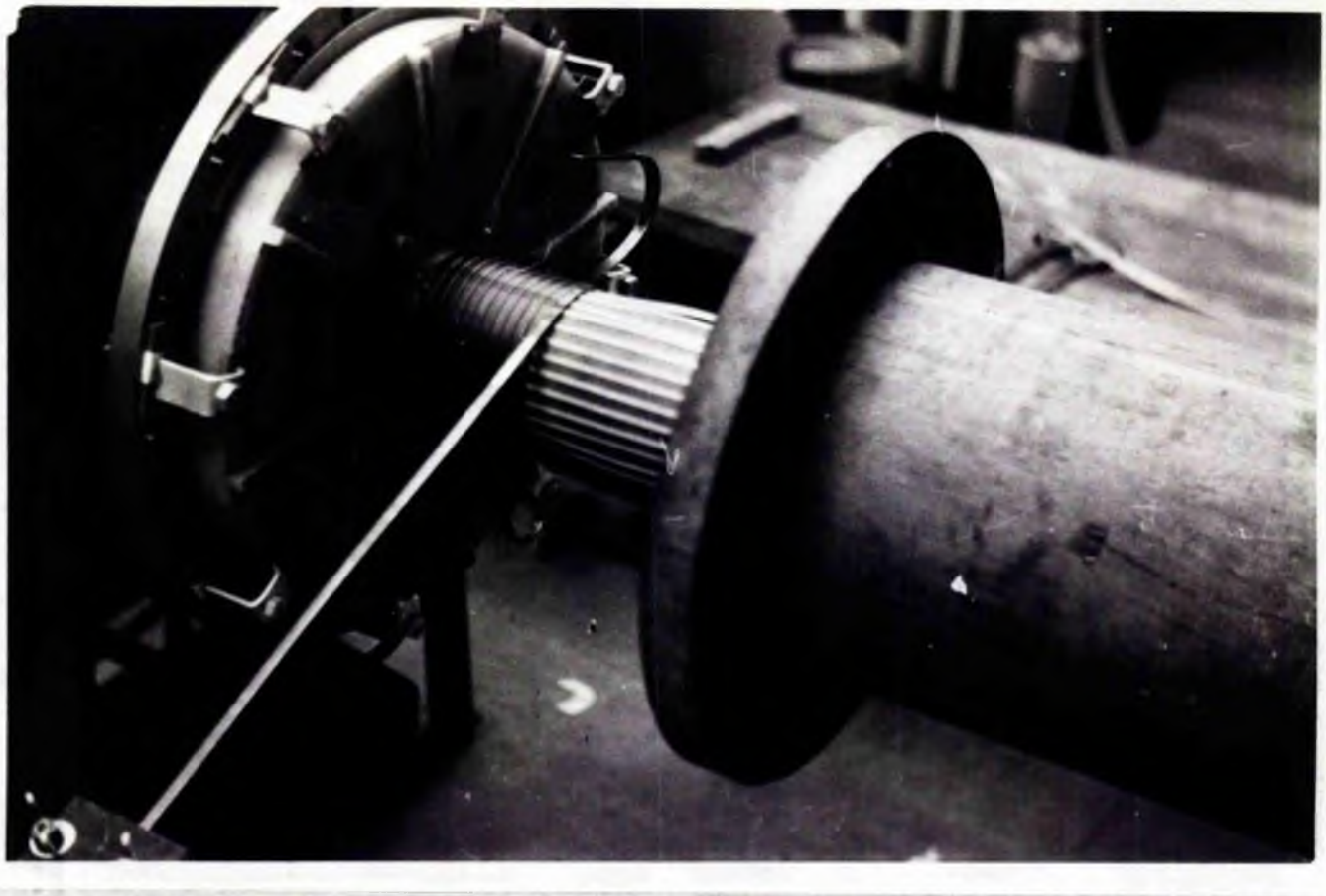

Plate 6. The Winding of the Solenoid.

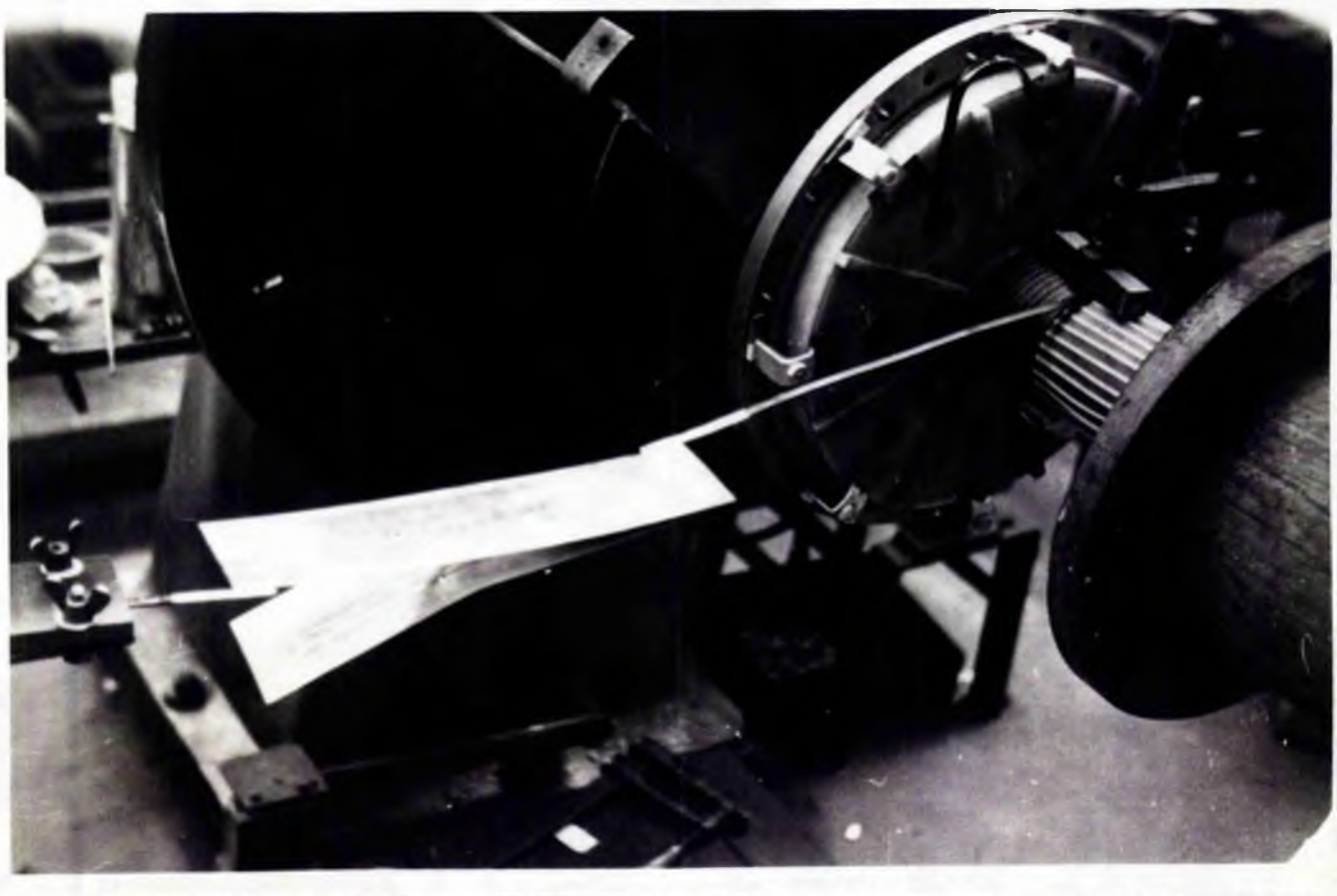

Plate 7. The Use of Copper Sheet to Replace Windings.

which were secured by brass rods. The casing was made water-tight with rubber O-ring seals. The casing and the former are shown in plates 5 and 4. Plate 6 shows the winding of the solenoid, and plate 7 shows the method of replacing some turns of B_1 with copper sheet.

The windings B_1 and B_2 were of varnished copper wire of rectangular sections $S = 14.20$ mm.^{2}, and 30.68 mm.^{2}, respectively. The resistances at 20°C of the two coils were, respectively, $R_1 = 0.26$ ohm, and $R_2 = 0.28$ ohm. The dimensions of the solenoid were:

internal radius of the coil B_1, $a_1 = 4.75$ cm.

external radius of the coil B_1, $a_2 = 9.45$ cm.

internal radius of the coil B_2, $a_2 = 9.45$ cm.

external radius of the coil B_2, $a_3 = 18.2$ cm.

The lengths of the coils were, respectively, $2b_1 = 25.0$ cm. and $2b_2 = 24.4$ cm. The coil B_1 was wound with 16 layers each of 34 turns, and B_2 with 24 layers each of 24 turns. The overall length of the solenoid case was 37 cm., the diameter of the brass cylinder was 38.3 cm., and one end plate was a square of side 44 cm. The varnished wire was wound layer by layer. The turns were insulated from each other by the varnish. The insulation between layers was ensured by strips of fibreglass 0.4 mm. thick and 3 mm. wide, separated from each other by 3.3 mm. By

this means channels were formed which allowed cooling water to circulate between the layers. Since the same power is dissipated in each set of windings, the same cooling surface was necessary for each set. This was achieved by introducing the separators between every layer in B_1 and between every second layer in B_2, so that the cooling surfaces were about equal. The replacement for the windings removed in B_1 to make the field homogeneous was arranged so that the cooling channels were not blocked.

The filling factor for B_1, was $\lambda_1 = 0.68$, and for B_2 was $\lambda_2 = 0.83$. The coefficient for the whole solenoid was $G = 0.178$.

The solenoid was cooled by demineralized water circulating in closed circuit which was cooled in a heat exchanger by water from the town supply. The rise in temperature of the water when the solenoid was operating at 150 kW was about $10^{\circ}C$. It was hoped that with improved heat exchange through the varnish, the solenoid could be operated with the windings in parallel at a power of about 1 MW producing a field of 50000 oe. The resistance between the windings and the casing was about 8000 ohms with water of resistivity 0.1 Megohm-cm.

The solenoid operating with the two windings in series at a power of 138 kW with a current of 500 amp. produced at the centre of the solenoid a magnetic

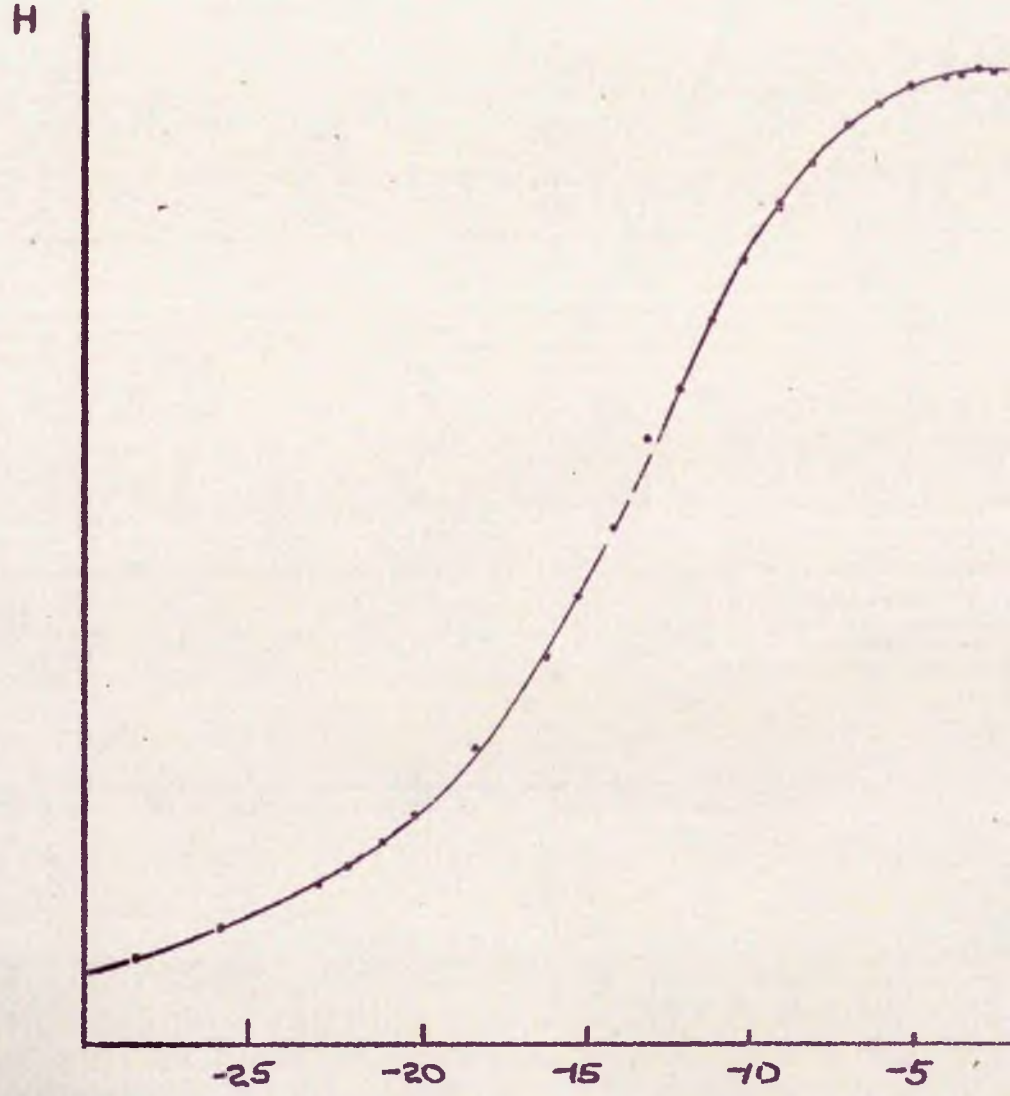

FIG. 13

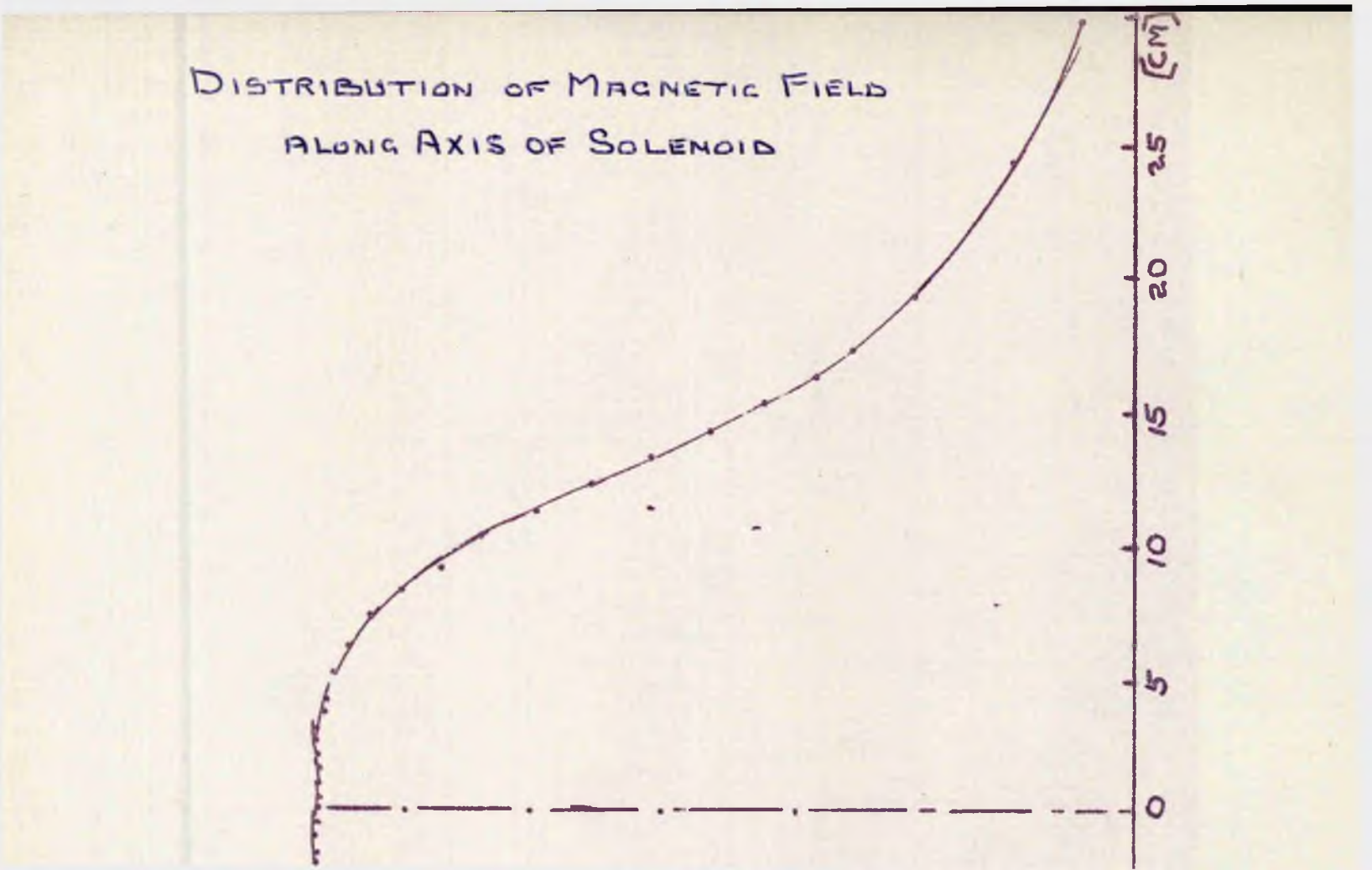
DISTRIBUTION OF MAGNETIC FIELD
ALONG AXIS OF SOLENOID
(CM)
25
20
15
10
5
0

field of 19000oersted, which was stable to about 1 p.c. (fig. 13).

CHAPTER VIII

The Conduct of a Run.

Preliminaries.

When the cryostat had been assembled and sealed, the inner and outer Dewars were mounted. Preliminary cooling was started with liquid nitrogen in the outer Dewar. The inner Dewar was pumped and tested for leaks. Gaseous helium was then admitted to the interior of the inner Dewar. The pressure of the helium in the inner Dewar was then measured with the mercury manometer with the inner Dewar closed to the helium gasometer. About 1 mm. Hg pressure of air was admitted between the walls of the inner Dewar to increase heat transfer from the cryostat to the liquid nitrogen in the outer Dewar. An estimate of the temperature of the cryostat could be made from the pressure of the helium gas in the inner Dewar.

When it was judged that the temperature of the cryostat had fallen far enough, the cryostat was evacuated, and tested for a leak. Helium exchange gas at about 40 mm. Hg pressure was then admitted to the

cryostat from the Dewar. The cryostat was not evacuated until it was cooled to near liquid nitrogen temperature so that damage to the salt pill by evaporation of the water in it could be avoided. The helium chamber was also evacuated, then filled with helium gas at atmospheric pressure. The apparatus was then left for another two hours to ensure complete cooling. The counting apparatus was switched on at this time so that it was thoroughly warmed up and stable by the time it was needed.

VIII.1 Helium Siphoning.

When the cryostat and the inner wall of the helium Dewar had been cooled to liquid nitrogen temperature, the interspace of the inner Dewar was completely evacuated. The interior of the Dewar was then refilled with gaseous helium and left open to the gas-holder at atmospheric pressure. Liquid helium was then transferred through a siphon into the Dewar with a pressure of 100 gm/cm^2. Cooling of the Dewar and the cryostat down to the boiling point of helium took about 20 - 30 minutes, then the Dewar was filled with about 5 litres of liquid helium, the whole process having taken 45 - 60 minutes. The cryostat was then evacuated, pumping being continued for about three hours while the temper-

ature of the helium bath remained at 4.2°K.

VIII,2 Calibration of the Thermometers.

The pressure above the helium bath was then lowered until the helium in the small chamber had liquefied. This was seen to be the case when the pressure in the chamber closely followed the pressure above the liquid helium. The helium in the chamber usually liquefied when the pressure in the helium bath was about 10 cm.Hg, corresponding to a temperature of about 2.6°K. The temperature of the helium chamber, and thus the temperature of the salt and the specimen, closely followed that of the helium bath.

The purpose of the helium chamber can now be seen. The chamber provided a thermal link between the salt pill and the helium bath by a process of evaporation and recondensation of the liquid helium in the chamber. This link could be broken by pumping all the helium from the chamber. The thermal isolation was good because the stainless steel capillary linking the chamber to the cryostat cap conducted very little heat at low temperatures. This system had the advantage that helium exchange gas in the cryostat was unnecessary, so that the cryostat could be pumped at the relatively high temperature of 4°K,

thus ensuring a much better vacuum at low temperatures than would be possible if the cryostat were pumped at $1^{\circ}K$. The helium chamber could be more easily evacuated at low temperatures because of its small volume. This resulted in much better thermal isolation of the salt pill and the specimen.

The temperature of the helium bath was reduced by stages by pumping, and at each stage measurements of the pressure in the helium chamber gave its temperature. Measurements of the mutual inductance of the large coil were made at each stage. It was found to be impossible to make measurements of the variation in mutual inductance of the small coils for the measurements of the susceptibility of the cerium magnesium nitrate, in spite of modifications to the coils and in the method of mounting the crystal which was found to shatter during cooling.

From the measurements of mutual inductance and helium vapour pressure, a calibration curve of mutual inductance against temperature, found from the 1958 He^{4} scale of temperatures, published by the National Bureau of Standards, was drawn.

When measurements of mutual inductance are made at different temperatures between $1^{\circ}K$ and $4^{\circ}K$, a curve is obtained which has the form $T = \frac{B}{A-M}$.

For the correct use of the curve it is better to consider the magnetic temperature T*, since this is what is measured at very low temperatures. Between $1^{\circ}K$ and $4^{\circ}K$, T and T* are related by:

$$\frac{T^*}{T} = 1 + \frac{1}{3}\left(\frac{4\pi}{3} - n\right)\frac{C}{vfT},$$

where $\frac{C}{V}$ is the Curie constant per unit volume, f is the filling factor of the salt pill, and $n = 4\pi\varepsilon$, where ε is the eccentricity of the ellipsoid.

$$\text{Let} \quad \Delta = \frac{1}{3}\left(\frac{4\pi}{3} - n\right)\frac{C}{vf}, \tag{50}$$

$$\text{then} \quad T = T^* - \Delta$$

$$\text{and} \quad T^* = \frac{B}{A-M} + \Delta \tag{51}$$

where A is the value of M at $\frac{1}{T^*-\Delta} = 0$, and B is the gradient of the curve. Hence, plotting M as a function of $\frac{1}{T^*-\Delta}$ we obtain a linear graph of equation:

$$A - M = \frac{B}{T^*-\Delta}.$$

Now, substituting in equation (50) the values for the salt pill used in the experiment,

$$\Delta = \frac{1}{3}\left(\frac{4\pi}{3} - 0.677\right)\frac{0.00204}{0.51}$$

$$\text{i.e.} \quad \Delta = 0.0047$$

$$\text{Then,} \quad T^* = \frac{B}{A-M} + 0.0047 \tag{52}$$

Thus from a measured value of mutual inductance one can find the corresponding magnetic temperature.

VIII.3 The Magnetic Cooling.

When the calibration of the salt thermometer was completed, preparations for the adiabatic demagnetisation were made. The solenoid was moved below the Dewars, and raised around them with the hydraulic jacks, and the cooling water turned on. The large valve in the helium pumping line was fully opened, and the pressure above the liquid helium reduced to the minimum possible. The temperature of the helium bath was then 1.15°K. The valve to the cryostat was closed and pumping on the helium chamber started. At this point the magnetic field was turned on slowly while pumping on the helium chamber continued. If the amount of helium admitted to the chamber were correctly chosen, the heat generated in the salt pill during magnetisation would be just sufficient to evaporate most of the helium in the chamber. The rapid pumping of what was left when the heat of magnetisation had been dissipated ensured a low starting temperature for the demagnetisation, about 0.8°K. If it appeared that too much helium had been admitted to the chamber, the chamber was gently heated with about 10^{-2} watts to speed up evaporation. Pumping on the cryostat was then restarted in order to maintain a hard vacuum. The magnetic field used for the magnetic cooling varied between 13000 and 17000 oersted, depend-

ing on the run.

When a hard vacuum had been attained, say 4 to 6×10^{-6} mm. Hg, the magnetic field was slowly reduced to zero, and the solenoid lowered. The scintillation counters were then mounted on a table fixed to the top of the solenoid in predetermined positions at the level of the specimen, the positions of the scintillation counters being arranged so that they were perpendicular and parallel, respectively, to the direction of magnetization of the specimen. Simultaneously, measurements of mutual inductance were started. One member of the team made measurements of mutual inductance as a function of elapsed time, the other measured the γ-ray count-rate as a function of elapsed time. Afterwards the two measurements were combined to express γ-ray count-rate as a function of temperature. The magnetic temperatures T* were found by substituting for M in equation (52). The thermodynamic temperatures were found from a curve of T against T* for potassium chromium alum provided by Dr J.A. Beun. Measurements of the γ-ray count-rate continued until about 0.2°K was reached. This took about 2 or 3 hours, so that it was usually possible to make 2 or 3 sets of measurements in the course of one run, by repeating the magnetic cooling process.

CHAPTER IX

Experimental Results

IX.1 The Nuclear Polarization of Co^{60} in a 50% Alloy of Cobalt and Nickel.

This experiment was carried out in order to verify the working of the apparatus. Nuclear polarization experiments have been done by Grace, Johnson, Scurlock and Taylor[13] on pure hexagonal cobalt, and by Johnson and Scurlock[14] on a dilute alloy of cobalt in nickel. We therefore considered that nuclear polarization of Co^{60} nuclei in a 50% alloy of cobalt and nickel should be fairly easy to achieve, and should provide a satisfactory test of the apparatus. The results of this experiment are reported here for interest.

The specimen was soldered to the end of the copper rod which was in thermal contact with the cooling salt, potassium chromium alum. The specimen was cooled to about 0.02°K by adiabatic demagnetization, and magnetized by a field of 1300 oersted which was applied by means of a Helmholtz pair of coils. The intensity of the γ-radiation emitted was then measured simultaneously

THE VARIATION OF γ-RAY INTENSITY AS A FUNCTION OF T^{-1}
FOR THE 1·17 MeV RADIATION FROM Co^{60}

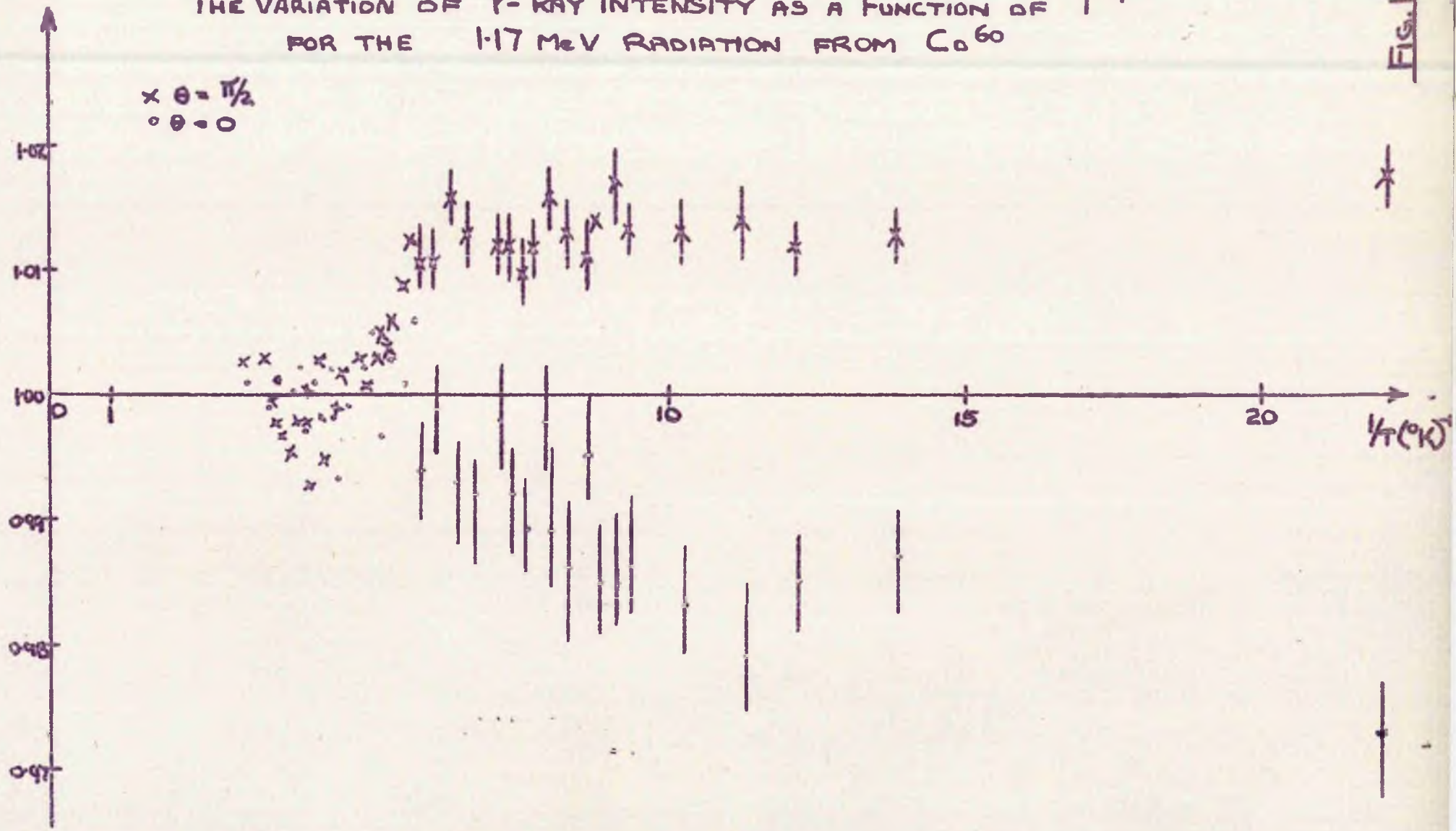

FIG. 14

FIG. 14

Fig. 15

√S as a function of T⁻¹ for the 1.17 MeV γ-radiation of Co⁶⁰
√S
0·20
0·15
0·10
0·05
5
10
15
20
1/T(°K)⁻¹

FIG. 15

parallel and perpendicular to the magnetic field, as a function of the temperature of the specimen.

The Co^{60} nuclei emit radiation of energy 1.17 MeV by the transition $4+ \longrightarrow 2+$, after a β^- disintegration of energy 312 keV arising from the transition $5+ \longrightarrow 4+$. If we estimate the number of β^- disintegrations which completely dissipate their energy in the specimen to be about 50%, then the energy dissipated in the specimen will be about 0.5 ergs/sec. The specimen receives about 0.5 ergs/sec. from other sources, so the total heat flux on the specimen was about 60 ergs/minute.

The variation of the intensity of radiation in the two directions parallel and perpendicular to the direction of magnetization of the specimen was measured over the temperature range $0.025^{\circ}K$ to $1^{\circ}K$ during about 3 hours, and is shown as a function of the reciprocal of the temperature in figure (14). $\sqrt{\varepsilon}$, as defined in equation (47), was then evaluated for each pair, $W(\pi/2)$ and $W(0)$, and plotted as a function of $1/T$ in figure (15). We see from equation (42) that $\sqrt{\varepsilon}$ is proportional to $1/T$ for small β, i.e. for values of T which are not too small. We see from figure (15) that a straight line can be drawn through the origin for small values of $1/T$. The slope of

the line was calculated by the method of least squares and gives the result $T.\sqrt{\varepsilon} = (1.6 \pm 0.2) \times 10^{-2}$.

The angular distribution of the 1.17 MeV γ-radiation from Co^{60} is $W(\theta) = 1 - \frac{60}{49}f_2(4)P_2(\cos\theta) - \frac{64}{21}f_4(4)P_4(\cos\theta)$, where the f_k are functions of the spin of the energy level. If we take into account the influence of the preceding β^- transition $5+ \longrightarrow 4+$ on the orientation of the nuclei, we find that the relation between the orientation parameters f_k before and after the transition is $f_k(4) = B_k f_k(5)$, where B_2 and B_4 are found to be given by

$$B_2 = \frac{11 \times 25}{16}\sqrt{\frac{14}{39}}\cdot\frac{2\sqrt{182}}{165\sqrt{3}} = \frac{35}{36}$$

$$B_4 = \frac{11\sqrt{7} \times (5)^4}{\sqrt{7} \times 33(4)^4} = \frac{625}{768}$$

The angular distribution of the 1.17 MeV γ-radiation is the given by $W(\theta) = 1 - \frac{25}{21}f_2(5)P_2(\cos\theta) - \frac{625}{252}f_4(5)P_4(\cos\theta)$. Now, if $\beta = \frac{\mu H}{kTI} \ll 1$, the anisotropy $\varepsilon = \frac{195\beta^2}{56}$, whence

$$\sqrt{\varepsilon} = 4.85 \times 10^8 \cdot \frac{H}{T}.$$

The effective magnetic field is thus $H = 2.06 \times 10^7 \cdot T\sqrt{\varepsilon}$ Using the value of $T\sqrt{\varepsilon}$ obtained from the curve, we calculate the effective magnetic field to be $H = (330 \pm 40) \times 10^3$ oersted. At $0.02^\circ K$, the degree of polarization of the orientated nuclei $f_1 = \frac{I_z}{I} = 0.7$, with $\beta = 0.43$. At this temperature, the sublevel m = 5 is at least

fifty times more heavily populated than the sublevel $m = -5$. At $0.05^{\circ}K$, $f_1 = 0.3$, and the ratio of the populations a_5/a_{-5} is less than 10.

Arp, Edmunds and Petersen[31] have obtained a value of (161 ± 3) kOersted for the hyperfine field in a 60% Co-40% Ni alloy, to which must be added about 5 kGauss to include the applied external field and the Lorentz field, for comparison with our result, but even so there is considerable disagreement with the result we have obtained. This could be due to differences in electron structure between alloys of different concentration, but it is more likely to be due to inaccurate measurements of temperature. It would appear that our measurements of temperature are too high by about a factor of two.

IX.2 The Nuclear Polarization of Au^{198} in a 1% Alloy of Gold in Gadolinium.

When the specimen of the alloy of 1% gold in gadolinium had been irradiated in the reactor, it was left until the activity of Gd^{159} of half-life 18 hours had declined to a negligible level. The specimen was then glued with araldite to the copper rod which was in thermal contact with the refrigerant salt.

The specimen was then cooled to about $0.02^{\circ}K$

Fig. 15

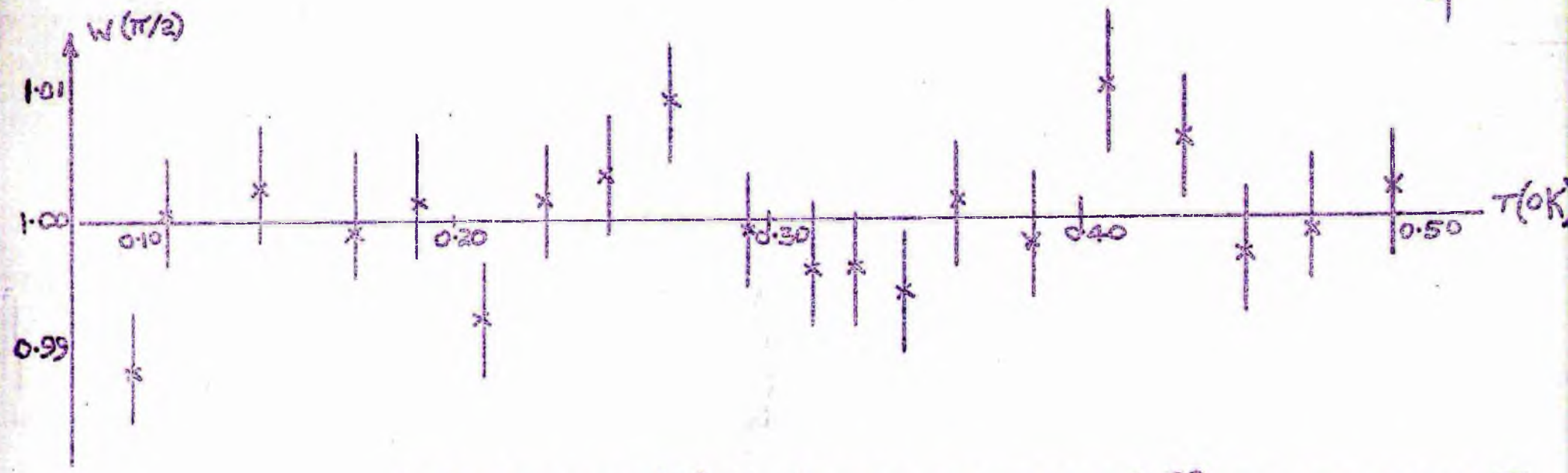

INTENSITY OF 411 KeV γ-RADIATION FROM Au^{198} AS A FUNCTION OF T

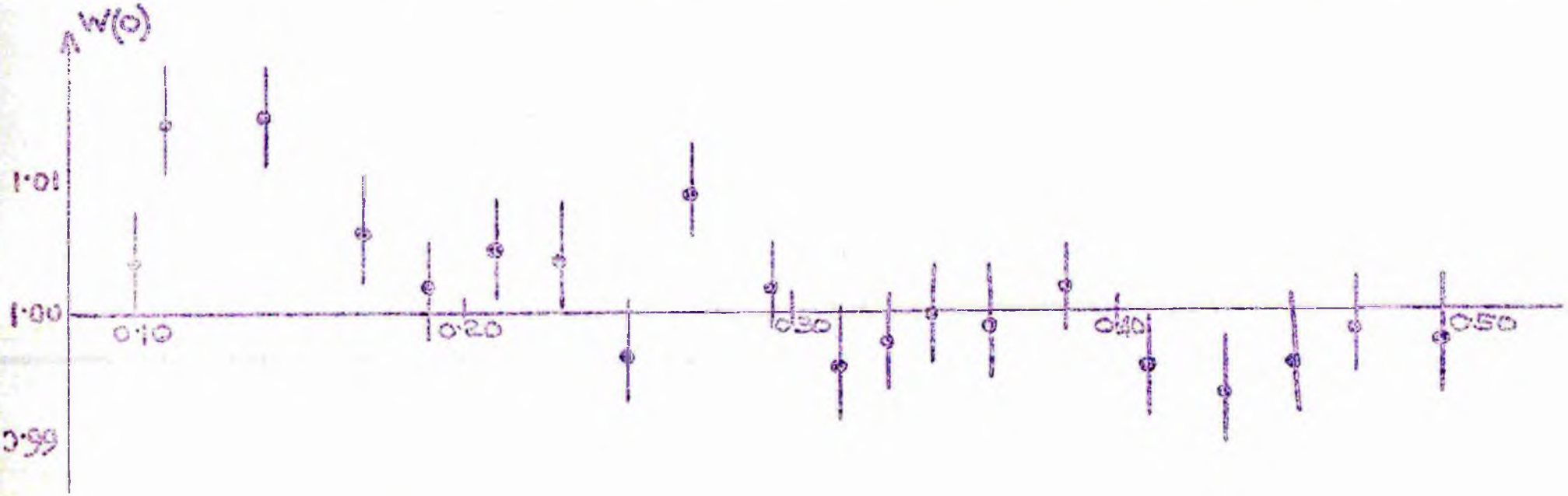

by adiabatic demagnetization of the salt, and magnetized with a magnetic field of 1300 gauss. The intensity of the 411 keV γ-radiation was then measured simultaneously parallel and perpendicularly to the direction of magnetization of the specimen as a function of elapsed time. The temperature of the salt pill was measured simultaneously, also as a function of elapsed time. Afterwards the two sets of measurements were combined to show the γ-ray count-rate as a function of specimen temperature. The salt pill and the specimen were assumed to be at the same temperature. The energy dissipated in the specimen by the β^- disintegrations was estimated to be 0.3 erg/second, giving a total heat flux on the specimen of about 50 ergs/minute.

A series of six experiments was carried out in the temperature range $0.02^{\circ}K$ to $1^{\circ}K$, each experiment lasting about three hours. Figures (16), (17) and (18) show the intensity of γ-radiation as a function of temperature for the experiments 4, 5 and 6. Each value of the count-rates $W(\pi/2)$ and $W(0)$ is obtained from a counting period of two minutes, and is normalized by dividing $W(\pi/2)$ and $W(0)$, respectively, by $W^1(\pi/2)$ and $W^1(0)$, which are the γ-ray count-rates for a specimen at $1^{\circ}K$. Error bars are shown for each point on the graphs, and are statistical errors which depend on

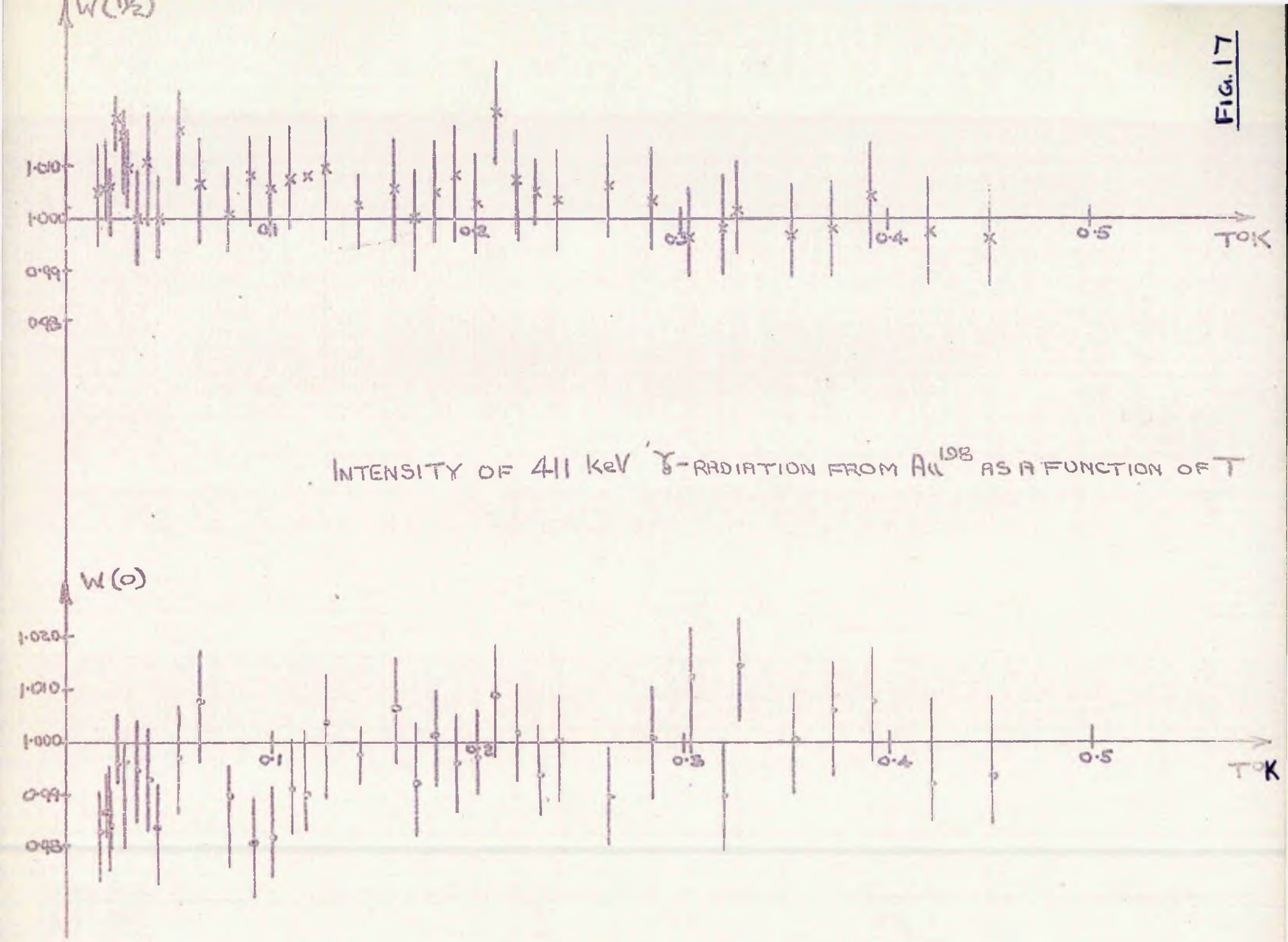

FIG. 17

INTENSITY OF 411 keV γ-RADIATION FROM Au^{198} AS A FUNCTION OF T

the activity of the sample and the distance from the sample to the scintillation counters. The error in the count-rate varied from three to eight parts per thousand.

The results of three of the six experiments performed have been selected as they are typical. Figure 16 shows normalized values of $W(\pi/2)$ and $W(0)$ for the fourth experiment. The normalized values of $W(\pi/2)$ show a normal scatter about the value $W(\pi/2) = 1$, and most of the error bars about those points are intersected by the line $W(\pi/2) = 1$. The normalized values of $W(0)$ show rather more scatter, but generally follow the same distribution. High values of $W(\pi/2)$ mostly coincide with high values of $W(0)$. From the angular distribution curve of quadrupolar γ-emission from Au^{198}, we should expect that $W(\pi/2)$ would be increased at the expense of $W(0)$ by the existence of nuclear orientation. In the temperature range up to $0.15^{\circ}K$, the opposite effect has occurred. Such anisotropy as exists is random.

This is seen even more clearly in figure 17, and in this case measurements were made from much lower temperatures. We concentrated in this experiment on the temperature range $0.01^{\circ}K$ to $0.1^{\circ}K$. We see quite clearly that while the γ-ray count-rate in the parallel direction $W(0)$ increases quite sharply in this

Fig. 18

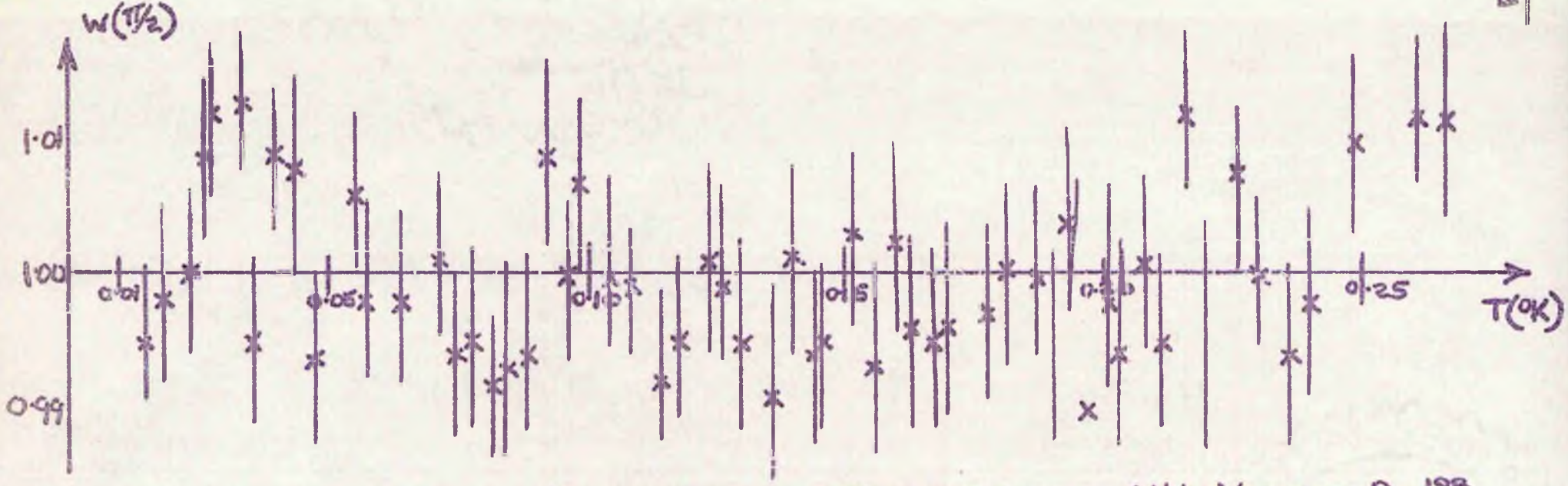

INTENSITY OF γ-RADIATION OF 411 keV FROM Au^{198}

AS A FUNCTION OF T.

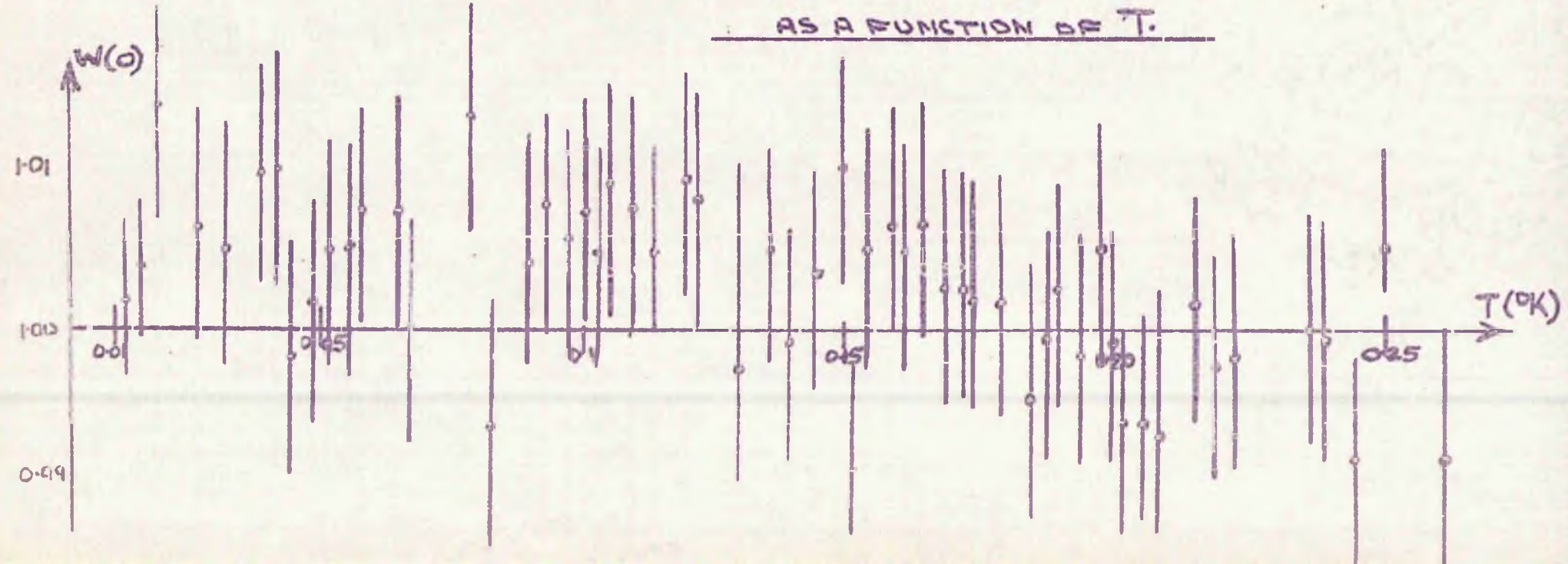

$\sqrt{E}$ AS A FUNCTION OF T^{-1} FOR 411 keV γ-RADIATION FROM Au^{198}

FIG. 19

range, so too does the γ -ray count-rate in the perpendicular direction, whereas, as remarked earlier, we should expect to see W(0) increase at the expense of $W(\pi/2)$ with rising temperature.

From the results of the sixth experiment, shown in figure 18, one might be tempted to suggest that there is an anisotropy present. This is particularly noticeable in the temperature range $0.1^{\circ}K$ to $0.2^{\circ}K$. Once again, however, the objection arises that the values of W(0) should increase with rising temperature if the anisotropy is due to nuclear orientation. In any case, nuclear orientation could only occur in this temperature range if the internal magnetic field were of the order of 10^7 oersted, which seems most unlikely. The fact that W(0) is consistently larger than unity is puzzling, but must be due to some statistical factor.

We must conclude, therefore, that the results obtained show no evidence of anisotropy in the angular distribution of γ -radiation from the specimen which is attributable to nuclear orientation.

We have plotted in figure 19 an 'anisotropy' obtained by subtracting W(0) from $W(\pi/2)$ as a function of temperature. From this we see that an anisotropy of 1% would be undetected in this experiment, taking into account statistical errors in W(0) and $W(\pi/2)$.

We can, therefore, put an upper limit to a possible anisotropy of 1%, which gives an upper limit to the field at the Au^{198} nuclei in alloy in gadolinium metal. Since

$$\sqrt{\varepsilon} = 0.79 \times 10^{8} \cdot \frac{H}{T} \leq 0.01 \text{ for } Au^{198}, \text{ we obtain}$$

$$H \leq 1.27 \times 10^{7} \cdot T \text{ oersted.}$$

The lowest temperature obtained was about 0.016°K, so we estimate the upper limit of the internal effective magnetic field at the Au^{198} nuclei to be about 2×10^{5} oersted, but if we consider that the measured values of temperature may be too high by a factor of about two, then the upper limit of the internal field is about 100 kOersted.

IX.3 An Estimate of the Effective Field on the Au^{198} Nucleus in the Gadolinium - Gold Alloy.

An estimate of the effective field at the gold nucleus was made by taking into account two terms. The first term is the contact interaction between the conduction electrons of the gadolinium and the gold nucleus. Using the expression (20) and the value for $\rho_{\uparrow}(0) - \rho_{\downarrow}(0)$ given by Freeman and Watson[26] evaluated at a lattice point for an average lattice spacing of 6.84 a.u., which is about 0.07, we find on evaluating expression (20)

$$\chi = \frac{4\pi}{1} \times \frac{1}{2} \times 0.07 \quad \text{a.u.}$$

Therefore $H_c = 2\pi \times 0.07 \times 4.21 \times 10^4$ oersted.

$= 18.5 \times 10^3$ oersted.

This calculation shows that polarised conduction electrons of gadolinium would produce a field of about 18.5 kGauss at a gold nucleus if the effect of magnetising the specimen were to make 1.5 6s electrons per atom align themselves with spin parallel to the direction of magnetisation and 0.5 6s electrons per atom with spin antiparallel to the direction of magnetisation, that is, producing one unpaired conduction electron per atom of gadolinium.

The second term we assumed to be due to hyperfine interaction between core s-electrons of the gold and its nucleus which were unpaired through interaction with the polarised conduction electrons of the gadolinium. If we assume that this interaction produces an increase in the orbital radii of the spin-antiparallel s-electrons of the order of 10%, we can estimate the possible effect by considering the non-relativistic Hartree wave functions for mercury s-electrons. Mercury is next to gold in the periodic table, and it is convenient to use the Hartree functions for Hg to enable us to make an estimate of the magnetic field.

The estimate was made by using the wave functions for an orbital radius of about 0.1 a.u. We supposed that the one electron spin densities at a radius of 0.1063 a.u. represented spin-parallel electrons, and that the spin densities at a radius of 0.1156 a.u. represented spin antiparallel electrons. The s-wave functions are given below, in the form $P/\sqrt{r}$, where P is the un-normalised radial wave function and r is the orbital radius. From the wave functions we evaluate the radial charge densities $P^2(r)$.

$P/\sqrt{r}$

r	1s	2s	3s	4s	5s	6s	$\sqrt{r}$
0.1063	0.006	-1.385	0.582	0.887	0.946	0.953	0.326
0.1156	0.003	-1.144	1.039	1.315	1.362	1.368	0.339

then $P(r)$

0.1063	0.0019	-0.451	0.190	0.289	0.309	0.311
0.1156	0.0010	-0.388	0.352	0.446	0.462	0.463

and $P^2(r)$

0.1063	----	0.203	0.0361	0.0835	0.0955	0.0967
0.1156	----	0.151	0.1240	0.1985	0.2130	0.2140

The normalizing factors are

$$24 \int P^2 dr = 0.0759 \quad 0.6900 \quad 3.109 \quad 12.55 \quad 62.99 \quad 1197.0$$

Then $$= \frac{4\pi}{\Omega} \cdot \frac{1}{2} \sum_S \left\{ P^2(r) - P^2(r) \right\}$$

$$= \frac{4\pi}{\Omega} \cdot \frac{1}{2} \cdot \quad 0.0394 \text{ a.u.}$$

If we suppose that there are 3 unpaired electrons per atom as a result of the exchange interaction, then $H_c = 3.2 \times 10^3$ gauss.

A possible third term could arise from polarization of the conduction electrons of the gold atoms by magnetic moments of the 4f shells of the gadolinium atoms, but calculation shows this to be only about 1% of the other terms so it can be ignored. For gold atoms which occupy gadolinium sites on the lattice, there would be three nearest neighbours, so that the total effective field due to the first term would be about 55 kOersted. If the gold atoms occupy interstitial sites, then the effective field at the gold nucleus due to polarized conductions electrons would be greater and could reach 90 kOersted. Addition of the two terms gives a magnetic field which could be between 20 and 100 kOersted, which gives reasonable agreement with the experimental results.

CHAPTER X

Conclusion

We have assumed in this work that the specimen is at the same temperature as the salt pill. This is doubtful because good thermal contact between the salt and the specimen is very hard to achieve. Araldite was used to join the gadolinium alloy to the copper rod because it was found to be impossible to solder gadolinium to copper, but it is difficult to judge how well araldite affords thermal contact between the specimen and the copper rod. We hoped to obtain measurements of the temperature of the specimen by measuring the magnetic susceptibility of a single crystal of cerium magnesium nitrate attached to the specimen, but we found that this was impossible because the crystal shattered during cooling.

The thermal contact between the cobalt-nickel alloy and the copper rod appeared to be adequate, since nuclear orientation was observed in this alloy. The layer of solder between this alloy and the copper rod is probably not superconducting in a field of

1300 oersted, but if it were, thermal conduction through it would probably be about the same as the thermal conduction through a similar layer of araldite.

The effective magnetic field at the nuclei of Au^{198} is not sufficiently large to produce an observable nuclear orientation. The effective magnetic field at the fluorine nucleus in gadolinium fluoride was calculated by Watson and Freeman to be -7200 oersted, which would certainly not be sufficient to produce nuclear orientation. This is not an analagous case, since the effective field due to contact interaction between s-electrons and the nuclear magnetic moment may be a function of nuclear charge, but it does provide some indication of the validity of our result.

Boyle and Hall[31] attempted to measure the effective field at the Sn^{119} nucleus as an impurity in gadolinium by the Mossbauer effect, but concluded that the effective field was insufficient to produce an observable broadening of the resonance absorption line, and must, therefore, be less than 10 kOersted. They are unsure that in their specimen the tin had properly dissolved in the gadolinium, and so consider the result not particularly trustworthy[32].

Bearing in mind that the result is unreliable, we may say that it corroborates our result to some extent since it places an upper limit of 10 kOersted on

the effective magnetic field on which our result places an upper limit of 100 kOersted, although this conclusion is affected by the fact that the distribution of electron spin density in Sn is different from that in Au. In this connection, however, it is worth remarking that Samoilov[1] found that an internal magnetic field of about 2×10^5 oersted orientated nuclei of Sb in solution in iron, whereas a field of about 7×10^5 oersted orientated nuclei of Au in solution in iron. Sn and Sb are adjacent in the periodic table, and must have a very similar electron distribution. On this basis, if we take the upper limit of the effective magnetic field on the Sn nucleus in gadolinium to be 10 kOersted, this gives an upper limit to the effective field on the Au nucleus in gadolinium of 35 kOersted. This to some extent corroborates our result.

X.2 Possible Further Developments.

It is apparent that much work remains to be done on exchange interactions between the electrons of neighbouring atoms, and on the possibility of admixture of the spin density of the magnetic electron shells of ferromagnetic metals into the closed shells of non-magnetic atoms so as to explain the presence or absence

of hyperfine fields sufficiently large to orientate nuclei. Nuclear orientation techniques have proved ineffective for measuring the internal magnetic field at gold nuclei in gadolinium, but may prove to be suitable for measuring the effective field at the gadolinium nucleus. Nuclear orientation methods are in any case very dependent on accurate temperature measurements for their accuracy.

The following possibilities for future development of the subject suggest themselves: it may be possible to make measurements of the effective magnetic field at gold nuclei as impurities in gadolinium by measurements of the Mossbauer effect or nuclear magnetic resonance of the gold in the gadolinium. It would also be interesting to carry out nuclear orientation measurements on the nuclei of a suitable isotope of gadolinium. Calculations by Freeman and Watson[26] indicate the presence of a negative electron spin density close to the gadolinium nucleus. This would lead to a negative hyperfine field of about 10 kOersted, which would not be enough to polarise the nuclei, but the effective field due to the unquenched orbital angular momentum of the 4f shell would dominate over the core polarization contact term, and would give an effective field of about 690 kOersted. It ought, therefore, to be possible to obtain a measurable nuclear

orientation in gadolinium metal.

Since the beginning of the work described in this thesis, much theoretical work (references 18, 25, 26 and 27a) has been published on the origin of effective magnetic fields in magnetic materials which might well have affected the series of experiments. Less time would have been devoted to attempts to obtain nuclear orientation of gold in gadolinium in favour of measurements on pure gadolinium specimens.

This would have yielded information on the internal magnetic field in pure gadolinium metal, which ~~would~~, in comparison with our result for gold in gadolinium, might have helped to elucidate the mechanism of formation of effective magnetic fields at the nuclei of impurities in a ferromagnetic metal.

References

(1) Samoilov, Skiyarevskii, and Stepanov, Soviet Physics, JETP, 11, 261, (1960).

(2) Overhauser, A.W., Phys. Rev. 92, 411, (1953).

(3) Jeffries, C.D., Phys. Rev. 106, 164, (1957).

(4) Abraham, Kedzie, and Jeffries, Phys. Rev. 106, 165, (1957).

(5) Dabbs, Roberts, and Bernstein, Phys. Rev. 98, 1512, (1955).

(6) Kurti, Robinson, Simon and Spohr, Nature, 178, 450, (1956).

(7) Gorter, C.J., Physica, 14, 504, (1948).

(8) Rose, M.E., Phys. Rev. 75, 213, (1949).

(9) Bleaney, B., Proc. Phys. Soc. A64, 315, (1951).

(10) Pound, R.V., Phys. Rev. 76, 1410, (1949).

(11) Dabbs, Roberts, and Parker, Physica, 24, S69, (1958

(12) Johnson, Scholey, and Shirley, Proc. Int. Conf. Low Temp. Phys., Toronto, 1960, p.1

(13) Grace, Johnson, Kurti, Scurlock, and Taylor, Phil. Mag. 4, 948, (1959)

(14) Johnson and Scurlock, reported by Marshall (17).

(15) Heer and Erickson, Phys. Rev. 108, 896, (1957).

(16) Kurti, Arp and Petersen, Bull. Am. Phys. Soc. 2, 388, (1957).

(17) Marshall, W. Phys. Rev. 110, 1280, (1958).

(18) Watson and Freeman, Phys. Rev. 123, 2027, (1961).

(19) Hanna, et al., Phys. Rev. Letters, 4, 177 and 513, (1960).

(20) Nagle, et al., Phys. Rev. Letters, 5, 364, (1960).

(21) Wertheim, G.K., Phys. Rev. Letters, 4, 403, (1960).

(22) Boyle, Bunbury and Edwards, Phys. Rev. Letters, 5, 553, (1960).

(23) Meyer-Schutzmeister, et al., reported by Watson and Freeman (18).

(24) Reference (1).

(25) Freeman and Watson, Phys. Rev., 127, 2058 (1962).

(26) Watson and Freeman, Phys. Rev., Letters, 6, 277, (19

(27)a Freeman and Watson, Jour. Phys. Soc. Japan, 17, B-I, 15, (1962).

(27)b Jaccharino, et al., Phys. Rev. Letters, 5, 251, (196

(28) Tolhoek and Cox, Physica, 19, 101, (1953).

(28a) Tolhoek and Cox, Physica, 19, 673, (1953).

(29) Stone and Turrell, Physics Letters, 1, 39, (1962).

(30) Geiser, R., Thèse, Université de Grenoble, 1963.

(31) Tournier, P., Thèse, Université de Grenoble, 1960.

(32) Arp, Edmunds and Petersen, Phys. Rev. Letters, 3, 212, (1959).

(33) Hartree and Hartree, Proc. Roy. Soc. A149, 210, (193

(34) Boyle, A.J.F., and Hall, H.E., Repts. Prog. Phys. 25, 513, (1962).

(35) H.E. Hall, Private communication.